INSTITUTE OF BIOPHYSICS

BIOLOGICAL RESEARCH CENTER - SZEGED

HUNGARIAN ACADEMY OF SCIENCES

LASER RAMAN STUDIES ON LIPIDS

Molecular interactions with phosphatidylcholine multilayers

Evgenija Loshchilova

PhD Thesis

Szeged

1979

CONTENTS

INTRODUCTION

One of the most active and rapidly changing areas of modern biology is the study of membrane structure and function. Many new hypotheses are evolving, leading to a concept of the membrane as a complex, dynamic structure with unique biological properties which receives signals from and transmits signals to the environment, controls the permeation of nutrients, regulates the action of certain drugs and hormones, modulates cell to cell interactions and communications, and influences cell growth and differentiation.

The present view of biomembrane structure is that a lipid bilayer is the basic matrix into which and around which the various proteins are situated. Not only can the proteins be attached to the outside of the lipid bilayer but in many cases the proteins are embedded within and can span the bilayer. In the living cell most of the membranes exist in a fluid, "liquid crystalline" state. The biochemical functions of membrane-bound proteins may be regulated by the physical state of the lipid matrix, and, in turn, the proteins might disturb their lipid environment, significantly changing its mobility.

Numerous physical methods have been applied to elucidate different aspects of membrane structure - from X-ray diffraction providing a static, time-averaged picture of the membrane to magnetic resonance methods which furnish information on the dynamic processes in the membranes and are sensitive to both environment and motion of different chemical groups. A detailed structural organization of unaltered biological membranes cannot be ascertained by direct observation or measurements, hence a solution to this problem has to be derived indirectly by piecing together partial informations obtained by several methods, critically estimating the relevance and relative importance of available data.

Recently it has been proved that laser Raman spectroscopy is a powerful method for structural investigations of both lipid and protein components of model and biological membranes. An advantage of this technique is that it does not require the introduction of a foreign probe molecule /as in the case of electron paramagnetic resonance/ which could perturb the membrane and disrupt the weak ordering interactions between the membrane constituents. Since water is a poor Raman scatterer /in contrast to its strong infrared absorption/ the drying of membrane preparations which often complicates the biological applications of IR spectroscopy, is not necessary. Unlike other physical techniques, Raman measurements can be made with ease in single crystals, powders, fibers, aqueous solutions or even intact biological specimens.

In the present work laser Raman spectroscopy has been applied to investigate lipid-ion interactions playing important role in excitation processes, ion permeation, ion binding and ion exchange properties of biological membranes. Prior to understanding the Raman spectra of naturally occuring membranes, it is necessary to examine model membrane systems. Among others, the phospholipid-water multilayer dispersions are accepted and widely used as a model for the more complicated cellular membranes. In our studies the structural behaviour of dipalmitoyl phosphatidyl choline--water multilamellar system was studied in the presence of mono- and divalent cations /K^+, Na^+, Cs^+, Rb^+, Ca^{2+}, Mg^{2+}, Cd^{2+}, Ba^{2+}/ and anions /Cl^-, Br^-, NO_3^-, SO_3^{2-}, SO_4^{2-}, $S_2O_3^{2-}$, $S_2O_8^{2-}$/. Special attention was paid to the influence of iodine species /I_2, I^-, I_3^-/ on the lipid bilayer structure in order to find supporting data for conduction mechanisms of iodine-doped bimolecular membranes /BLM/, suggested pre-

viously on the basis of electric measurements. The Raman spectroscopic data have been evaluated quantitatively by calculating and comparing the intensity ratios of conformational sensitive Raman bands and *trans* and lateral order parameters of which the first gives the fraction of all-*trans* bonds in the lipid hydrocarbon chains while the second provides a measure of the lateral order between the chains. Detailed analysis has been performed on the applicability of the introduced order parameters in the case of interactions of ions with lipid polar groups.

I. RAMAN SPECTROSCOPY AND ITS APPLICATION TO STRUCTURAL INVESTIGATIONS

Raman scattering /or combination scattering/ is one of the processes resulting from the interaction of radiation with matter. A characteristic feature of Raman scattering is the change in the frequency of the scattered light in comparison with the primary /exciting/ radiation /1-5/.

Raman scattering was discovered in 1928 simultaneously, by C.V. Raman and K.S. Krishnan in liquids and G.S. Landsberg and L.I. Mandelstam in quartz crystals. Long before these discoveries, Lommel developed the mathematical theory of light scattering by anharmonic oscillator, according to which the scattered radiation should contain shifted /combination/ frequencies. Smecal /1923/ suggested similar results on the basis of quantum concepts. These theoretical predictions, however, had no relation to the actual discovery of Raman scattering.

If radiation with frequency ν_o and intensity I_o illuminates a suitable transparent specimen along with the strong scattering at unshifted frequency ν_o /elastic scattering/, due to Rayleigh and Tindal effects, a low-intensity scattered light at altered frequencies $\nu_o \pm \nu_v$ /unelastic scattering/ is observed and is called Raman scattering.

The frequency shifts ν_v are equal to the frequencies of molecular motions /vibration or rotation/ in the sample. The frequency units usually employed in vibrational spectroscopy are reciprocal centimeters /cm^{-1}/, or wave-numbers defined as ν /cm^{-1}/ = $\frac{1}{\lambda / cm}$, where λ is the wavelength.

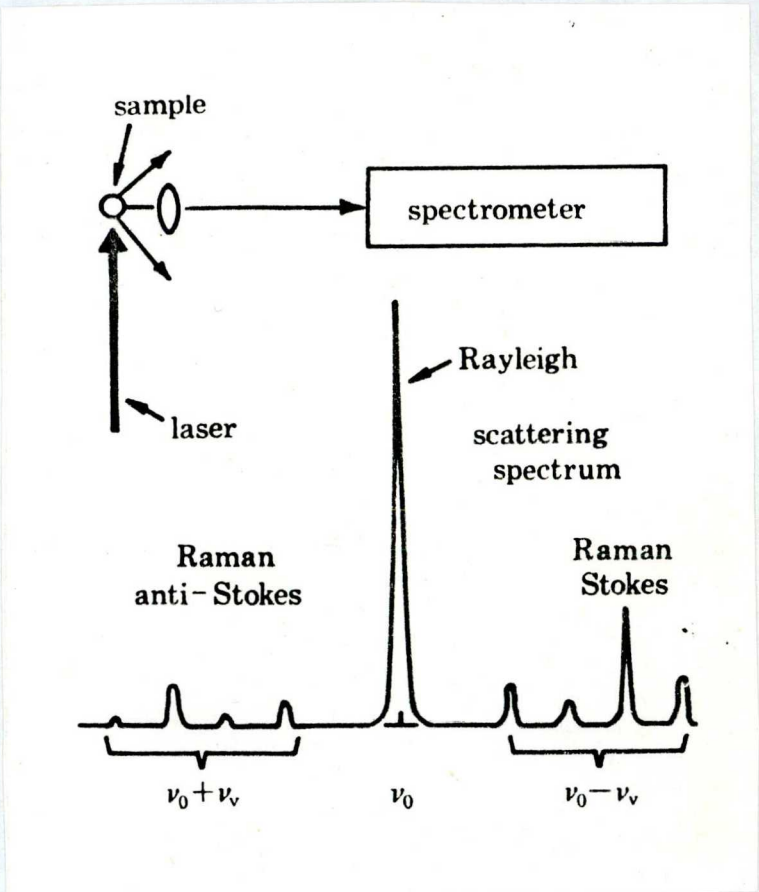

Fig. 1.

Schematic illustration of an arrangement for obtaining a Raman spectrum with a laser light source. ν_o is the frequency of the incident light and vibrational frequencies are represented by ν_v. /The Rayleigh peak in an actual scattering spectrum is several orders of magnitude larger than the Raman peaks./

Usually the position of a Raman band is characterized not by the absolute value of its frequency ν' /cm^{-1}/ but by its shift $\Delta\nu$ from the excitation band ν_o /cm^{-1}/, i.e.

$$\Delta\nu[cm^{-1}] = \nu_o[cm^{-1}] - \nu'[cm^{-1}]$$

Radiation which has increased frequency /$\nu_o + \nu_v$/ as a result of energy transfer from the scattering system is known as anti-Stokes radiation and that which has decreased energy, i.e. lower frequency /$\nu_o - \nu_v$/ is known as Stokes radiation. For energy to be removed from the scattering system, some excited energy states must be populated initially. In the equilibrium the population of states is given by the Boltzman distribution equationand it decreases exponentially with increasing energy difference between the ground and excited state. From this follows that the intensity of anti-Stokes bands is lower than that of the corresponding Stokes bands and decreases rapidly with increasing frequency shift from the exciting band.

Both infrared /IR/ and Raman spectroscopy provide information on the vibrational and rotational motion of the molecules /Fig. 2./. However, the factors which determine the Raman scattering intensities are different from those involved in the absorption of IR radiation. The activity of a particular vibrational mode in the IR spectrum is a function of dipole moment change during vibration. In contrast, Raman active vibration modes are accompanied by a change in the polarizability of the molecule. This makes the two techniques complementary in the studies of molecular motions.

It is important to sharply distinguish Raman scattering from fluorescence, where the frequency of the re-emitted radiation is also changed /Fig. 2./. In the latter resonant absorption occurs and, after a measurable /10^{-8}-10^{-9} sec/ life-time of the excited electronic state, is followed

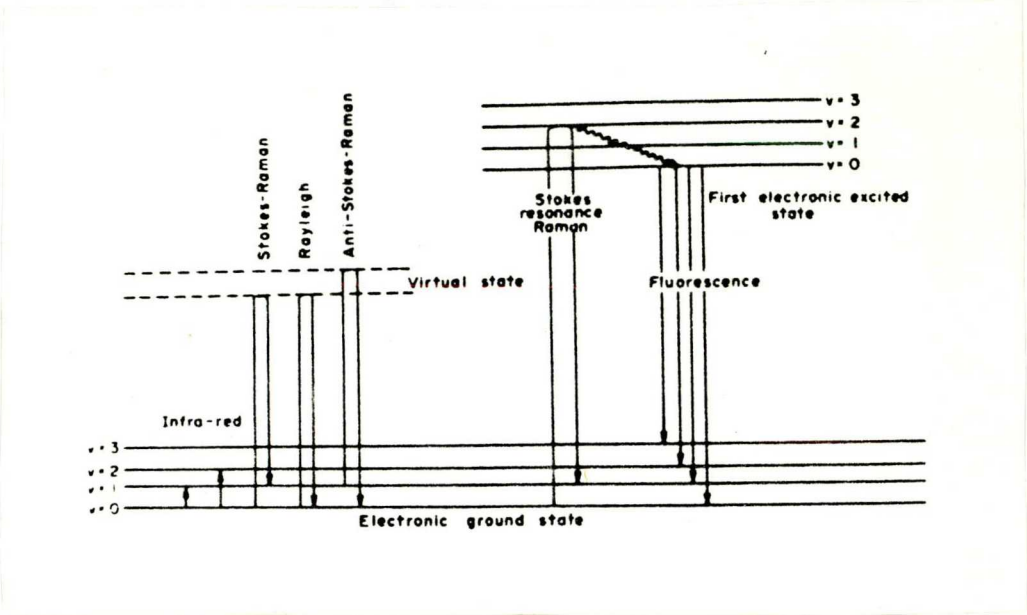

Fig. 2.

Schematic comparison of various processes: Rayleigh, Stokes Raman, anti-Stokes Raman, infrared, resonance Raman, and fluorescence.

by emission involving either the same or different lower state.

Raman effect takes its origin from the transitions between rotational and vibrational levels of the ground electronic state. In the Raman scattering the life-time of the excited states is of the order of the vibrational period-about 10^{-12} - 10^{-14} sec, and excitations are considered as purely virtual states. In spite of this, especially for weakly-fluorescent materials, it is difficult to separate experimentally Raman scattering and fluorescence and the theoretical difference is also not so clear-cut, as could be supposed, if the excitation frequency is within the absorption band of the scattering material /resonance Raman effect/.

I. 1. Raman scattering - classical approach

I.1. A. Origin of Raman scattering . Polarizability tensor

No complete theory of Raman scattering can be built without extensive use of quantum concepts. Some basic conclusions, however, can be derived from classical treatment also. The fundamental physical principles used in the classical theory of Raman effect can be formulated as follows:

1. The light is scattered as a result of forced oscillations of the molecular dipole induced by the electromagnetic field of the incident light.
2. The light in the visible and near UV is mainly scattered by the electron shell of the molecule, the atomic nuclei being displaced insignificantly due to the incident radiation.
3. Raman scattering reflects the coupling between the movement of electrons and the movements of atomic nuclei. As the nuclei oscillate about their respective equilibrium positions /and also during their periodic motions e.g. molecular rotations/ the deformability of the electron cloud and consequently the induced dipole, vary with the oscillation frequency of the nuclei. On the other hand, deformation of the electron cloud may induce addition vibrations of the molecular nuclei, as well.

From this classical point of view Raman scattering is associated with the modulation of the induced dipole moment by the molecular skeletal vibrations. An elementary classical justification for this is as follows. If a light wave $\vec{E} = \vec{E}_o \cos\omega t$ hits the molecule, it induces in it a dipole moment $\vec{p}(t) = \alpha\vec{E}$

Here α is the polarizability of the molecule. In the classical theory polarizability is a phenomenological quantity, which depends on the distance between the atomic nuclei at any given time and reflects the deformability of the molecular electron cloud. In general, the scattering system is anisotropic, i.e. the ability of the electrons to move away from their equilibrium positions under the action of the electromagnetic field depends on the orientation of the field relative to certain preferred axes in the scattering system. Consequently, the polarizability, in general, is not a scalar and the induced dipole moment $\vec{P}$ does not point in the direction of the electric field vector $\vec{E}$. The components of the induced dipole moment and the exciting electric field are related as follows

$$P_i = \sum_{\kappa} \alpha_{i\kappa} E_{\kappa} \quad (i, \kappa = x, y, z) \qquad /1/$$

The nine coefficients $\alpha_{i\kappa}$ involved are called components of the polarizability tensor /or scattering tensor/, which describes the properties of the scattered radiation. In fact, the polarizability tensor is symmetric and only six of its components are independent.

In harmonic approximation any vibrational movement of a polyatomic molecule can be represented as a superposition of vibrations of simple harmonic oscillators. Assuming that $q_i = q_{i0} \cos(\omega_i t + \delta_i)$ is the coordinate corresponding to vibration with frequency ω_i, the polarizability α as a function of q_i can be expanded in a power series

$$\alpha(q_i) = \alpha_0 + \left(\frac{\partial \alpha}{\partial q_i}\right)_0 q_i + \ldots \qquad /2/$$

Substituting /2/ in the expression for $\vec{P}$ gives

$$P(t) = \left[\alpha_0 + \left(\frac{\partial\alpha}{\partial q_i}\right)_0 q_{i0} \cos(\omega_i t + \delta_i)\right] E_0 \cos\omega_0 t =$$

$$\alpha_0 E_0 \cos\omega_0 t + \frac{1}{2}\left(\frac{\partial\alpha}{\partial q_i}\right)_0 E_0 q_{i0} \cos[(\omega_0 - \omega_i)t + \delta_i] + \quad /3/$$

$$\frac{1}{2}\left(\frac{\partial\alpha}{\partial q_i}\right)_0 E_0 q_{i0} \cos[(\omega_0 + \omega_i)t + \delta_i]$$

This is to be understood as implying for each of the components of the induced dipole moment $\vec{P}$ taking into account all the components of the applied electric field $\vec{E}$. The first term in the expression /3/ for $\vec{P}$ is responsible for the Rayleigh scattering of the incident light at unchanged frequency ω_0. The second and the third terms at shifted frequencies $\omega_0 - \omega_i$ and $\omega_0 + \omega_i$ are responsible for the Stokes and anti-Stokes Raman scattering, respectively. At low incident intensities the values of the phase angles δ_i are different for different scattering centers and in this case Raman scattering is incoherent. Evidently the condition that a particular molecular frequency ω_i shall be active in Raman scattering is that the factor $\left(\frac{\partial\alpha}{\partial q_i}\right)_0$ shall be different from zero. If higher terms in the expansion are taken into consideration, the intensities of overtones /vibrations with frequencies $2\omega_i, 3\omega_i, \ldots$/ and combination frequencies $\omega_i + \omega_k$ can be related to the higher derivatives of α.

I.1.B. Intensity and state of polarization of scattered light

According to classical electrodynamics a small oscillating dipole $\vec{P}$ /induced dipole in the case of Raman scattering/ emits electromagnetic radiation at the frequency

of its oscillation. The radiation intensity dI in a solid angle $d\Omega$ is defined as the quantity of energy passing in unit time through a surface element $R^2 d\Omega$ of a sphere of radius R, centered at the origin. The scattered intensity in the direction $\vec{n}'$ at distances much greater than the diameter of the scattering system for a dipole $\vec{P}$, vibrating as a harmonic oscillator of frequency ω' is

$$dI = \frac{\omega'^4}{4\pi c^3} \left| [\vec{P}\,\vec{n}'] \right|^2 d\Omega \qquad /4/$$

It is clear from /1/ and /4/ that the intensity of scattering depends on the relative directions of observation, illumination and the electric field vector.

A typical experimental configuration is shown on Fig. 3, where the incident laser beam travels along the X axis with

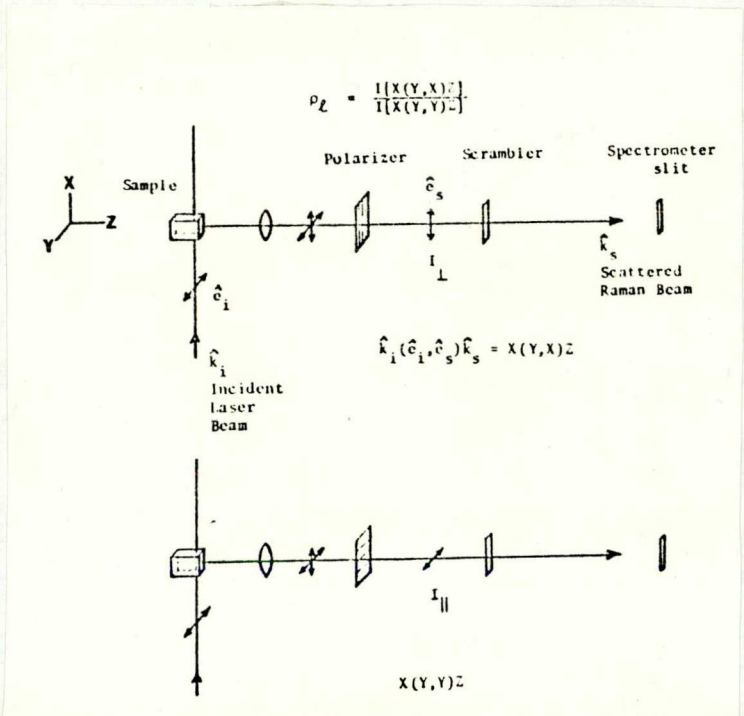

Fig. 3.
A typical 90° Raman scattering configuration.

electric field $\vec{E}$ polarized in the direction Y /i.e. $E_y \neq 0$, $E_x = 0$, $E_z = 0$/ and the scattered light is observed along the Z axis. In case of light scattering by a single molecule with a fixed orientation in space, the intensities of the scattered light polarized in the X and Y directions /i.e. with electric vector parallel to X and Y axes, respectively,/ are expressed according to /1/ and/ 4/ as follows

$$I \text{ /polarized along the X axis/} \sim \alpha_{xy}^2 E_y^2 \qquad /5/$$

$$I \text{ /polarized along the Y axis/} \sim \alpha_{yy}^2 E_y^2 \qquad /6/$$

and

$$I \text{ /total/} \sim (\alpha_{xy}^2 + \alpha_{yy}^2) E_y^2 \qquad /7/$$

For a system consisting of randomly oriented molecules in case of incoherent Raman scattering the total scattering intensity is proportional to the number of scattering molecules, and the expressions /5/ - /7/ should be averaged over all the various orientations the molecules can have, relative to a system of fixed axes.

The components of the polarizability tensor α /in our case α_{xy} and α_{yy}/ will change upon rotation of the molecular coordinate system. For special coordinate system the matrix α will take a diagonal form, its components /α_1, α_2, α_3/ known as the principle polarizabilities. Of considerable importance in Raman spectroscopy are certain functions of the polarizability tensor components which are invariant towards the rotation of the coordinate system. These are the mean polarizability

$$\bar{\alpha} = \frac{1}{3}(\alpha_{xx} + \alpha_{yy} + \alpha_{zz}) = \frac{1}{3}(\alpha_1 + \alpha_2 + \alpha_3) \qquad /8/$$

and the anysotropy

$$\beta^2 = \frac{1}{2}\left[(\alpha_{xx} - \alpha_{yy})^2 + (\alpha_{yy} - \alpha_{zz})^2 + (\alpha_{zz} - \alpha_{xx})^2 + 6(\alpha_{xy}^2 + \alpha_{yz}^2 + \alpha_{xz}^2)\right] = \frac{1}{2}\left[(\alpha_1 - \alpha_2)^2 + (\alpha_2 - \alpha_3)^2 + (\alpha_3 - \alpha_1)^2\right] \qquad /9/$$

It can be also shown that the mean square quantities $\overline{\alpha_{xy}^2}$ and $\overline{\alpha_{yy}^2}$, and consequently the intensity of the scattered radiation are expressible in terms of invariants of the scattering tensor $\bar{\alpha}$ and β^2. In terms of the scattering tensor invariants the total scattering intensity of a system of randomly oriented molecules is proportional to $(45\bar{\alpha}^2+4\beta^2)N_v I_o$, where N_v is the number of molecules per unit volume and I_o is the intensity of the excitation source.

Usually to characterize the polarization of the scattered radiation the so-called depolarization ratio ρ_l is introduced, which in notations used on Fig.3., is expressed as

$$\rho_l = \frac{I[X[Y,X]Z]}{I[X[Y,Y]Z]} \qquad /10/$$

The subscript l indicates linearly polarized incident radiation. Two spectra are needed to determine this ratio: one with the polarizer oriented parallel to the axis X and the other with the polarizer oriented parallel to the Y axis. The scrambler between the polarizer and the spectrometer slit is to eliminate the polarization dependence of the monochromator response. $I[X(Y,X)Z]$ and $I[X(Y,Y)Z]$ are often referred to as $I_\perp$ and $I_\parallel$, respectively.

In terms of the polarizability tensor invariants the depolarization ratio is expressed as

$$\rho_l = \frac{3\beta^2}{45\bar{\alpha}^2+4\beta^2} \qquad /11/$$

The Rayleigh scattering is accounted for by that part of the incident dipole moment which is determined solely by the polarizability tensor α_o of the molecule in its equilibrium configuration. That is why considering intensities and the state of polarization of Rayleigh bands, the components of α_o should be used in calculations of tensor invariants $\bar{\alpha}_o$ and β_o^2. The mean-value invariant $\bar{\alpha}_o$ of the polarizability

tensor α_o can never vanish, for all molecules are electrically polarizable to some extent. On the other hand the anysotropy invariant β_o^2 may be zero, as in the case of electrically isotropic molecules. For these reasons in Rayleigh scattering ρ_l is always less than 3/4.

The Raman scattering for a particular vibrational mode of normal coordinate q_α is determined by the derived polarizability tensor $\left(\frac{\partial \alpha}{\partial q_\alpha}\right)_o$ or α' in the same way as the Rayleigh scattering is determined by α_o. In this case the components of α' should be used in calculation of the invariants $\bar{\alpha}'$ and β'^2. There is a very important difference between α_o and α'. α_o must be always positive, whether α' may be either positive or negative, or zero. Thus for Raman scattering $o \leq \rho_l \leq \frac{3}{4}$. In certain circumstances both α' and β'^2 may be simultaneously zero and Raman scattering will be forbidden. Rayleigh scattering, in contrast is never forbidden.

When $\rho_l = 3/4$ for a Raman line, it is conventionally described as depolarized. Any line for which $\rho_l < 3/4$ is said to be polarized. In particular when $\rho_l = 0$ the line is said to be completely polarized. As will be discussed later, it is the molecular symmetry which determines not only whether a certain normal mode shall be permitted or forbidden in the Raman scattering but also whether its Raman line shall be polarized or depolarized.

I.1.C. Vibrational frequencies and modes

In terms of classical mechanics a polyatomic molecule is treated as a system of point masses and in case of known geometry and known forces resisting deformation of bonds and bond angles /known intramolecular force field/, the vibrational frequencies and the amplitudes of atomic displacements can be calculated. As in classical dynamics of

isolated systems the problem is to find the form and periodicity of the displacements which are consistent with invariance of the total energy of the system.

In a first order of approximation the molecular vibrations can be treated independently of rotational-translational and electronic motions. The vibrations of a molecule can be described by a classical equation of motion of Hamiltonian type. It has especially simple form if special so called normal coordinates, which are linear combinations of mass-weighted nuclear displacement coordinates are chosen. The normal coordinates describe normal modes of vibrations in which all of the atoms in a molecule move with the same frequency and the same phase, that is, they all pass through their equilibrium positions at the same time. Any complex molecular motion can be regarded as a superposition of normal modes. There are as many different normal vibrations as there are vibrational degrees of freedom, that is 3N-6 or 3N-5 /for linear molecules/, where N is the number of atoms in the molecule. After solving the Hamiltonian equation of motion, the internal vibrational frequencies of the molecule are obtained together with the amplitudes of the atomic displacements at the corresponding frequencies, which determines the actual mode of the particular vibration.

In practice, it is the vibrational frequencies which are known /experimentally observable/ and from them, in principle, the force constants of the intramolecular field could be calculated. However, grave difficulties arise in these calculations, for the experimental evidence /the number of the observed vibrations/ is usually insufficient to determine the field completely. Another serious problem is the correct assignment of the observed vibrations.

I. 2. Raman scattering - quantum approach

In quantum theory a system of particles immersed in a radiation field is described by a wave function $\Psi(t)$, which satisfies the wave equation

$$i\hbar \frac{\partial \Psi}{\partial t} = \hat{H} \Psi \qquad /12/$$

Here $\hat{H}$ is the system Hamiltonian which is written as a sum of the molecule Hamiltonian $\hat{H}_m$, the electromagnetic field Hamiltonian $\hat{H}_s$ and the interaction Hamiltonian $\hat{H}_{int}$ which are generally assumed to be Hermitian operators. In order to allow for damping, a molecule Hamiltonian is taken as a sum of a Hermitian operator $\hat{H}_m$ and a non-Hermitian "damping operator" $\hat{H}_d$, which is assumed to be small compared to $\hat{H}_m$. In terms of Dirac's time-dependent perturbation theory the damping-free molecule and the radiation field are considered as the "unperturbed" system with the Hamiltonian $\hat{H}_o = \hat{H}_m + \hat{H}_s$, whereas $\hat{H}' = \hat{H}_d + \hat{H}_{int}$ is regarded as the perturbation operator.

The solution of the wave equation /12/ for the unperturbed system in the state n with energy E_n can be represented as $\Psi_n(x,t) = \Psi_n(x)\, e^{-iE_n t/\hbar}$
The perturbation alters the state of the system. The solution of the fundamental equation /12/ for the perturbed system is sought as a superposition of the eigenfunctions of the unperturbed system:

$$\Psi(x,t) = \sum_n b_n(t)\, \Psi_n(x,t) \qquad /13/$$

Physically, $|b_n(t)|^2$ is the probability that at the time t the system occupies the unperturbed state n.

$|b_n(t)|^2$ can as well be considered as a probability for the transition from the initial state m occupied by the system to the state n during the time t under the action of the electromagnetic field.

In general, the solution of the differential equations for $b_n(t)$ is a highly conplicated problem. In the particular case when in certain interval $\hat{H}_{int}$ can be considered constant with time and the perturbation operator can be represented as $\hat{H}'(x,t) = \hat{H}_d + \hat{H}_{int} = \hat{H}_d + \eta \hat{H}'(x)$ /η is a constant/, the following expression is obtained for $b_n(t)$:

$$b_n(t) = -\frac{\eta H'_{mn}}{E'_m - E'_n} f_{nm}(t) - \frac{\eta^2}{E'_m - E'_n} \cdot \sum_\ell \frac{H'_{m\ell} H'_{\ell n}}{E'_m - E'_\ell} f_{nm}(t) + \qquad /14/$$

$$+ \eta^2 \sum_\ell \frac{H'_{m\ell} H'_{\ell n}}{(E'_m - E'_\ell)(E'_\ell - E'_n)}$$

Here $H'_{\kappa i}$ is the matrix element of the operator $\hat{H}'(x)$ for the transition of the system from state i to state κ, defined as

$$H'_{\kappa i} = \int \psi_i^*(x)\, \hat{H}'(x)\, \psi_\kappa(x)\, dx \qquad /15/$$

$E'_\kappa = E_\kappa - \frac{1}{2} i \Gamma_\kappa$, where Γ_κ characterized the width of the K-th energy level and is determined by the matrix elements of $\hat{H}_d$. $f_{ki}/t/$ are products of oscillating and damping factors, giving the time-dependence of $b_k/t/$.

Equation /14/ contains three termes: the first describes direct transitions of the system from the initial state m to the state n /light absorption and emission/ and the second and third terms correspond to transitions through intermediate states - Raman scattering and re-

sonance fluorescence, respectively.

The expressions for the transition probabilities can be applied in principle to determine the intensities of the spectral bands corresponding to these transitions. This requires the calculation of the matrix elements H'_{ki} /15/. In practice, these calculations can be carried out only partially since the wave functions of complex molecules are not known. The solution of the problem is nevertheless of the greatest significance even in particular cases, since it gives the actual expressions for the matrix elements and sheds light on the entire question of line intensities.

Taking into consideration the possibilities for the realization of the Raman scattering through different intermediary states and introducing in /14/ the perturbation operator from the known expression for the particle Hamiltonian in the electromagnetic field, the probability of Raman scattering is found to be proportional to

$$S_{nm} = \sum_{\ell} \frac{(\vec{e}\, P_{\ell m})(\vec{e}' P_{n\ell})}{\omega_{\ell}^{e} - \omega_0 + i(q_m - q_\ell)} + \frac{(\vec{e}' P_{\ell' m})(\vec{e}\, P_{n\ell'})}{\omega_{\ell}^{e} + \omega' + i(q_m - q_\ell)} \quad /16/$$

Here $\vec{e}$ and $\vec{e}'$ are the unit vectors for the direction of polarization of the exciting and scattered radiation, respectively, ω_0 and ω' are the frequencies of the exciting and scattered radiation, respectively, $q_i = \frac{\Gamma_i}{2\hbar}$, $\omega_{\ell}^{e} = E_\ell - E_m$, P_{kl} represents the transition moment. $P_{kl} = \int \psi_k^* |\vec{P}| \psi_\ell \, dx$ where $\vec{P}$ is the molecular dipole inclusive of the induced moment. In the case of $\omega_{\ell}^{e} \gg \omega_0$ the following expression is obtained for the intensity of the Raman scattering

$$I_R = a I_0 \omega'^4$$

/17/

Here I_o is the intensity of the exciting radiation and a is determined by S_{mn} and the term showing the time-dependence of the probability of Raman scattering. From the comparison of the classical and quantum expressions for the Raman scattering intensity, the scattering tensor $\alpha_{\rho\sigma}$ formally introduced in /1/ can be written as follows:

$$(\alpha_{\rho\sigma})_{nm} = \frac{1}{\hbar} \sum_{\ell} \left(\frac{(P_{n\ell})_\rho (P_{\ell m})_\sigma}{\omega_\ell^e - \omega_o + i(q_m - q_e)} + \right. \qquad /18/$$

$$\left. + \frac{(P_{\ell' m})_\rho (P_{n\ell'})_\sigma}{\omega_\ell^e + \omega' + i(q_m - q_e)} \right)$$

Consequently, all the results obtained in classical approximation are valid for the quantum mechanic expression /18/ which gives the actual form of the scattering tensor.

When the frequency of the incident light approaches that of a given electronic transition /$\omega_o \approx \omega_\ell^e$/, i.e. it is within an absorption band of the scattering system, Resonance Raman effect is observed. In this case the first term in the summation /18/, and consequently the induced dipole moment, can become very large for an allowed electronic transition. It is prevented from reaching infinity by inclusion of the damping term, which is a measure of the width of the electronic transition. Most of the ordinary Raman lines are attenuated by the absorption, but some lines can be greatly enhanced in intensity. In the Resonance Raman scattering only those vibrations are enhanced which are coupled to the resonant electronic transition. The magnitude of resonant enhancement is predicted to vary directly with the oscillator strength of the resonant electronic transition and inversly with its breadth. Maximal resonance effects are therefore expected for strong sharp absorption bands.

I. 3. The concept of symmetry and its application to the vibrational problem

Molecular symmtery is a very powerful concept. From symmetry considerations alone without any quantitative calculations, it can be determined how many energy states a molecule may have and what interactions and transitions between them may occur. However, to determine the actual energy difference between the states of the system and the actual probabilities of the allowed transitions, calculations or measurements must be made.

The symmetry properties of a molecule in its equilibrium configuration are described by saying that it possesses certain symmetry elements, with which are associated certain symmetry operations. The symmetry elements include reflection planes σ, rotation C_p and reflection-rotation axes S_p and center of symmetry i. Here the subscript "p" identifies the order of the axis. A symmetry operation is defined as one which, when performed upon the molecular model /i.e. upon the model of the molecule in its equilibrium configuration/ produces a result which is indistinguishable from the original model. The full set of symmetry operations, appropriate to the model of a molecule in its equilibrium configuration /when certain requirements are fulfilled/ constitutes a mathematical point group. Each such group is designated by a conventional symbol. Detailed descriptions of different point groups and their symmetry elements can be found in a number of text books /1, 4, 6, 7/.

If a coordinate system is appropriately chosen in the configuration space, each symmtery operation may be

represented by a matrix, relating the atomic coordinates before and after the application of the symmetry operation. Since the complete set of symmetry operations constitutes a mathematical group, it can be shown that a complete set of matrices, corresponding to these operations also forms a group and is called a representation of the group. By suitable choice of the basis it is possible to bring /reduce/ each matrix of a group representation into a diagonal-block form. In a completely reduced representation the blocks have dimensions 1, 2 and 3 and are called irreducible representations. One-dimensional, non-degenerate representation is designed A_I, if the coordinate transformed according to this representation remains unchanged under any symmetry operation of the point group, and A_2 if under some of the group operations the coordinate is unchanged and under the other - it reverses its sign. Two- and three-dimensional representations are designed E and F, respectively, and are called degenerated representations. Coordinates mixing under the symmetry operations of the group, are transformed according to these representations. Double degenerate species E appear in case if two directions in the space are symmetrically equivalent and three-fold degenerate species F occur where all three directions in physical space are symmetrically equivalent.

For the purposes of applying symmetry considerations to the problem of molecular vibrations it suffices to know the characters /the sum of the matrices, diagonal elements/ of the matrices forming irreducible representations without knowing the individual matrix elements for any particular basis choice. Using the characters of the irreducible representations it is possible to derive the

structure of the completely reduced form without the necessity of actually carrying out the complete reduction at all. Since the representation of any molecular point group is completely reduced, when based upon the complete set of normal coordinates, the above considerations can be used in determining the number of normal coordinates /and vibrational modes/ which belong to various symmetry species. The actual introduction of normal coordinates is not necessary for this.

Each class of normal coordinates belonging to particular symmetry species constitutes a separate vibrational problem and therefore it is apparent that theoretical analysis can be greatly facilitated by considering each class separately. The following notation is used for the normal modes of various symmetry classes. A and B are reserved for non-degenerate modes, E designates a doubly degenerate modes, and F triply degenerate modes. In general A is assigned to symmetric modes and B to antisymmetric modes /relative to the preferential axis of the molecule/. For symmetry groups without preferential axes, the letter A signifies symmetry relative to three mutually perpendicular two-fold axes, and the letter B antisymmetry to two out of the three two-fold axes. The subscript g and u designate symmetry or antisymmetry relative to the center of symmetry i ; a prime and double prime indicate symmtery or antisymmetry relative to a plane of symmetry σ . The indices $+$ and $-$ for degenerate modes indicate symmetry relative to an axis rotation. If the system has another symmetry element, the subscript 1 is generally introduced to indicate symmetry relative to this additional element.

Symmetry considerations are extremely helpful in deriving the selection rules in IR and Raman spectroscopy, i.e. one can find the transitions with non-zero matrix ele-

ments and, correspondingly, non-zero band intensities. A matrix element

$$(\beta_\lambda)_{\kappa n} = \int \psi_n^* \beta_\lambda \psi_\kappa \, dx \qquad /19/$$

does not vanish only if the integrand in /19/ is invariant under a symmetry transformation. The wave functions ψ_n^* and ψ_κ have definite transformation properties under symmetry operations, which depend only on the symmetry of the system and are well known for any symmetry type. The derivation of selection rules thus reduces to the determination of the symmetry properties of the triple products of the form $\psi_n^* \beta_\lambda \psi_\kappa$. A transition is allowed if the product is not affected by symmetry operations, and it is forbidden if the product reverses its sign /then $(\beta_\lambda)_{\kappa n} = 0$ /. The function β_λ may be a tensor, a vector or a component of a tensor or a vector. To derive the selection rules for Raman scattering we have to consider the behaviour of the components of the scattering tensor, under symmetry operations. The selection rules for IR absorption are determined by the behaviour of the components of the dipole moment vector.

When sufficiently comprehensive experimental data are available on the molecular vibrational spectra/ IR and Raman,/ the selection rules can be applied together with the numerical values of the depolarization of the Raman bands to identify the corresponding vibrational modes thus providing information on the symmetry of the molecule.

I. 4. Raman experiment

The total intensity of scattered radiation from a dust-free transparent liquid is approximately 0.1 % of that of the source I_o. Most of it occurs at ν_o /Rayleigh scattering/ and only less than 10^{-7} I_o occurs as Raman scattering. For these reasons high performance equipments are required in Raman work. In the basic Raman spectrometer the sample under examination is irradiated by a suitable excitation source and the Raman spectrum is observed through a system comprising optics for collecting the Raman emission, monochromator/s/, detector /photomultiplier/, photon-counting electronics and recorder.

In a Raman spectrometer an intense, monochromatic, preferably highly polarized light source with minimal background is required. In this respect lasers offer unique possibilities as compared to other sources of radiation. It is generally accepted that a laser source of at least 10 mW power is necessary for routine Raman spectroscopy. Helium-neon and ruby lasers provide an intense stable source of red light, especially useful in studying coloured materials. The ionized inert gas /especially argon/ lasers and some solid state lasers offer higher power /up to 1 watt/ in the green-blue region. For wide selection of wave lenghts mixed gas lasers /krypton-argon/ are applied.

Almost every laser Raman instrument seems to have its own unique sampling system and pre-slit optics. However, the basic requirements are the same in each case: to illuminate the sample in such a way that an acceptable image is produced and passed efficiently to the entrance slit of the monochromator. By focussing the laser beam an extremely high flux density can be created in the sample and the volume of the substance required for the investigation is very small.

Since the intensities of Raman bands are very weak relative to the radiation at the exciting frequency ν_0 and the band positions are close to it in frequency, it is essential to use a monochromator system with very high resolution. This is why almost all currently available laser Raman spectrometers incorporate two or more monochromators. Commercially available spectrophotometers usually assure spectral resolution 0.1-0.3 cm^{-1} and wave number accuracy 0.5-1. cm^{-1}.

Photoelectric recording is achieved normally with the aid of low-noise, often cooled photomultiplier, amplification system /usually in photon-counting mode/ and millivolt chart recorder.

For polarization measurements Raman spectrometers are supplied with polarizers which transmit radiation with particular orientation of the electric vector. Using polarizer the intensity of scattered ligh with electric vector perpendicular /$I_\perp$/ or parallel /$I_\parallel$/ to the electric vector of the exciting radiation can be measured and the degree of depolarization can be calculated. Accurate experimental measurement of the degree of depolarization is possible for high-quality single crystals and some liquids, whereas, in samples with structural inhomogeneities the depolarization data tend to be inaccurate because of the depolarization of the exciting laser beam and the Raman radiation by multiple reflections.

The measurement of absolute intensities is a very complicated process and usually relative intensities of the Raman bands are measured. Appropriate reference bands are choosen either from the spectrum of the sample under investigation or from the spectrum of a standard compound added in small quantity to the sample.

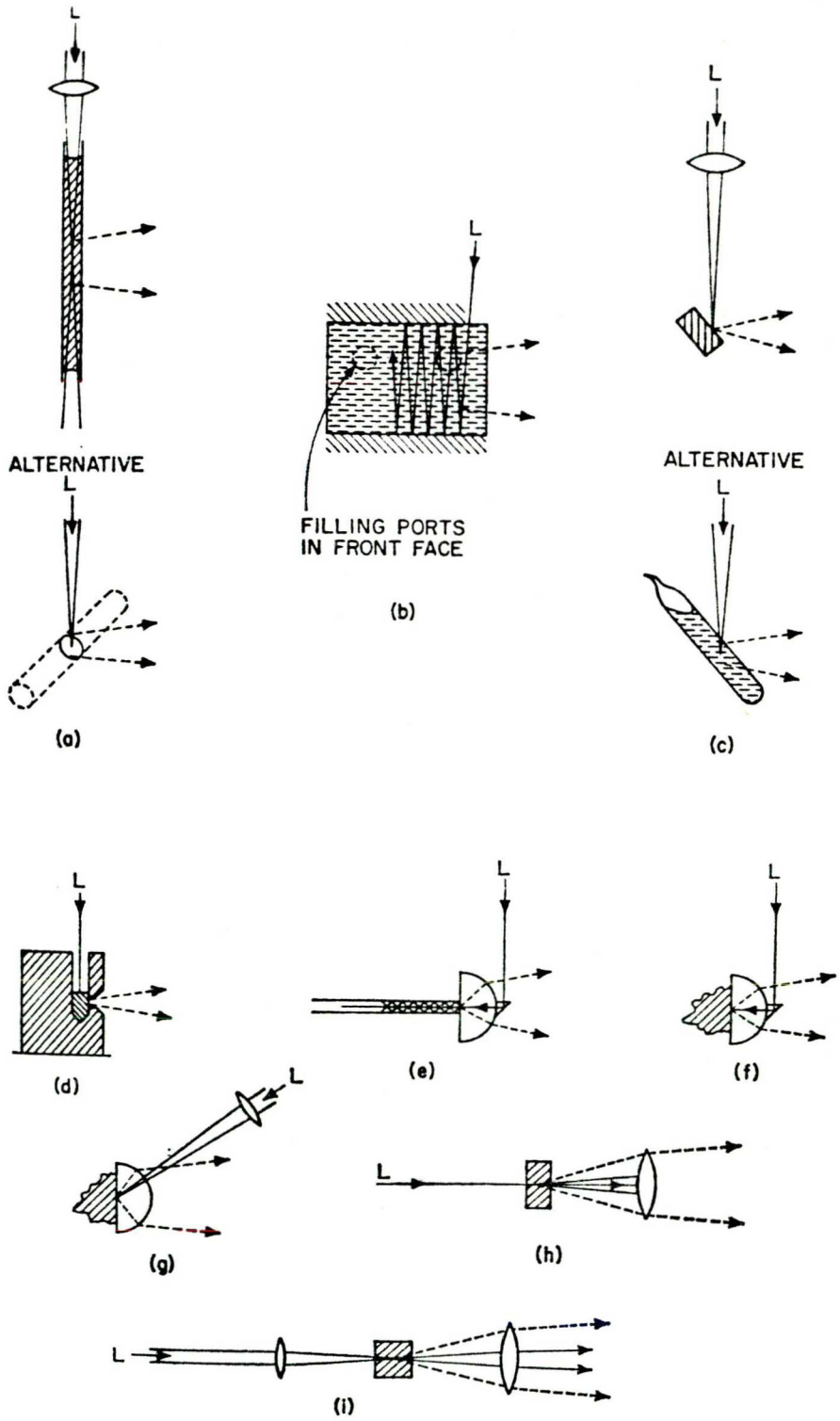

Fig. 4. Some of the sample arrangements found in laser Raman Spectrometers. L sifnigies the incoming laser beam, and the broken arrows indicate the rays proceeding to the monochromator. In cases /b/, /d/ and /h/ the laser need not be focused on the sample; in /e/ and /f/ a convergent beam is used. /from ref. 3/.

Usually no special sample preparation is required for Raman work. Depending on the amount of the substance and the aims of investigation, liquids can be placed in capillary tubes, ampoules, sample bottles and even flasks /Fig. 4/. Solid materials of suitable rigidity and size can be simply held in the laser beam in an appropriate orientation. Powders are usually contained in transparent vessels as for liquids, and one of the best methods is capillary tube. Single crystals can be easily mounted for Raman examination in the same fashion as for X-ray work. For photosensitive materials approperiate wavelength /usually red/ and appropriate laser power should be choosen. Care should be taken to free the sample from fluorescent impurities. In many cases the fluorescence can be reduced by prolonged exposure to the laser beam. Special sample holders and cuvettes have been constructed for Raman work at high pressure, different temperatures, kinetic studies, etc. Detailed information on the techniques used in Raman spectroscopy can be found in a number of text books and reviews /1, 3, 8, 9/.

It should be emphasized that an advantage of Raman spectroscopy is that practically samples in any state can be investigated and no perturbation occurs in the natural state of the system. Unlike in IR absorption the water content of the sample does not limit the application of Raman spectroscopy.

II. RAMAN SPECTROSCOPY OF BIOLOGICAL MEMBRANES

II. 1. Structure of biological membranes

The central task of research on membrane structure and its correlation with physiological and biochemical functions is to determine the organization principles for the constituent molecules, lipids and proteins, which endow the biological membranes with unique functional features, qualitatively different from the simple sum of its parts. The organization of proteins in a lipid bilayer lends itself to several possibilities and therefore, to considerable speculation in terms of membrane models. It must be pointed out that most membrane models are not mutually exclusive, they seem rather to emphasize the different aspects of membrane organization /for reviews see 11-15 and ref. therein/.

Gorter and Grendel were the first to suggest the existence of a lipid bilayer structure in biomembranes, which was confirmed later by a large number of physical and physico-chemical techniques. Inability of a simple lipid bilayer structure to account for a variety of biomembrane characteristics led to numerous modifications of the basic bilayer model, introducing layers of adsorbed proteins /Dawson - Danielli mode, Fig. 5A/ on the both sides of the lipid bilayer, "pores" or "active regions", selective carriers embedded, etc. The polar interactions were considered the predominant mode of binding proteins to lipid, though some hydrophobic interactions and partial or total penetration of protein into the bilayer were not excluded.

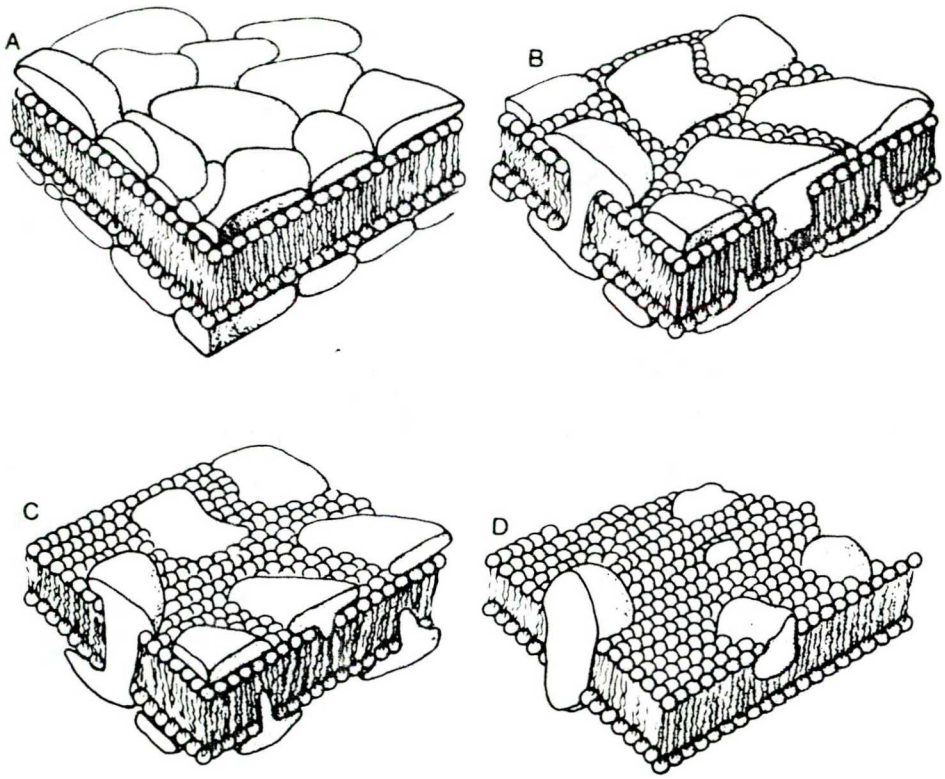

Fig. 5.

Diagramatic representation of possible molecular arrangements of proteins and phospholipids in the cell membrane. The small circles and connected wavy lines represent a phospholipid bilayer. The amorphous structures on the outer surfaces, and in some cases, penetrating the bilayer represent proteins /from R.W. Hendler /1974/ in "Biomembranes" vol. 5. /L.A. Manson ed./ pp. 251-273.

Some quantitative discrepancies of the lipid bilayer hypothesis and specialized functions of the biomembranes could be explained only by the presence of proteins embedded in the lipid bilayer. A large number of models tried to visualize the orientation of proteins into lipids. These models, generally speaking, range from proteins dipped in the lipid matrix to lipid embedded in a protein matrix, the organization features depending on the biochemical function of a particular membrane /Fig. 5, B and C/. The importance of hydrophobic interactions for stabilizing the lipid-protein association and existence of hydrophilic regions in the proteins for the passage of polar solutes was suggested by several authors /"iceberg" models/. Others emphasized higher proportion, asymmetric distribution, specific interactions and association of proteins /"protein crystal" models/. Lipoprotein subunit organization of the membranes was suggested accounting for allosteric interactions, that is, transfer of information over long distances.

Further development of membrane models was made by Lenard, Singer and Nicolson /"fluid mosaic" model, Fig. 5D/. They visualized membrane proteins as globular and folded up so as to be amphipatic, their hydrophobic end embedded in the interior of the lipid bilayer, while the hydrophilic end would project out into the aqueous medium. This model emphasized the balance between the structural organization and the fluid disorder of membrane lipids and proteins. It postulates that some membrane proteins in order to perform their functions must be free to rotate within their lipid matrix and to move in the plane of the membrane. So the basic assumption implicit in the fluid-mosaic model is, that there is little or no specificity of lateral intermolecular interactions among membrane compounds, especially lipids, and that they are randomly distributed in the plane of the membrane. However, experimental evidence which has

accumulated in the last decade suggests clustering of membrane proteins, phase separation of lipids and association of proteins with specific lipid coat of functional importance, which all may have yet unappreciated functional significance. A considerable amount of work has been done in the past few years to understand the non-covalent interactions among various membrane components and the heterogeneity of biomembrane organization. However, since the clustering and associations are based on weak interactions, none of the teqchniques available thus far are capable of providing unambiguous evidence for their existance. The use of molecular probes in membranes, generally speaking would tend to disrupt the weak interactions leading to the ordering of the components in biomembranes. For these reasons it is important to look for techniques to investigate the alignment of membrane constituents at the molecular level, without altering the natural state of the membrane. Recently, laser Raman spectroscopy has been applied with increasing success in the membrane research, providing a powerful method for studying lipid-protein assemblies in aqueous environment.

II. 2. Raman spectroscopy of the main membrane constituents

The main experimental approach in the Raman studies of complex biological macromolecules is the investigation of the so-called "group-frequencies" and the spectral changes with changing molecular environment and conformation.

The spectra of the molecules containing the same characteristic groups of atoms or bonds often show certain common or slightly shifted frequencies, termed characteristic group frequencies. The main technique of this method calls for a systematic examination of large classes of compounds with progressively increasing complexity of molecular structure. These structural elements, whose presence in a molecule produces a stable persistent series of characteristic structural lines, may be referred to as characteristic structural elements. The spectra of complex polyatomic molecules with several characteristic structural elements are often formed by additive superposition of the spectra of the individual structural elements. In some cases a complex "interaction" breaks the additivity and the molecules contain a dominant characteristic structural element, whose presence determines the main features of the Raman spectrum. Since every characteristic structural element is a constituent of the molecule, its vibrations strictly speaking, are the vibrations of the entire molecule. Therefore, any change in molecular structure is reflected to a certain extent in the parameters of the characteristic lines.

The fundamental difficulty in interpretation of the Raman spectra of biological macromolecules is, that, often several characteristic elements give contribution to the same narrow spectral region, which is difficult to ascribe to any particular group. In some cases it is useful for band assignment to prepare oriented samples from biological macromolecules by drawing fibers and to examine the Raman-band polarization. Hydrogen-deuterium exchange studies as well help in band assignment and evaluation of the contributions of different atomic groups to the Raman spectrum.

In the following the results from Raman studies of biologically important molecules and systems are briefly summarized.

II. 2. A. Lipids

Thermodynamic considerations as well as physico-chemical evidence show rather convincingly that molecules of amphypathic lipids dispersed in a high enough concentration in an aqueous medium tend to aggregate to a bilayer structure with the hydrocarbon chains pointing inward and the polar heads facing the water. There is a more or less stiff region of the hydrocarbon chains near the polar heads and a region with gradually increasing flexibility towards the center of the bilayer. The thickness of the bilayer depends on the repulsive forces between the two planes of lipid polar heads, hydration, presence of electrolites and other solutes in the bathing solution, etc. The lateral packing of the lipids in the bilayer depends primarily upon the branching and the degree of unsaturation of the fatty acid residues and presence of non-polar lipids. The most profound changes in the physical properties of lipids occur during temperature- or ion-induced phase transitions from gel to liquid crystalline state, during which so-called "melting" or disordering of the hydrocarbon chains occurs /16-18/.

In biological membranes lipids provide more than a suitable, inert matrix, in which the proteins are embedded. In last few years evidence has been gained that the physical state of the lipid has marked impact on the activity of the membrane-bound proteins by influencing or determining their tertiary or quaternary structure and, in turn, that the proteins affect the state of the surrounding lipids /19-21/.

First Raman studies of simple model systems /23, 25, 27, 32/ and biologically important lipids /22, 24, 26/ had shown the existence of several spectral regions sensitive

to the conformation, motion, molecular packing and immediate environments of the hydrocarbon moiety of the lipids/Fig.6/. The spctral regions most frequently used for monitoring the state of the hydrocarbon chains in lipids are around 1100 cm^{-1} and 2900 cm^{-1}. In the region 1000 - 1140 cm^{-1} the peaks were assigned to skeletal optical modes of the acyl chains /22, 24, 28/. The two intense bands at 1066 and 1128 cm^{-1} are C-C stretching vibrations of the rigid chains in all-*trans* configuration and they dominate in ordered state of lipid systems. The band at about 1090 cm^{-1} increases its intensity upon disordering of the system and appearance of gauche rotations in the hydrocarbon chains /Fig. 7 /. The C-C stretches being extremely delocalized over the hydrocarbon chains provide information on the intrachain conformation /64/. The delocalization is reduced by the appearance of gauche conformers upon disordering of the system which is manifested in the Raman spectra of lipids in frequency shift and collapse of the above three bands in this region towards a broad central maximum at ab out 1100 cm^{-1}.

The bands at about 2900 cm^{-1} have been assigned to C-H stretching vibrations of the hydrocarbon chains /25, 26, 28, 61/. The C-H stretches are not strongly coupled to the chain but are particularly sensitive to interchain or lateral interactions in the bilayer /64/. Experimental observations have shown that the band at 2850 cm^{-1} /CH_2 symmetric stretch/ dominates in the disordered state, whereas, that at 2880 cm^{-1} /CH_2 antisymmetric stretch/ is peculiar to the crystalline state of the lipids. The intensities of the 2930 cm^{-1} and 2960 cm^{-1} bands depend on the polarity of the chain environment /27, 36, 49/.

Detailed assignment of the Raman bands of dipalmitoyl phosphatidyl choline will be discussed later.

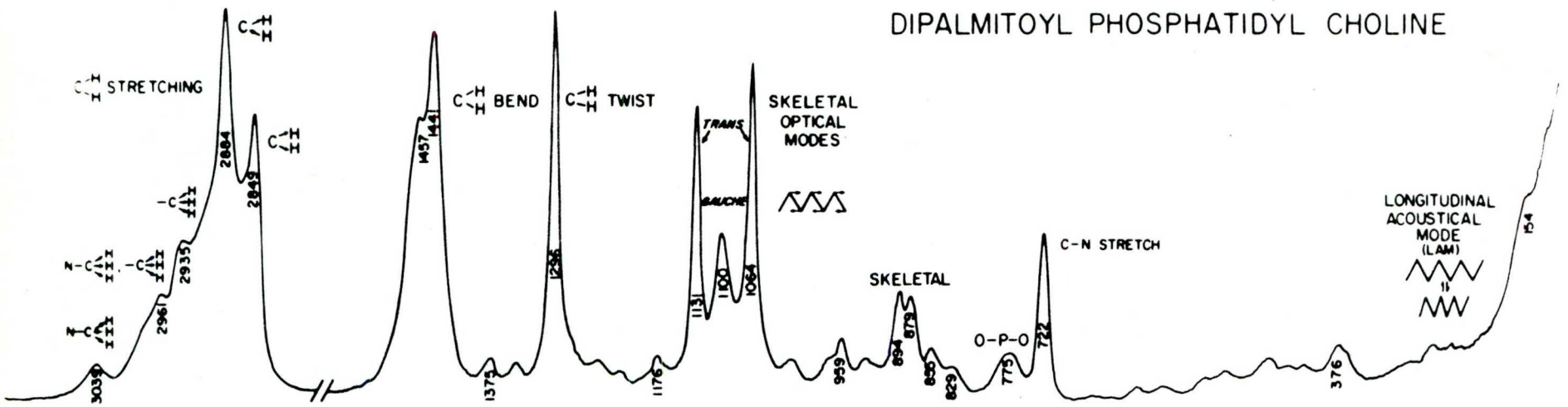

Fig. 6.

Raman spectrum and band assignment of solid dipalmitoyl phosphatidylcholine /from. ref. 43/

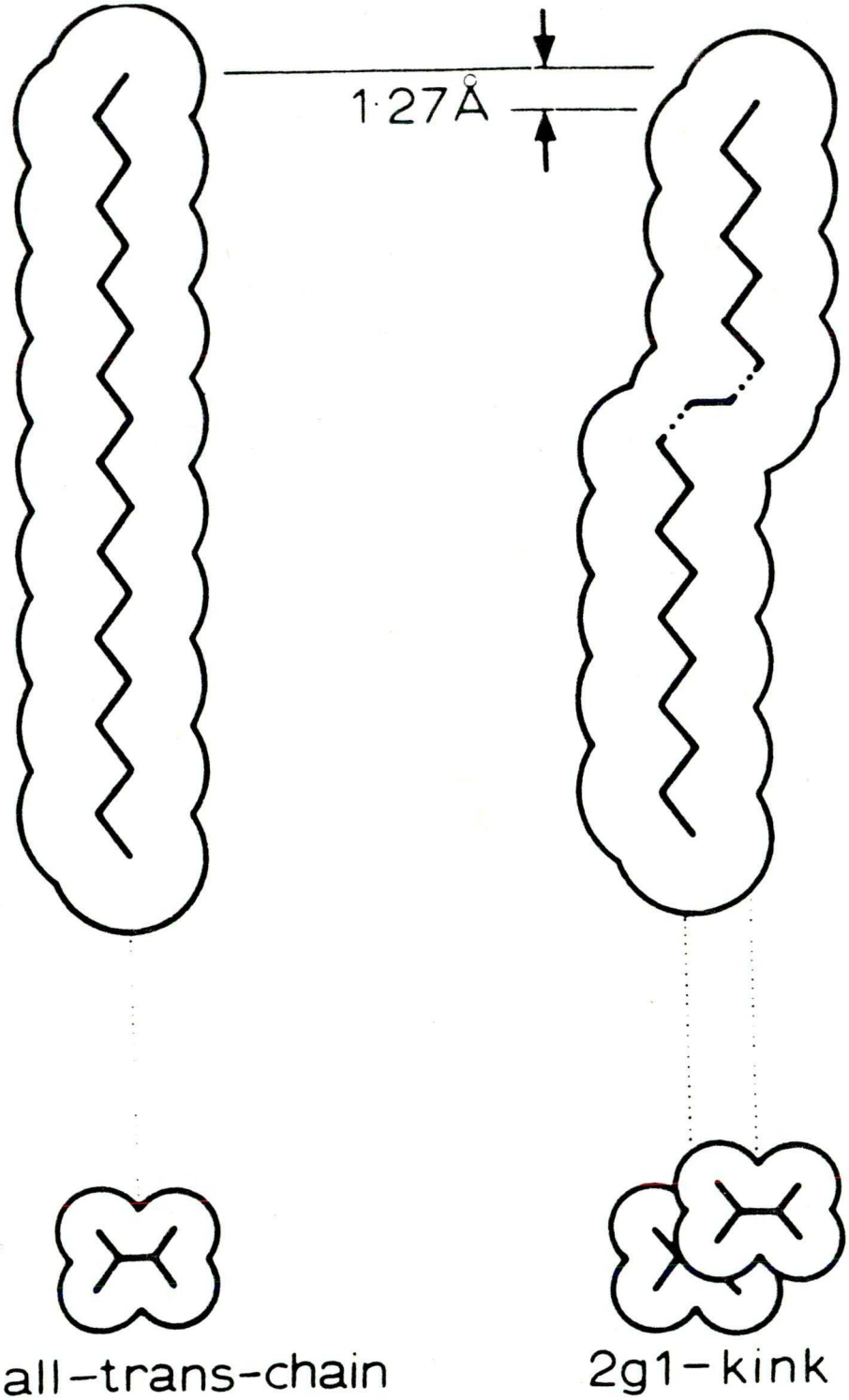

Fig. 7.

The formation of a 2g1-kink in a fatty acid chain /from G. Lagaly and A. Weiss /1971/ Angew. Chem. internatl. Edit. 10, 558/.

In spite of the complicated structure of the C-C and C-H stretching spectral regions and some difficulties in band assignments, the changes in relative intensities /22--34/ and frequency shifts /35/ of the Raman bands have been correlated with altering conformation, interactions and environment of the hydrocarbon chains and widely used to monitor the structure of the lipid bilayer.

Raman spectroscopy has been applied to study the polymorphism of the lipid-water systems and proved to be extremely sensitive to the structure of the mesophase /25, 27, 33/.

It was also possible to reveal by Raman spectroscopy that lipid vesicle curvature causes alterations in the packing arrangement of lipids and increases *trans*-gauche isomaerization as compared to the planar multilayers /31, 40/.

Phase transitions have been extensively investigated in pure lipids and lipid mixtures and the cooperativity of the process could be estimated from Raman spectroscopic data /22-24, 26, 35, 44/. The values of the transition temperatures obtained by Raman spectroscopy are in a good agreement with those provided by other techniques. Recently Raman difference spectroscopy has been applied in studies of lipid phase transitions showing details of Raman spectral changes with greater clarity than the conventional Raman technique since only perturbed Raman bands are observed in the difference spectra and the invariant bands are missing /53,54/. Some thermodynamic parameters connected with the phase-transitions and the onset of the hydrocarbon chain trans-gauche isomerization at low temperatures were obtained from Raman spectroscopy /44, 50, 51/.

Attempts were made to investigate ordered samples of fatty acids, which were suggested to be a useful refer-

ence in quantitative studies of the packing order in lipid phases /47/.

Theoretically order parameters were introduced recently as a quantitative molecular interpretation of the spectral events accompanying conformational changes /43/.

Besides the most widely studied lipids - diacyllecithins, Raman spectra were obtained from dietherlecithins /62/, triglicerides/88/, sphingomyelin/30,60/, phosphatidyiethanolamine /24,26,30,59/ and cholesterol/22,46/. Among the lipid mixtures special attention was paid to lecithin-cholesterol complex. The mechanism of the cholesterol action on the bilayer structure - abolishing the phase transition cooperativity, fluidizing the lipids in gel state and rigidifying them in the liquid crystalline state,was suggested on the basis ofRaman data /22,24,34,35,37,46/. Especially useful in Raman studies of complex lipid mixtures and biomembranes as non-perturbing probes, are deuterated phospholipids /39, 52, 58, 59/. They form a thermodynamically ideal mixture with the normal phospholipids and, therefore, do not perturb the structure of the bilayer. However, the influence of the deuteration itself on the bilayer is not yet completely understood and caution is necessary in the interpretation of results obtained with isotopically labelled compounds /56/.

The spectral changes in the conformational sensitive regions in the Raman spectra of lipids were used in numerous studies of lipid interactions with biologically important substances as ions /29/, antibiotics /38, 42, 57/, hydrocarbons /45/, polypeptides /63/ and aminoacids /63/.

In the last years some Raman studies appeared on the conformation of the lipid polar heads /65/, although IR spectroscopy is more suitable for this purpose /66-68/.

II. 2. B. Proteins

Although proteins represent usually more than a half of the total membrane weight, no general pattern of their organization in membrane appears to exist. Various optical methods have shown the proteins to be 30-50 % in the α-helical configuration, with a predominance of random-coil arrangement in the rest. Membrane proteins are now generally assumed to be of two types - peripheral and the integral proteins. Peripheral proteins are thought to blanket the surface of the membrane and are mostly water-soluble. Integral proteins, on the other hand, are embedded to a greater or lesser degree in the lipid continuum and may span the entire thickness of the membrane.

It is now well established that laser Raman spectroscopy is a powerful technique to investigate the structure of proteins, since one can either study their conformations by non-resonance Raman scattering, or probe their chromophoric sites by resonance Raman scattering /for review see 69-72 and ref. therein/. The obvious advantage of this technique is the possibility to investigate the structure of a protein in vivo.

A peptide bond gives rise to many different types of vibrational modes. Among them Amide I and Amide III yield very prominent Raman bands which are correlated with the structural properties of protein molecules /Fig. 8/. Both Amide I and Amide III bands arise from in-plane vibrations of the peptide bond. From the Raman spectra of model compounds /different polypeptides / it has been established that α-helical structure generate and Amide I bands at 1650 $\pm$5 cm^{-1} with strong intensity and sharp peak. The β-sheet structure also generate a strong and sharp Amide I

Fig. 8.

One possible correlation of /a/ the structurally distinct subregions of myosin, /b/ their proposed conformational structures, and /c/ the Raman spectrum of the Amide III region of myosin .
/from E.B. Carew, I.M. Asher and H.E. Stanley /1975/

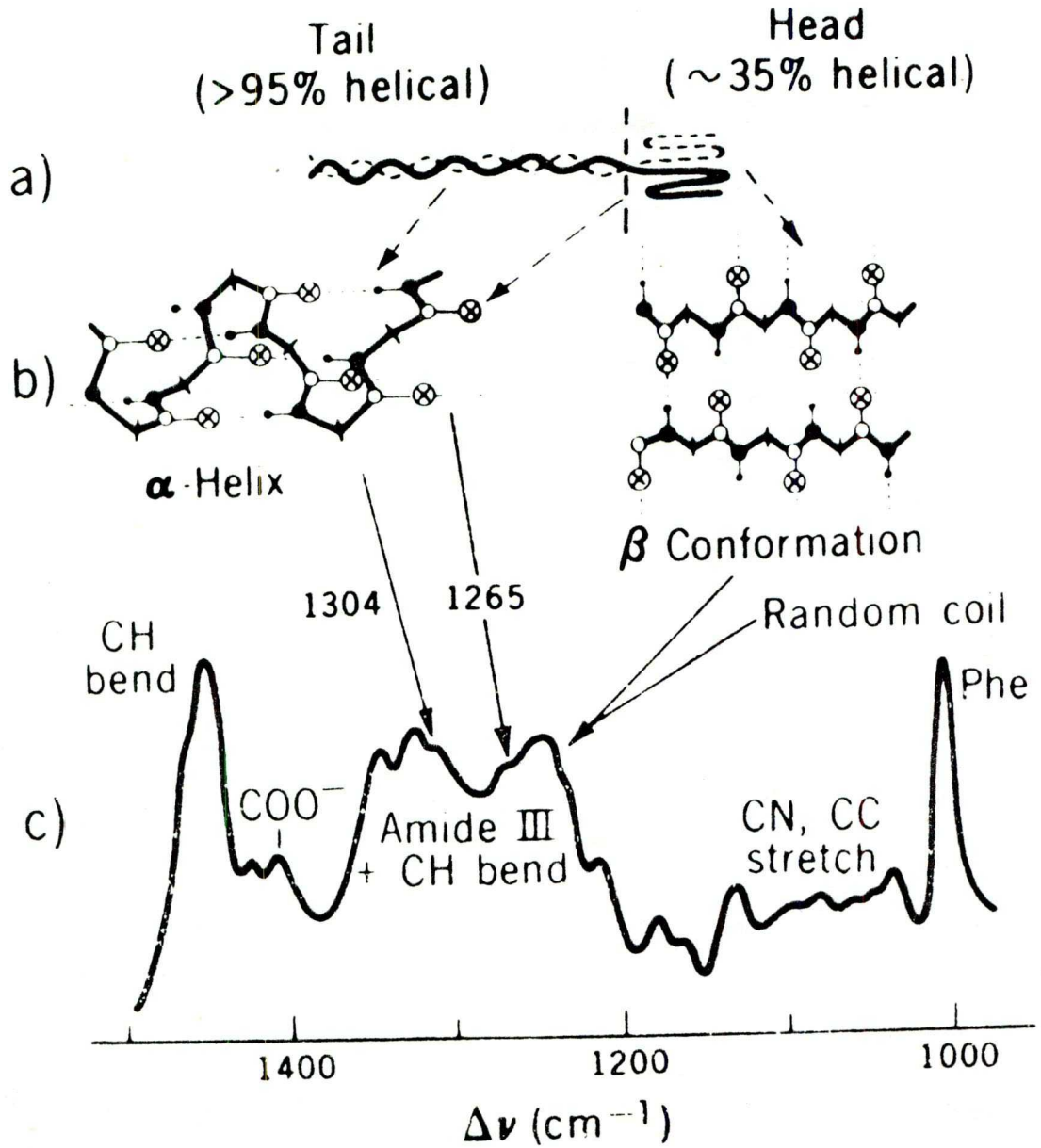
Tail
(>95% helical)
Head
(~35% helical)
a)
b)
α-Helix
β Conformation
1304
1265
Random coil
CH
bend
Phe
c)
COO⁻
Amide III
+ CH bend
CN, CC
stretch
1400
1200
1000
Δν (cm⁻¹)

line but at higher frequency of 1665 ± 5 cm^{-1}. Random coiled proteins usually yield a strong but broad Amide I band at about 1665 cm^{-1}.

For the Amide III band α-helical structures usually show a relatively weak band in the region of 1265 to 1300 cm^{-1}, while β-sheet structures show a strong line at 1235 ± 5 cm^{-1}. Random coil structuregives a medium intensity line at 1248 ± 10 cm^{-1}..

The presence and conformation of disulfide bonds can also be detected by Raman spectroscopy. Gauche - G - G shows a strong and sharp band at 510 cm^{-1}, the trans- G - G and T - G - T give bands at 525 and 540 nm^{-1}, respectively.

Raman spectroscopy provides infromation as well on the environment of side chains such as tyrosine, tryptophan and methionyne.

Laser Raman spectroscopy has been applied to the study of various polypeptide and proteins, for example Bovine serum albumine, snake toxins, myosine, ribonucleases, -lactoglobulin etc. The influence of different ions, pH, temperature has been monitored by the changes of the conformational sensitive Raman bands. Information on the peptide backbone structure under different conditions, disulfide bonds, denaturation mechanisms has been obtained from these studies.

In biological macromolecules the sites of physiological importance usually contain a chromophore such as haems, flavins or methal ions, hence the potential importance of Resonance Raman /RR/ spectroscopy is obvious. In the RR scattering only these vibrations are enhanced which are coupled to the resonant electronic transition. This allowes selective enhancement of the vibrations of different chromophores and is a sensitive probe of their conformation and local environment.

In studies of the visual pigments the resonance enhancement of the chromophore vibrations without enhacing the protein vibrations allowed to obtain the vibrational spectra of the chromophore in different bleaching intermediates. Each isomer is characterized by a specific intensity pattern serving as a "fingerprint". The resulting spectra contain important information about the conformation of the chromophore and its interaction with the opsin.

Heme proteins contain iron-porphyrin as the active group. These classes include such important proteins as hemoglobin, cytochromes and oxidases. RR studies of porphyrins provide an important correlation between the vibration frequencies and the oxidation and spin states of the central metal. Identification of the spin and oxidation state markers can help in understanding the detailed function of the heme system in heme proteins. In systems containing more than one heme selective enhancement of the vibrations of different hemes could be obtained. The main point that emerges from all these studies is the great usefulness of the RR technique in detailed studies of large multi-component biological systems that can hardly be studied by other approaches. In studies of enzymatic reactions RR spectroscopy can provide detailed information about the substrates inside the enzyme active site and thus, contribute to the understanding of the factors that determine the catalytic activity of the enzymes. For the investigation of biological systems which do not possess natural chromophores in their active site RR label technique has been developed /73/. This technique is analogous to the spin label method used in ESR spectroscopy. It consists of introducing into the molecule being studied a chemical grouping chosen to become an intrinsic part of the interaction under study and to yield a RR spectrum. Information can be obtained that relates specifically to the label and its environment.

II. 3. Raman spectroscopy of reconstituted system, isolated membranes and intact tissues

Recently attempts have been made to investigate the structure of lipids and proteins in isolated membranes, as well as the interactions between these components by Raman spectroscopy /89/.

These studies have been preceded by extensive experimental and theoretical examinations of the main membrane components and various lipid-protein model systems.

The characterization of the protein-lipid interaction is essential to the study of biomembranes and lipoprotein complexes. The lipid-protein interaction can be modeled by interactions between lipids and protein subunits such as polypeptides and amino acids. Using the information from the conformational-sensitive areas of the lipid Raman spectra it was shown /80/ that the amino acid-lipid interaction is highly specific and lacks any simple correlation with amino acid polarity. The lipid-polypeptide interactions were found to cause conformation changes in the hydrocarbon chains, probably arising from interactions between the phospholipid head group and the polypeptides /80/.
It has been proved by laser Raman spectroscopy /81/ that intrinsic, extrinsic and plasma proteins produced different changes in the lipid hydrocarbon C-H stretch Raman modes. The interaction of these three types of proteins can thus be used to define the interactions of proteins of unknown type on the bases of the changes in the Raman spectra of lipids. Raman studies on lipid-protein systems /85/ provide evidence for the existance of a "boundary layer" of partially immobilized lipid around membrane proteins and that the proteins tend to "buffer" membrane fluidity and to reduce the cooperativity of acyl chain transitions.

In the Raman spectra of isolated membranes the phospholipid structural information is contained primarily in the 1000-1200 cm^{-1} region, while evidence of the protein secondary structure is found in the Amid III region at 1250-1300 cm^{-1}. The CH_2 regions are complicated by contributions from both protein and phospholipid and so are difficult to interpret. By comparison of the conformation sensitive regions in the Raman spectra of isolated membranes and those of model lipid and protein systems, the percentage of all-*trans* configuration of the lipid n.c. chains and the relative amount of different protein structures in the membrane can be calculated.

As suggested by several authors /76, 77, 79/ resonance enhanced Raman bands of membrane carotenoids which are sensitive to carotenoid configuration and environment, can be used as sensitive natural Raman-active probes of membrane structure.

Well resolved Raman spectra were obtained from hemoglobin-free erythrocyte ghosts /74, 79, 83/, sarcoplasmic reticulum /77/, thymocyte plasma membranes /75, 78/. The thermotropism of thymosite plasma membranes /75/ and erythrocyte membranes /79/ has been investigated and on the bases of comparison with model system, conclusions about the cooperativity and role of the membrane proteins in the phase transitions have been reached.

Raman spectroscopy has been successfully applied in the studies of virus structure /82, 86/ and intact systems like single muscle fiber /84/ and living lenses /87/.

III. MATERIALS AND METHODS

III. 1. Chemicals

High purity synthetic β,γ-dipalmitoyl-DL-α- phosphatidylcholine /DPPC/, exhibiting a single spot in thin layer chromatography, was purchased from Fluka A.G. /Switzerland/ and was used without further purification. Aqueous solutions containing analytical-grade purity salts /Reanal, Hungary/, were made in tridistilled water.

III. 2. Sample preparation

Several membrane model systems from phospholipids have been developed and applied to model different membrane processes: hydrated smectic mesophase, isolated bimolecular membranes /BLM/, monolayers /90/. Lipid-water multilamellar dispersions are considered to be a suitable model for various structural investigations. Lipid molecules form planar bilayers separated by layers of water. The thickness of the aqueous layers depends on the lipid-water ratio. The polar groups of the lipids face the aqueous phase and can interact with the solutes present in it. This system was chosen in our investigations since it provides a suitable lipid concentration in the sample and does not require sonication as the preparation of lipid vesicles, which may influence the structure of the bilayer /31, 40, 43/.

Lipid multilamellar systems were prepared by mixing dry dipalmitoyl phosphtidylcholine /usually about 5 mg/ with aqueous solutions /added by a microsyringe/, in 1:4 weight ratio of lipid-to-water.

The samples were stirred thoroughly and left to swell for 2 hrs at 55°C /above the phase transition tempera-

ture of dipalmitoyl phosphatidylcholine/ to achieve homogenization. Anhydrous samples were dried at 60°C under vacuum for 48 hrs over P_2O_5. After preparation the samples were sealed in capillary tubes with an inner diameter of 1 mm.

III. 3. Raman experiment

Raman spectra were recorded with a Cary 82 Raman spectrophotometer with a Spectra Physics 164 argon ion laser operating at 448 nm with a typical power of 500 mW. The optical diagram of the Cary 82 Raman spectrometer is shown in Fig. 9.

The samples sealed in capillaries were illuminated at right angle to the tube axis. Scattered light was collected at right angles to both the incident light beam and the capillary axis /Fig. 4a/.

The scan speed was usually 0.4 $cm^{-1}.sec^{-1}$ and the count rate was between 1000 and 15000 $counts.sec^{-1}$ full scale. All spectra were obtained with a band pass of 4 cm^{-1}.

All the measurements were carried out at room temperature.

The Raman band intensities were judged by peak heights, measured from a base line determined individually for each spectrum. Two-three independent sample preparations were made for each system studied and at least three spectra were taken of every sample. The numerical data are averages of at least 6 measurements. The standard error of the mean of all intensity ration was 0.02. According to /43/ the usage of the bands' area instead of the peaks' intensities does not result in any substantial reduction in the scattering of the data.

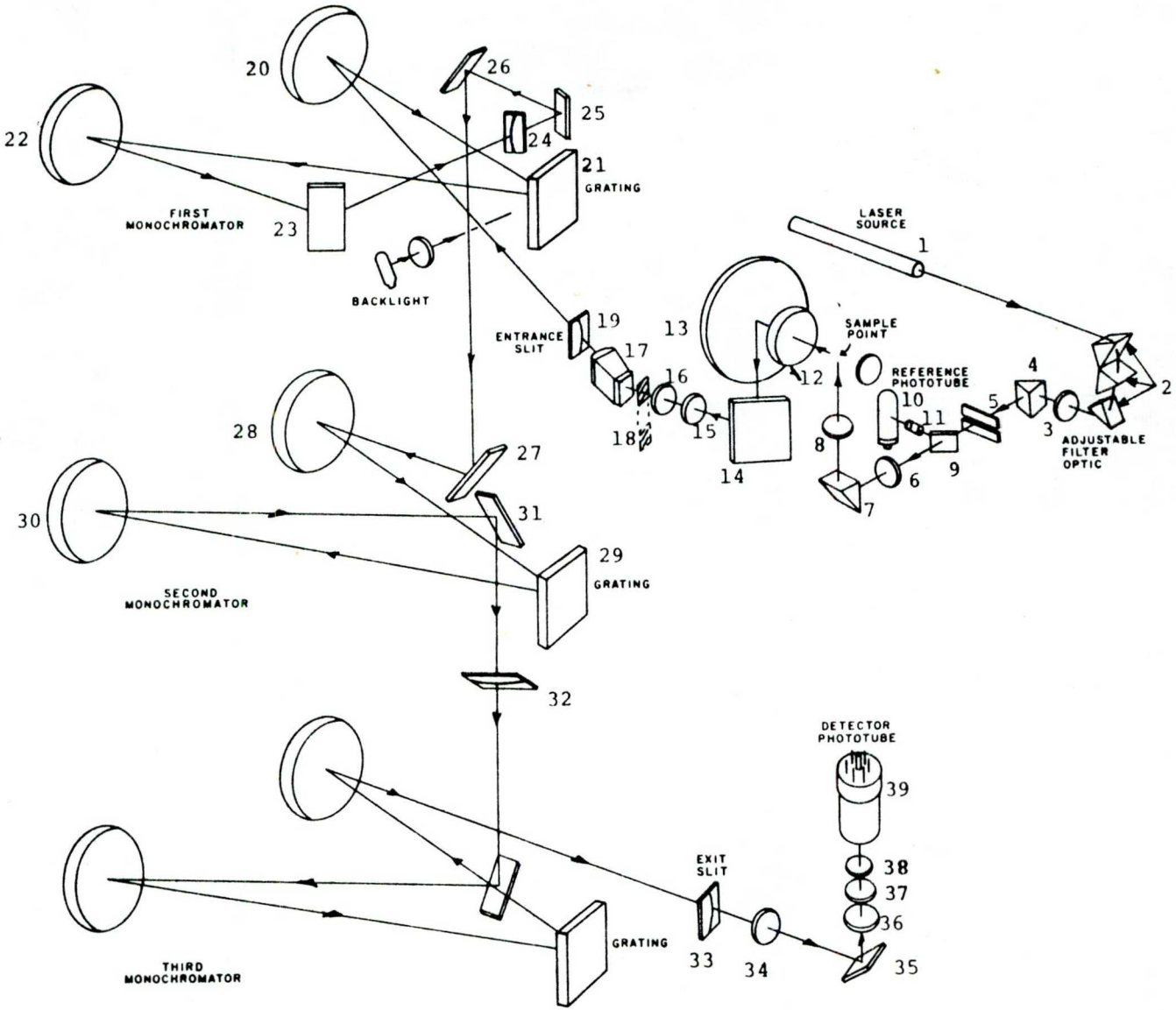

Fig. 9.

Optical diagram of Cary 82 Raman spectrometer.

IV. RESULTS AND DISCUSSION

IV. 1. Qualitative features of the Raman spectra of phospholipids

In general the Raman spectrum of a phospholipid is dominated by vibrations of the fatty acid chains with superposition of a few bands from the head group. The dominant features of a phospholipid spectrum are depicted on Fig. 6. Comparative Raman spectra of solid dipalmitoyl phosphatidylcholine/DPPC/ and DPPC-water dispersion /1:4 w/w/ are presented on Fig. 10. In what follows the Raman bands of DPPC are described in terms of their origin and conformation sensitivity.

40 - 400 cm^{-1} region

The vibrations in this region in the Raman spectra of lipids have been assigned mainly to acoustical, accordian-like stretches of the whole molecule /22, 26/. Investigations of different hydrocarbons andfatty acids /23, 32/ have shown that the frequencies of acoustical vibrations are chain-length dependent. In complex lipid molecules the low-frequency vibrations are sensitive to particular details of chain packing /26/ and provide information on the length of the all-*trans* segments in the lipid hydrocarbon region /30,43/. According to some authors, several weak bands in the low-frequency region arise from skeletal deformations of the polar head as well /65/. However, the usage of this region for structural investigations is hampered by the low intensity of the acoustical spectral bands.

720 - 1050 cm^{-1} region

Several bands originating from the polar head vibrations

Fig. 10.

Laser Raman spectra of dipalmitoyl phosphatidyl-choline.

a/ crystalline

b/ DPPC:H_2O - 1:4 w/w at room temperature

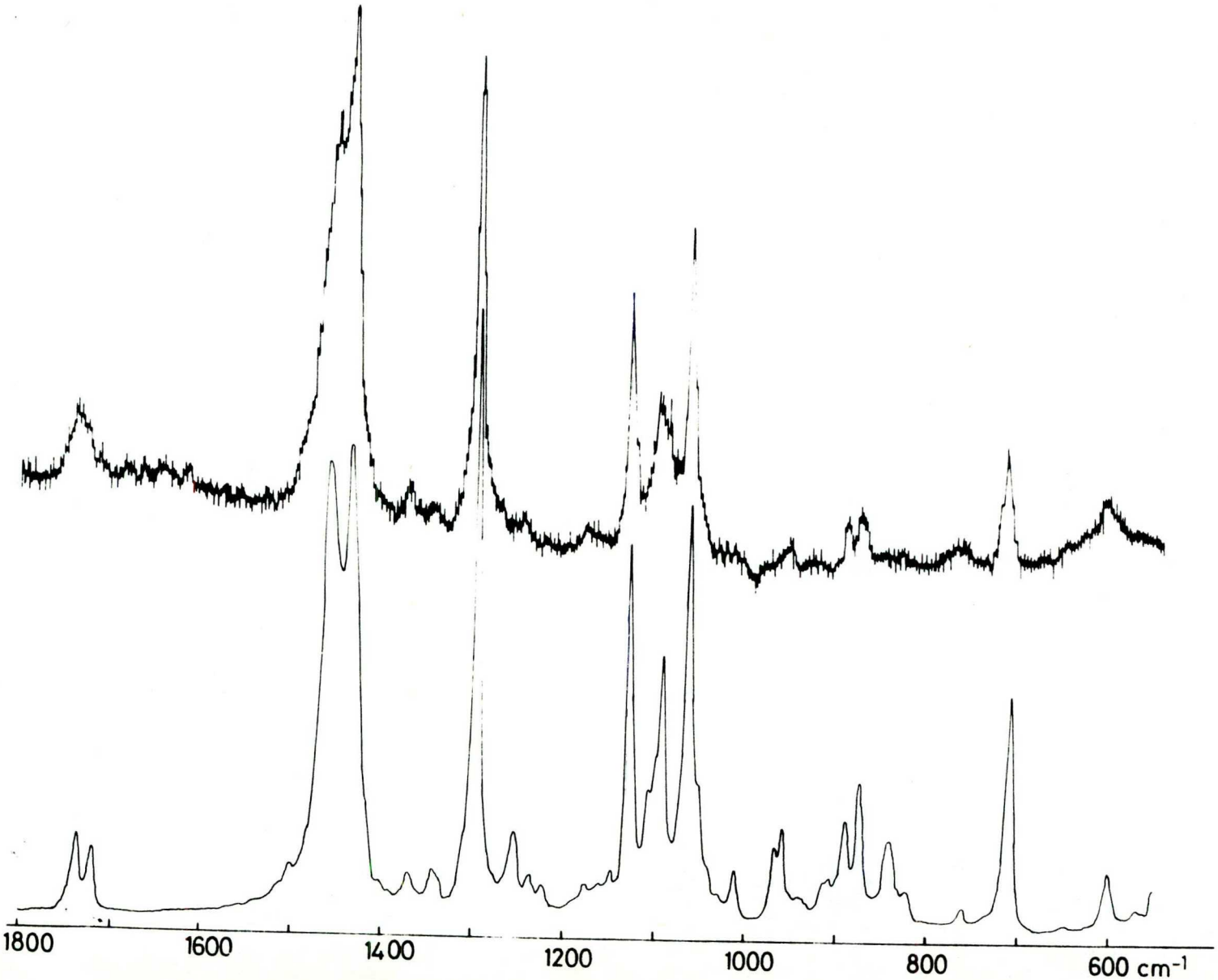
1800
1600
1400
1200
1000
800
600 cm-1

are observed in this region.

The most intense band at about 712 cm^{-1} has been assigned to the symmetrical C -N stretch of the choline group /24, 26/. The band is strongly polarized and shows nearly tetrahedral structure of the choline group /28/. Upon hydration the band shifts slightly towards higher frequencies in comparison to the anhydrous crystal. The band is a temperature invariant and is often used as an internal standart for measuring peak intensities in studies of lipid thermotropic behaviour /43, 53/.

Two weak bands at 763 cm^{-1} and 833 cm^{-1} have been assigned to O-P-O diester symmetric /26,28/ and antisymmetric /28/ stretches, respectively.

In the 800 - 900 cm^{-1} region weak bands originate from vibrations of the hydrocarbon chains as well.

The band at 872 cm^{-1} has been assigned to CH_2 deformational vibration /24/, while other authors attribute the bands in this region to skeletal vibrations of the hydrocarbon chains sensitive to the *trans*-gauche isomerization /26, 35/.

1050 - 1150 cm^{-1} region

As mentioned above this spectral region has been widely used for obtaining information on structural behaviour, particularly *trans*-gauche isomerization in lipids and membrane systems.

The bands at about 1063 cm^{-1} and 1128 cm^{-1} have been assigned to skeletal optical modes of the hydrocarbon chains with a motion such that alternate carbon atoms move in opposite directions along the chain axis /22, 24, 26, 28, 30/. Both vibrations are characteristic for the all-*trans*, fully

extended zig-zag conformation of highly ordered hydrocarbon chains and lose their intensity upon disordering of the system /22, 24, 63/. The 1063^{-1} band has been assigned to B_{Ig} vibrational mode /43/. The 1063 cm^{-1} feature is relatively pure stretching mode and although its intensity changes with temperature, no significant frequency shifts arise /26, 40, 51/. In gel state the 1063 cm^{-1} band is both chain length and temperature insensitive /22, 50/. The band at 1129 cm^{-1} has been assigned to A_g vibrational mode /43/. According to normal coordinate calculations in hydrocarbons this mode is coupled to a C-C-C · angle bending mode /40/, and/or to the acyl chain terminal methyl rocking mode /51/. Since the frequencies of the last two molecular motions depend on conformational rearrangements of the hydrocarbon chains, the C-C stretching coupled to them exhibits frequency shifts upont the structural changes in the system /50/.

The band at about 1100 cm^{-1} is a superposition of the C-C stretching modes of hydrocarbon chains in all-*trans* conformation /if the system is in gel or crystalline state/, the C-C modes of the hydrocarbon chains containing gauche bonds and the symmetric PO_2^- streching mode /28/. Some authors suggest as well contributions from methylene twist and wagg to the 1100 cm^{-1} band /53/. The band at 1100 cm^{-1} is characteristic for the liquid crystalline state of the hydrocarbon chains and increases its intensity upon disordering of the system and appearance of gauche conformers /22, 24, 28, 35/. The contributions from different vibrations forming the feature at 1100 cm^{-1} are briefly discussed, since its complexity has been the reason for certain confusion in the band assignment and interpretation of the experimental results.

The weak contribution to this region from the all-*trans* chains is highly chain-length /22, 49, 53/ and temperature /49/ dependent. It was suggested that it might be the k = 1 mode of the skeletal stretch at 1130 cm^{-1}/53/. The frequency of the PO_2^- symmetric stretch shifts downwards upon phase transition, probably because of the exposure of the phosphate group to aqueous environment /26/. The PO_2^- and all-*trans* C-C streching bands are not observable as distinct features in dipalmitoyl phosphatidyl choline Raman spectrum.

According to normal coordinate calculations on normal paraffines vibrations of hydrocabron chains containing gauche bonds should appear in the 1065 - 1100 cm^{-1} region /35/. The asymmetry of the 1080 cm^{-1} gauche band indicates that it is a composite of bands which arise from a variety of local gauche-type conformations /53/. The gauche band at about 1080 cm^{-1} is weak when a hydrocarbon chain contained gauche-bonds separated by long *trans* segments and gains intensity upon appearance of closely coupled gauche bonds /53/.

The overall behaviour of the 1100 cm^{-1} band in the Raman spectra of dipalmitoyl phosphatidylcholine is as follows: below the primary gel-liquid crystalline phase transition the 1090 - 1085 cm^{-1} gauche feature is weak and is partially obscured by the 1100 cm^{-1} all-*trans* C-C stretching mode, while above the phase transition the 1090 - 1085 cm^{-1} feature predomintes and has considerable intensity /50/. In DPPC a frequency shift of this band occurs from 1097 cm^{-1} in crystalline state to 1088 cm^{-1} in liquid crystalline state /35/. It was shown /51/ that the main contribution to the 1100 cm^{-1} band comes from the hydrocarbon chains. The contribution from the polar head has been considered constant with temperature /43, 50, 51/.

Taking into consideration the above assignment of the skeletal vibrations in the hydrocarbon chains, it is clear that the intensity ratios of either of the *trans* bands /1064 cm^{-1} or 1130 cm^{-1}/ to the gauche band /1100 cm^{-1}/ is a reliable measure of the degree of *trans* order in the hydrocarbon chains of phospholipids.

1200 - 1500 cm^{-1} region

The main bands in this region have been assigned to modes involving bending and rocking of the methylene groups /Fig. 11/ and all undergo sudden alterations in shape as the temperature of the system passes the melting point /26/.

The band at about 1298 cm^{-1} has been assigned to CH_2 twisting mode /24, 40, 53/. It shifts toward higher frequencies, broadens and decreases its intensity in comparison to 1438 cm^{-1} CH_2 deformational band upon disordering of the system caused by increased temperature /24/, and/or changes in the packing of lipid molecules /40/. The frequency shift of the 1296 cm^{-1} mode upon phase transition is consistent with a melted state conformation, containing a broad distribution of gauche rotamers. In this case the changed molecular symmetry activates a number of intense IR wagging modes near 1300 cm^{-1}. Some of this vibrations may enter into resonance with the Raman active twisting mode, perturbing the Raman band and shifting its frequency /53/.

The band at about 1450 cm^{-1} has been assigned to CH_2 deformational /bending/ modes /24, 26, 40, 49/. Below the phase transition temperature a strong band exists at 1440 cm^{-1} /A_g CH_2 bending/ and a shoulder at 1460 cm^{-1} /B_{3u} CH_2 bending/. Above the phase transition temperature a single peak at 1450 cm^{-1} appears as a consequence of changed selection rules in disordered hydrocarbon chains /26, 43/.

Fig. 11.

a/ Section of a polymethylene chain

b/ Vibrations of the methylene groups in the chain.

/from I. Fischmeister /1975/ Progr. Chem. Fats Other Lipids, 14, 91-162./

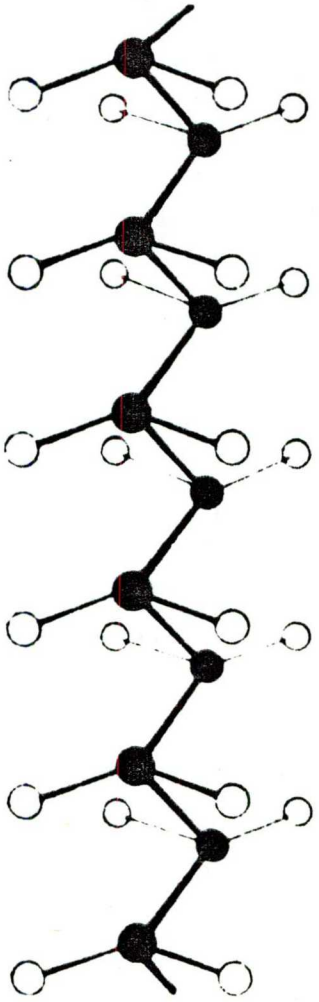

(a)

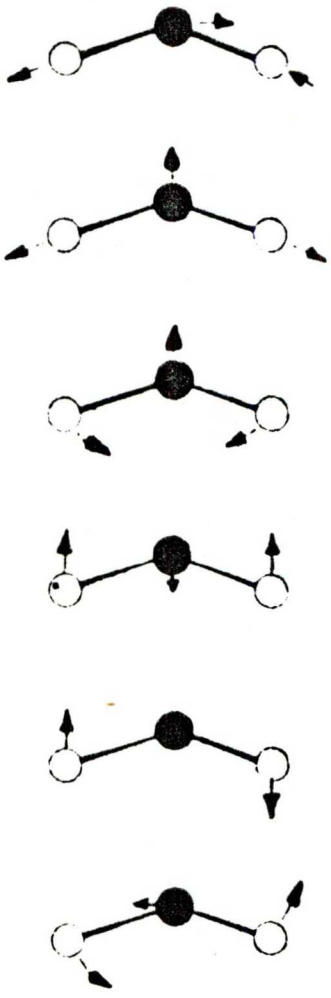
ASYMMETRIC
STRETCHING
SYMMETRIC
STRETCHING
DEFORMATION
WAGGING
TWISTING
ROCKING

(b)

The spectral changes in the 1450 cm^{-1} region appear to be related primarily to interchain interactions, though formation of chain rotamers as well affects the band /30, 40, 49, 55/. It was found that the band shape of 1450 cm^{-1} feature is sensitive to the packing of lipid molecules /25/ and to the radius of lipid bilayer curvature /40/. Selective deuteration of the hydrocarbon chains in lipids has shown that the head group methylene vibrations occur at 1451 cm^{-1} - higher than those of the acyl chain methylens /56/.

2800 - 3000 cm^{-1} region

Since the 2800 - 3000 cm^{-1} spectral region contains the most intense vibrations in the lipid spectrum, the C- H stretching modes are the most accessible for reflecting conformational changes under non-ideal conditions of small molecular perturbations, low lipid concentration, small sample size or high fluorescence background /52/. Moreover, it has been shown /25, 33/ that C-H vibrations are more sensitive than the C-C stretching region to differences in mesophase structure. A disadvantage arises, however, in that an overlapping of methyl and methylene modes from both lipid acyl chains and polar head groups contributes toward severely congesting this spectral area. In membrane bilayer systems containing other non-lipid components spectral contributions from the additional C-H containing moieties complicate the vibrational analysis and require an examination of the other parts of the spectrum. Considerable progress in the assignment of complex overlapping bands arising from the C-H vibrations in the Raman spectra of lipids has been achieved by using selectively deuterated fatty acids /39, 48/ and

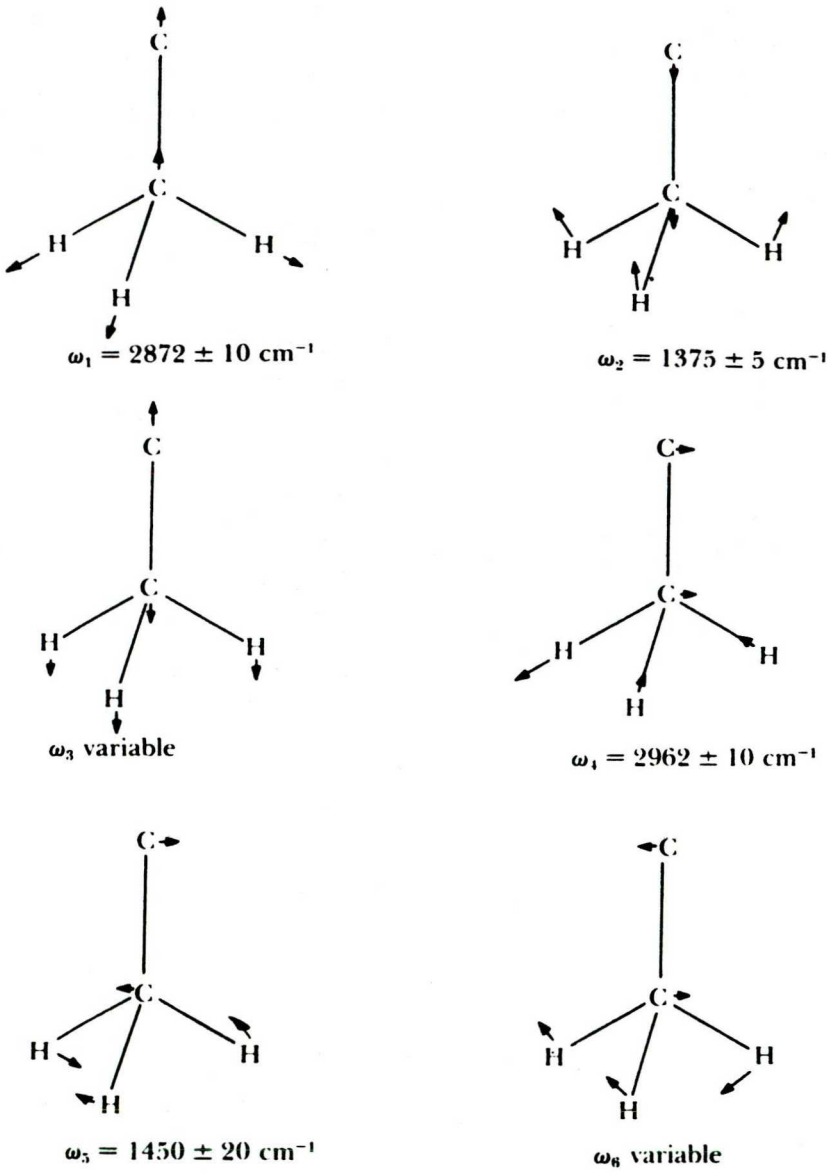

Fig. 12.

The vibrational modes of the $C-CH_3$ grouping /from ref. 5./

and lipids /52, 54/. In this way methyl and methylene vibrations, as well as the vibrations arising from the hydrocarbon chains and polar heads could be observed separately and more precisely assigned /55-59/.

The experimental observation of the drastic changes in the C-H region upon phase transitions in lipids - domination of the 2850 cm^{-1} band in liquid state and of 2880 cm^{-1} feature in the highly ordered state of the hydrocarbon chains, led to extensive investigation of this spectral region.

Attempts were made to assign the C-H vibrations on the basis of normal coordinate analysis of polyethylene and normal paraffins. It was assumed that the lipid hydrocarbon chains though not possessing as a whole the C_{2h} symmetry characteristic for extended n-paraffines, retain this local symmetry in gel and crystalline state /Fig. 11/, which leads to different selection rules in the IR absorption and in the Raman scattering /28/. The terminal methyl groups have C_{3v} symmetry /Fig. 12/ and hence the same selection rules in IR and Raman.

The band at 2850 cm^{-1} has been assigned to C-H methylene symmetric stretches of the hydrocarbon chains /25, 26, 28, 34, 40/, which conclusion has been confirmed by the band's polarized character /36, 39/. Contrary to some suggestions /52/, selective deuteration of DPPC showed no significant contribution to the 2850 cm^{-1} band from the head group methylene or terminal methyl groups of the acyl chains /57/. It was observed that 2850 cm^{-1} band only slightly changes with temperature /30/.

The band at 2880 cm^{-1} has been initially assigned to methyl symmetric stretch /25, 26/ and its broadening and loss of intensity upon heating were interpreted as reflecting different environment and increased mobility of the

terminal CH_3 groups in liquid state of the hydrocarbon chains as compared to the crystalline state. However, on the basis of theoretical analysis and experimental observations the band was later reassigned to CH_2 antisymmetric stretch /28, 32, 34, 39, 40/. An alternative assignment originating from the analysis of polyethylene spectra can be made interpreting 2883 cm^{-1} and 2848 cm^{-1} bands as resulting from splitting of the symmetrical CH_2 strechting mode by Fermi resonance with an overtone of the methylene deformational mode about 1430-1450 cm^{-1} /28,36/. The 2880 cm^{-1} band was found to be depolarized /36/ and was assigned to degenerate B_{3g} and B_{2u} vibrational mode /43/. Combination of crystal splitting and Fermi resonance was as well suggested to explain the antisymmetric character of the band and its predominance in the crystalline state /36/. It was shown /54, 57/ that the head group does not contribute intensity to 2880 cm^{-1} but there could be some contribution from the acyl chains' terminal methyl groups /57/. The terminal methyl groups, however, do not participate significantly in the temperature dependent changes of the 2880 cm^{-1} band /57/. The conformational sensitivity of the 2880 cm^{-1} band could be explained on the basis of Fermi resonance of 2865 cm^{-1} fundamental with environment sensitive CH_2 deformational mode /61/.

The band at about 2930 cm^{-1} seems to be composed from overlapping symmetric methyl streching at 2930 cm^{-1} and normally IR-active conformation-sensitive methylene antisymmetric stretch at 2920 cm^{-1}, which becomes allowed in the RAMAN scattering as the molecular symmetry changes upon disordering of the hydrocarbon chains /25, 26, 42, 49/. Two types of effects are tentatively assumed to contribute toward an intensification of the 2930 cm^{-1} feature: extensive disorder in the packing of the hydrocarbon chains,

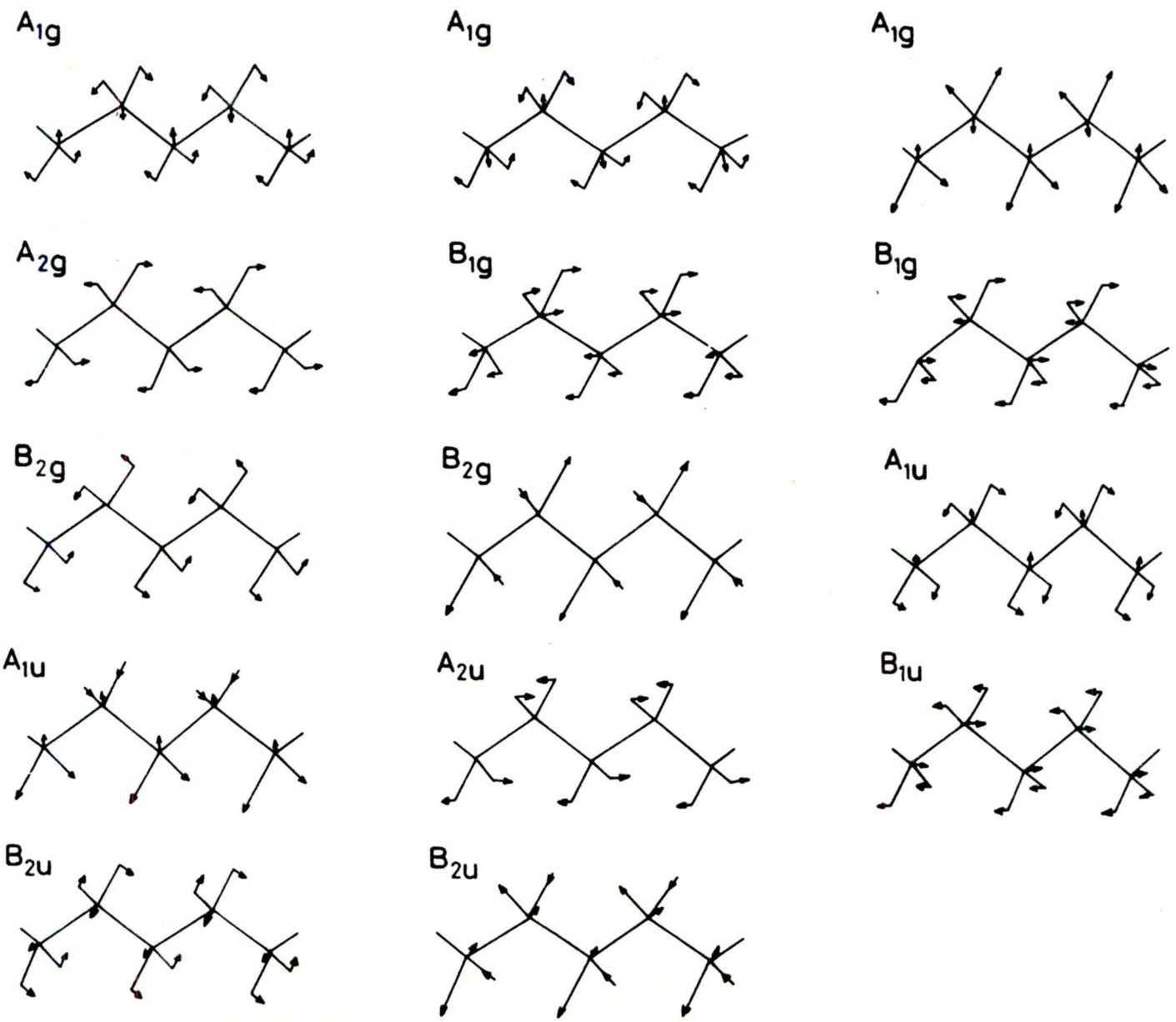

Fig. 13.

The vibrational modes of $/-CH_2-CH_2-/_n$ chain. /from T. Simanouti and S. Mizushima /1949/ J. Chem. Phys. 17,1102/.

Table 1.

Assignments for the Raman bands of the DL-DPPC crystal

Raman bands* /cm^{-1}/	Assigments	
	Groups**	Vibrational modes
40 - 500 /w/	sc, hg	Acoustic stretch of the entire molecule skeletal deformation
600 /w/	sc	$>C$ = o in-plane deformation
712 /m/	hg	Choline c-N symmetric-stretch
762 /w/	hg	O-P-O diester symmetric stretch
844 /w/	hg	O-P-O diester antisymmetric stretch
877 /m/	hg	Choline C-N antisymmetric stretch
890 /m/	sc	CH_3 rock + C-C stretch
910 /w/	hg	Skeletal stretch
960 /w/	hg	
967 /w/	hg	
1014 /w/	hg	
1052 /sh/	sc	C - O stretch
1064 /s/	sc	C - C stretch /all-*trans* conformation/
1092 /m/	sc, hg	C - C stretch /gauche conformation/ PO_2^- - symmetric stretch
1100 /sh/	sc	C - C stretch /all-*trans* conformation/
1130 /s/	sc	C - C stretch /all-*trans* conformation/

/cont. of Table 1/

Raman bands* /cm^{-1}/	Assignments	
	Groups**	Vibrational modes
1174 /vw/	sc	CH_2 rock
1252 /w/	hg	PO_2^- antisymmetric stretch
1296 /s/	sc	CH_2 twist
1342 /w/	hg	N^+ - CH_3 symmetric deformation
1371 /w/	sc	CH_2 wagg
1438 /s/	sc	CH_2 deformations
1460 /s/	hg	
1722 /w/	sc	C = O stretch
1738 /w/		
2846 /s/	sc	Acyl chain /CH_2/C - H symmetric stretch
2882 /s/	sc	Acyl chain /CH_2/C-H antisymmetric strech and /CH_3/C-H symmetric stretch /Possible involvement of crystal splitting and Fermi resonance with overtones and combination bands of CH_2 deformations/
2936 /m/	sc	Mainly /CH_3/C-H symmetric stretch /Possible resonance with /CH_2/C-H antisymmetric stretch/
2965 /m/	sc	Side chain /CH_3/C-H antisymmetric stretch
	hg	Choline /CH_3/C-H symmetric stretch
3024 /w/	hg	Choline /CH_3/C-H antisymmetric stretch
3040 /w/		

* s - strong; m - medium; w - weak; vw - very weak; sh - shoulder

** hg - head-group; sc - side chain

and increased polarity of the acyl chain environment /27, 31/. Unfortunately, the broad feature at about 2930 cm^{-1} cannot be resolved in separate peaks and cannot be used alone for characterization of the terminal methyl groups' motion /49/.

Still the intensity ratio I_{2930}/I_{2850} is expected to reflect the mobility of methyl termini relative to long methylene segments /34/. No significant contribution from the polar head was found to 2930 cm^{-1} region /57/.

The bands at 2962 cm^{-1} and 30 35 cm^{-1} were assigned to antisymmetric methylene vibrations of acyl chains /25, 26, 28, 39, 52/, and choline group /28, 52/, respectively. No coupling was observed between the vibrations of methyl and methylene groups /39/. Some contribution to the 2962 cm^{-1} band from methyl symmetric stretch of the choline groups is suggested /28, 36, 49/.

The bands' assignment in the Raman spectrum of dipalmitoyl phosphatidylcholine and the possible vibrational modes of $/-CH_2 - CH_2-/_n$ chain are summarized in Table 1 and on Fig. 13., respectively.

IV. 2. Quantitative evaluation of Raman spectroscopic data

IV.2.A. Intensity ratios

In the present work the following intensity ratios of the conformational sensitive Raman bands were used to evaluate the structural changes in the DPPC bilayers caused by lipid--ionic interactions:

$$\frac{I_{1128}}{I_{1100}}, \quad \frac{I_{1064}}{I_{1100}}, \quad \frac{I_{2880}}{I_{2850}} \qquad /20/$$

As was discussed above the first two intensity ratios in /20/ reflect the degree of *trans* order in the hydrocarbon region of the lipid systems.

Our observations showed that the tendencies in the results obtained by using either of the two *trans* bands - 1064 cm^{-1} or 1128 cm^{-1} were the same, although the absolute values of the intensity ratios for the 1128 cm^{-1} band were higher than those for the 1064 cm^{-1} band /Table 6/. Some authors /91/ prefer to use the 1064 cm^{-1} band since it is an almost pure *trans* C-C stretching mode and its frequency is independent of temperature. However, at least at constant temperature, the scattering of the data obtained by us tended to be less for $\frac{I_{1128}}{I_{1100}}$ intensity ratio, especially in disordered systems. As was mentioned above in disorder-er systems the 1100 cm^{-1} band shifts to lower frequencies /Fig. 22/ and its partial overlapping with the 1064 cm^{-1} makes the determination of $\frac{I_{1064}}{I_{1100}}$ intensity ratio less accurate. The $\frac{I_{2880}}{I_{2850}}$ intensity ratio reflects the changes in

the packing of the lipid hydrocarbon chains. The two C-H stratching bands - 2850 cm^{-1} and 2880 cm^{-1}, have considerable intensity and the scattering of the values of their intensity ratio was less than for the first two intensity ratios /usually 0.01/.

The decreased values of I_{1069}/I_{1100} and I_{1128}/I_{1100}, as well as of I_{2880}/I_{2850} intensity ratios in the presence of additives were interpretted as a reduction in the *trans* or lateral order, respectively, in the lipid hydrocarbon chains in comparison with DPPC - H_2O dispersion.

IV. 2. B. Order parameters

Recently an attempt has been made by Gaber and Peticolas /43/ to evaluate quantitatively the laser Raman spectra of lipids. Following order parameters have been introduced:

a/ The *trans* order parameter defined as

$$S_T = \frac{/I_{1128}/I_{ref}/ \text{ observed}}{/I_{1128}/I_{ref}/ \text{ DPPC solid}} \qquad /21/$$

The 1128 cm^{-1} band is considered as a *trans* marker and increases its intensity in systems with ordered, all-*trans* configuration of the hydrocarbon chains. I_{ref} is the intensity of a reference line. As reference bands the authors suggested those at 1100 cm^{-1} or 722 cm^{-1} / the 722 cm^{-1} band is the C-N symmetric stretch of the choline group/. Solid dipalmitoyl phosphatidylcholine was chosen as a standard for S_T, assuming it has the highest possible *trans* order.

As an approximation Gaber and Peticolas suggested that for an all-*trans* standard the intensity of the *trans* bands is the sum of intensities associated with individual bands. Assuming a similar additive relationship for shorter *trans* segments, S_T becomes a measure for the fraction of C-C bonds

in a *trans* conformation under a given set of conditions.

b/ The lateral order parameter defined as

$$S_{lat} = \frac{I_{CH_2}/\text{sample}/ - I_{CH_2}/\text{liq.hexadecane}/}{I_{CH_2}/\text{cryst.hexadecane}/ - I_{CH_2}/\text{liq.hexadecane}/} \qquad /22/$$

where $I_{CH_2} = I_{2890}/I_{2850}$

After substitution in /22/ of the experimentally obtained values of the intensity ratios for hexadecane the following expressions for S_{lat} was obtained:

$$S_{lat} = \frac{I_{CH_2}/\text{sample}/ - 0.7}{1.5} \qquad /23/$$

Since the change in the intensity of the 2890 cm^{-1} band is due both to decrease in vibrational coupling /change in the lateral packing/ and phonon dispersion broadening /appearance of several chain conformations/, the expression for S_{lat} is only approximate. It is a good estimate of the degree of lateral interaction if the frequency of the antisymmetric CH_2 stretch remains constant. Both order parameters were interpreted as probabilities. S_T was introduced as a measure of the all-*trans* chain probability /S_T = 1 for crystalline dipalmitoyl phosphatidylcholine, if all C-C bands are in *trans* conformation and S_T = 0 if none of them is in *trans* conformation/. S_{lat} was considered to be a measure of the closest packing probability /S_{lat} = 0 for the completely disordered state, as in liquid hexadecane, S_{lat} = 1 for the closest possible packing, as in crystalline hexadecane/.

The order parameters , as defined above, were applied by Gaber and Peticolas to show the thermally-induced structural changes in vesicles and aqueous lamellar dispersions of dipalmitoyl phosphatidylcholine. The convincing agreement between the data obtained by laser Raman and calorimetric techniques may give the impression that the suggested procedure of standardization and quantitation of the Raman data is of general validity. The sensitivity of the membrane structure to the ionic composition of the aqueous solution is particularly intersting physiologically, while the thermal effects are usually of secondary importance. For this reason we examined the applicability of the order parameters suggested by Gaber and Peticolas to ion-induced structural alterations of model membranes /92/ and suggested some refinements and modifications of the order parameters /100/ in order to achieve a more correct molecular interpretation of the laser Raman spectra of lipids in either aqueous disperions or biomembranes if ion-membrane interactions take place.

Obviously, in the choice of reference bands it was tacitly assumed by Gaber and Peticolas that temperature does not affect the head-group vibrations and thus their contributionto to I_{722} and I_{1096}. This implies on an entirely theoretical basis that hydrocarbon chain order-disorder transitions induced by interactions with polar head groups cannot be included in Gaber and Peticolas' picture. Considerable deviations and inconclusive data can be expected in these cases, primarily in the S_T values. To demonstrate this, the effects of some simple ions in high concentrations on the structure of lipid-water dispersion were monitored by laser Raman spectroscopy. The laser Raman spectra, in the relevant spectral regions, of dipalmitoyl

phosphatidylcholine in the presence of different ions are shown on Fig. 14.

Both 722 and 1096 cm^{-1} lines were taken as reference in accordance with Gaber and Peticolas' suggestions. Intensity ratios and order parameters S_T/S_T^1 for $I_{ref} = I_{722}$ and S_T^2 for $I_{ref} = I_{1096}$/ and S_L calculated via Eqns /21/ and /23/ are listed in Table 2. These data reveal that /a/ the intensity ratios I_{1096}/I_{722} usually deviate from unity and, /b/ the *trans* order parameters may exceed the theoretically predicted maximum value, the deviations being far above the inherent experimental measurement error. These imply that the structural changes induced by ions in multi-bilyaer systems cannot be conclusively described by the *trans* order parameters defined by Eqn. /21/.

On the basis of the assignments of the Raman bands used in the calculations of S_T^1 and S_T^2, it is plausible that the anomalously high values of S_T for various ions are to be ascribed to the interactions between ions and the zwitter-ionic polar head of phosphatidylcholine. The nature and points of attack of these interactions are not yet completely understood, but there is evidence /93/ that they can change the hydration state of the phospholipid molecules, Such interactions certainly may affect the polarizability of the phosphoryl moiety, and are reflected in the Raman spectra of lipids as changes in the intensities of the corresponding bands. Such changes were, in fact, observed. /Fig. 14/.

As regards the lateral order parameter, S_L, no anomaly appeared. According to the S_L data, none of the salts considered loosened the packing density of the hydrocarbon tails, whereas molecular iodine did /Table 2/. This latter observation coincides with Szundi's recent results obtained in monolayer investigations /unpublished results/, indicat-

Fig. 14.

Laser Raman spectra of dipalmitoyl phosphatidylcholine in lamellar aqueous dispersions containing different ions in the Raman spectral range 1000- 1200 cm^{-1}. a - 1 M $CaCl_2$; b - 1 M $MgCl_2$; c - 1 M $BaCl_2$; d - 1 M NaCl; e - 1 M $CdCl_2$; f - 10^{-2} M $Na_2S_3O_3$.

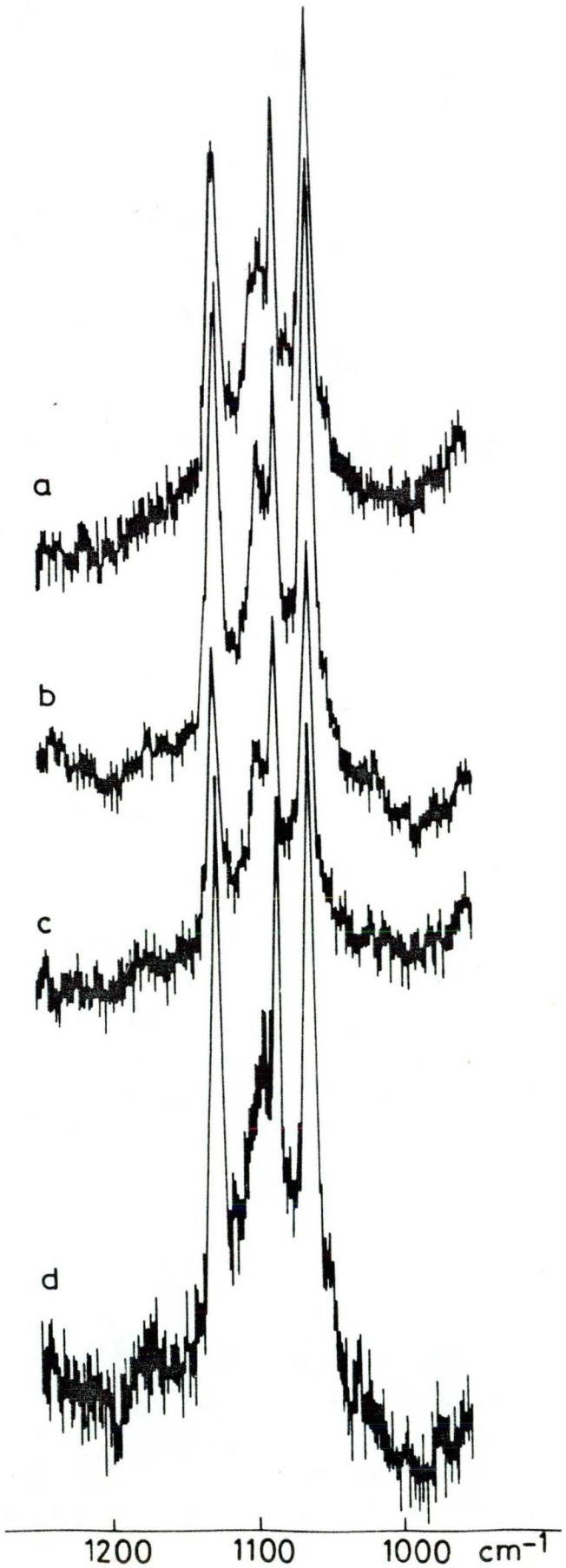
a
b
c
d
1200
1100
1000
cm⁻¹

ing the suitability and fairly high sensitivity of S_L for quantitative description of lateral order and packing density in aqueous lipid dispersions. Since the divalent ions considered have only a very slight ordering effect on the hydrocarbon moiety, it indicates that the ordering is probably due to secondary /perhaps head-group mediated/ interactions /"tightening"/ or ion-head group interactions may equally be the cause of any apparent changes observed.

To summarize, it is shown on theoretical and experimental grounds that the *trans* order parameter defined in Eqn 21 can only be applied to quantitative characterization of the all-*trans*- gauche relations in lipid systems if the polar head groups are not influenced by the external effect inducing the phase transition. There is only a restricted correspondence between the structural transitions and intensity ratios I_{1128}/I_{722} and/or I_{1128}/I_{1100}, they being determined not only by the *trans*-gauche relationship but even by the changes in the C-N stretching modes and PO_2^- vibrations, etc. as well. Thus, the concerted action of the different events may result in an unreal variation of S_T with respect to the *trans*-gauche isomaerization and therefore, the comparison of different structures on the basis of S_T with either I_{722} or I_{1100} as reference may lead to misinterpretation of the *trans* order situation. If the perturbation of the polar heads of lipids results in a decrease of the polarizability /dehydration or partial dehydration /94//, S_T may exceed the theoretical maximum, unity, indicating that the polar head is also involved. Since S_T was originally considered as a probability, there is no reasonable way to interpret values higher than 1.

The structural arrangments of fatty acid chains in the solid and differently hydrated states are rather multifarious

as revealed by X-ray diffraction technique /95-99/. For this reason we consider the quantity

$$\alpha = \frac{\frac{I_{1128}}{I_{ref}}_{sample}}{\frac{I_{1128}}{I_{ref}}_{hydrated\ lipid}} - 1 \qquad /24/$$

to be somewhat more correct from the viewpoint of physics than the analogous S_T parameter, and may give more realistic measure of the *trans* structure-modifying effectiveness of the solute /100/. α is only a phenomenological parameter for monitoring the conformational states of fatty acid residues and polar head groups in membranes, as compared to those of an identically hydrated lipid sample at a fixed reference temperature. Recently the hydrated lipid was accepted as a reference system by other authors as well /91/. In the following apparent ordering means that $\alpha > 0$, while apparent disordering is used when $\alpha < 0$; In the effectiveness sequences to be introduced below $H_2O < A$ denotes if ion A causes apparent ordering, and $A > H_2O$ applied appparent disordering. Otherwise the ions will be arranged according to $|\alpha|$. Clearly, no probability meaning is ascribed to α.

The intensity ratios I_{1128}/I_{722}, I_{1128}/I_{1100} and I_{2880}/I_{2850}, as well as the parameters and S_L were primarily used to evaluate the effects of various cations and anions on the structures of the aqueous disperions of lecithin at constant temperature. For the sake of comparison the S_T values will also be given in the tables below. S_T^1 and α_1 were obtained with $I_{ref}=I_{722}$, while S_T^2 and α_2 correspond to $I_{ref}=I_{1100}$.

IV. 3. Laser Raman studies of molecular interactions with phosphatidylcholine multilayers

IV. 3. 1. Effects of mono- and divalent ions on the lipid bilayer structure

There is understandable interest in the interactions of phospholipids with ions as regards excitability, ion permeation, ion binding and ion exchange properties at the surfaces of biological membranes. The lipid moiety of membranes is affected directly by ionic interactions depending upon the chemical nature of the polar head groups, and indirectly by the charge-induced structural changes in the vicinal and absorbed water. Although the influences of ions on phospholipid-water systems have been extensively investigated, the results obtained by different authors with various techniques are rather contradictory. Several investigators have observed in mono-, bi- and multibilayer studies /101-109/, thermal phase transition /110,111/ and X-ray diffraction /95/ experiments, NMR /112,113/ measurements that divalent cations interact directly with neutral phospholipids, Ca^{2+} having been found especially effective. Other authors failed to observe any cation binding /114-118/, or it appeared only at fairly high ionic concentrations /119/. Because of the diverse experimental antecendents we have reexamined the effects of various mono- and divalent ions on the lipid conformation and conformational changes at constant temperature by using laser Raman technique.

Monovalent cations

Due to the slight changes in the spectra, monovalent salt effects were examined only at high salt concentrations, such as 1 M /Figs. 15 and 16/. The experimental results show

Fig. 15.

Laser Raman spectra of DPPC:H_2O in lamellar aqueous dispersions containing 1 M chloride salts of different monovalent cations in the Raman spectral range of 950 - 1250 cm^{-1}.

a - NaCl; b - KCl; c - RbCl; d - CsCl

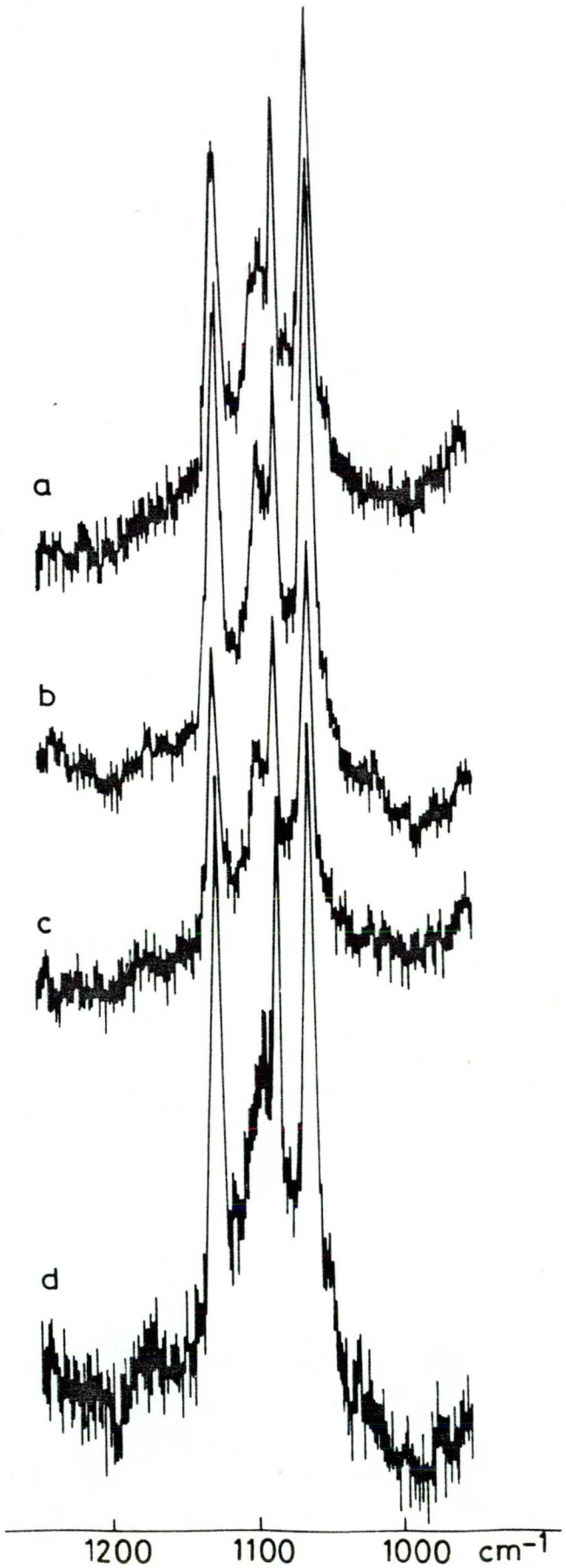
a
b
c
d
1200
1100
1000
cm⁻¹

Fig. 16.

Laser Raman spectra of DPPC:H_2O in lamellar aqueous dispersions containing 1 M chloride salts of different monovalent cations in the Raman spectral range of 2650 - 3050 cm^{-1}.

a - NaCl; b - KCl; c - RbCl; d - CsCl.

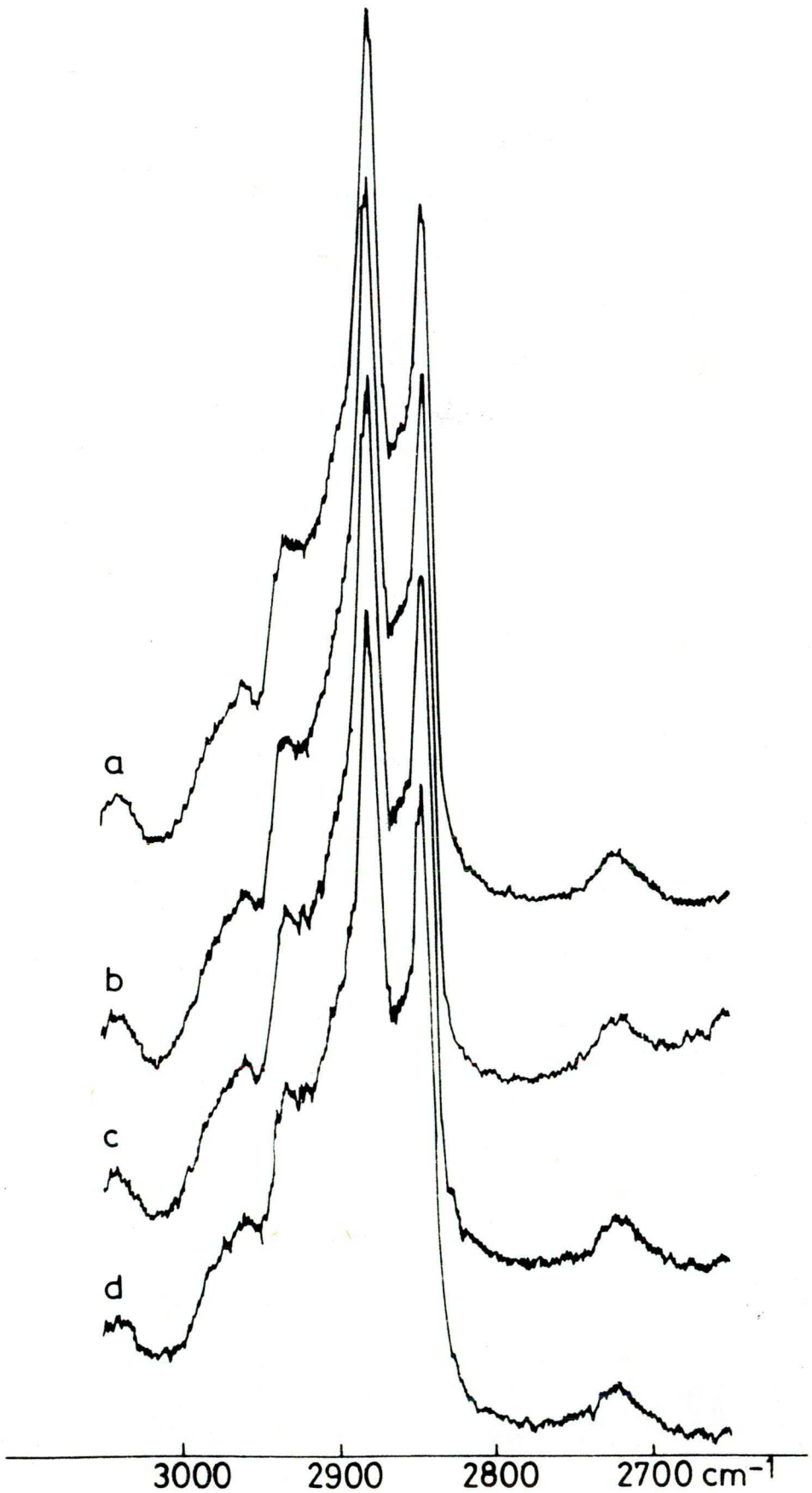
a
b
c
d
3000
2900
2800
2700 cm⁻¹

Table 3

Characteristic intensity ratios and order parameters for dry dipalmitoyl phosphatidylcholine and aqueous dipalmitoyl phosphatidylcholine dispersions in the presence of 1 M chloride salts of different monovalent cations. Phospholipid: :water = 1:4 /w/w/.

Composition of lipid sample	$\frac{I_{1100}}{I_{722}}$	$\frac{I_{1128}}{I_{722}}$	$\frac{I_{1128}}{I_{1100}}$	$\frac{I_{2880}}{I_{2850}}$	S_T^1	S_T^2	α_1	α_2	S_L
Dry	1.18	1.76	1.49	1.37	1.00	1.00	-	-	0.45
H_2O	1.20	1.74	1.45	1.28	0.99	0.97	0.00	0.00	0.39
NaCl	1.10	1.49	1.35	1.28	0.85	0.91	-0.15	-0.07	0.39
KCl	1.38	1.92	1.39	1.28	1.09	0.93	+0.10	-0.04	0.39
RbCl	1.45	2.10	1.45	1.28	1.19	0.97	+0.21	0.00	0.39
CsCl	1.45	1.96	1.35	1.28	1.12	0.91	0.12	-0.07	0.39

that in 1 M concentration all of them cause detectable alterations in the Raman spectra and order parameters /Table 3/. On the basis of the phenomenological parameter α_1 the following effectivenes order can be defined:

$$Na^+ > H_2O < K^+ < Cs^+ < Rb^+ \qquad /25/$$

The same sequence is obtained with S_T^1 and I_{1128}/I_{722} /see Table 3/. Since S_T^1 was originally interpreted as a measure of the all-*trans* probability the obtained numerical values for it, for K^+, Rb^+ and Cs^+, are lacking in meaning, they being higher than the theoretical maximum, unity. This is probably due to the interactions between the polar head

groups of lecithin molecules and cations as it was suggested above. The effectiveness sequence /25/ alos suggests that the interaction of Na^+ with hydrated lecithin may be different from those of K^+, Cs^+ and Rb^+. respectively.

Another effectiveness sequence for monovalent cations can be given on the bases of the intensity ratios I_{1128}/I_{1100} and the corresponding order parameters S_T^2 and α_2 as follows

$$Na^+ \approx Cs^+ > K^+ > Rb^+ \approx H_2O \qquad /26/$$

This is in agreement with the sequence obtained by differential scanning calorimetry /111/ except for Na^+, but non of the criteria suggested in ref. 111 provided a satisfactory explanation for our results. According to effectiveness order /26/ Na^+ and Cs^+ are the most effective in producing structural changes in the phospholipid multibilayer system. These behaviours of Na^+ and Cs^+ are, at first glance, in line with their structure breaking effects on water /120/. Most plausibly, the monopositive ions interact with the hydrated polar head both electrostatically and by changing its hydration shell. This latter may alter both the hydrogen bond network at the interface /99, 121/ and the polarizability of some Raman-active groups /probably the phosphoryl group, etc./ in the polar head, and lead to an apparent enhancement in gauche formation as revealed by the decreasing values of I_{1066}/I_{1100}, I_{1128}/I_{1100}, S_T^2 and α_2 respectively. Since no appreciable alteration in S_L accompanied the changes of the intensity parameters used above during monovalent salt exposure, one inclines to believe that the effectiveness order is determined by both cation-head group interactions and the perturbation /26/ of the acyl chains and, in fact, a smaller increase, if any, in the gauche formation occurs than would follow from the corresponding intensity ratios and order parameters. Interestingly, the order parameter S_T^2

does not exhibit any anomaly, indicating that the 1100 cm^{-1} line as reference is probably less sensitive to ion-head group interactions and can be, at least for monovalent cations, more suitable than the 722 cm^{-1}.

The intensity ratios of the two reference lines, I_{1100}/I_{722} vary ion to ion and depend also upon concentration /see Tables 3-5/. They can be considerably higher and lower than that for hydrated phosphatidylcholine, 1.18, and exhibit the following sequence.

$$Na^+ < H_2O \approx \text{dry dipalmitoyl phosphatidylcholine} < K^+ < Cs^+ \approx Rb^+ \qquad /27/$$

This reminds very much of sequence /25/, indicating that sequences /25/ and /27/ are determined basically by the same interactions. Considering the origins of the Raman lines at 722 and 1100 cm^{-1} sequence /27/ seems to reflect the effectiveness of the different monopositive ions in their interactions with the polar head of lecithin. If so the changes in all the quantities defined by means of I_{722} may be dominated by the cation-head group interactions.

Divalent cations

The influence of the divalent cations Ca^{2+}, Cd^{2+}, Mg^{2+} and Ba^{2+} on the structures of dipalmitoyl phosphatidylcholine-water lamellar phases were investigated in the concentration range 0.5 mM - 1 M of their chloride salts. /Figs. 14, 17 and 18/. Detectable changes in the Raman spectra occurred even at lower salt concentrations, depending upon the dipositive ion.

Fig. 17.

Laser Raman spectra of dipalmitoyl phosphatidylcholine in lamellar aqueous dispersions containing $CaCl_2$ in different concentrations, in the Raman spectral range 950 - 1250 cm^{-1}.

a - 1 M; b - 100 mM; c - 50 mM; d - 10 mM; e - 5 mM; f - 1 mM; g - 0.5 mM.

/from BBA, 514 /1978/ 274-285/.

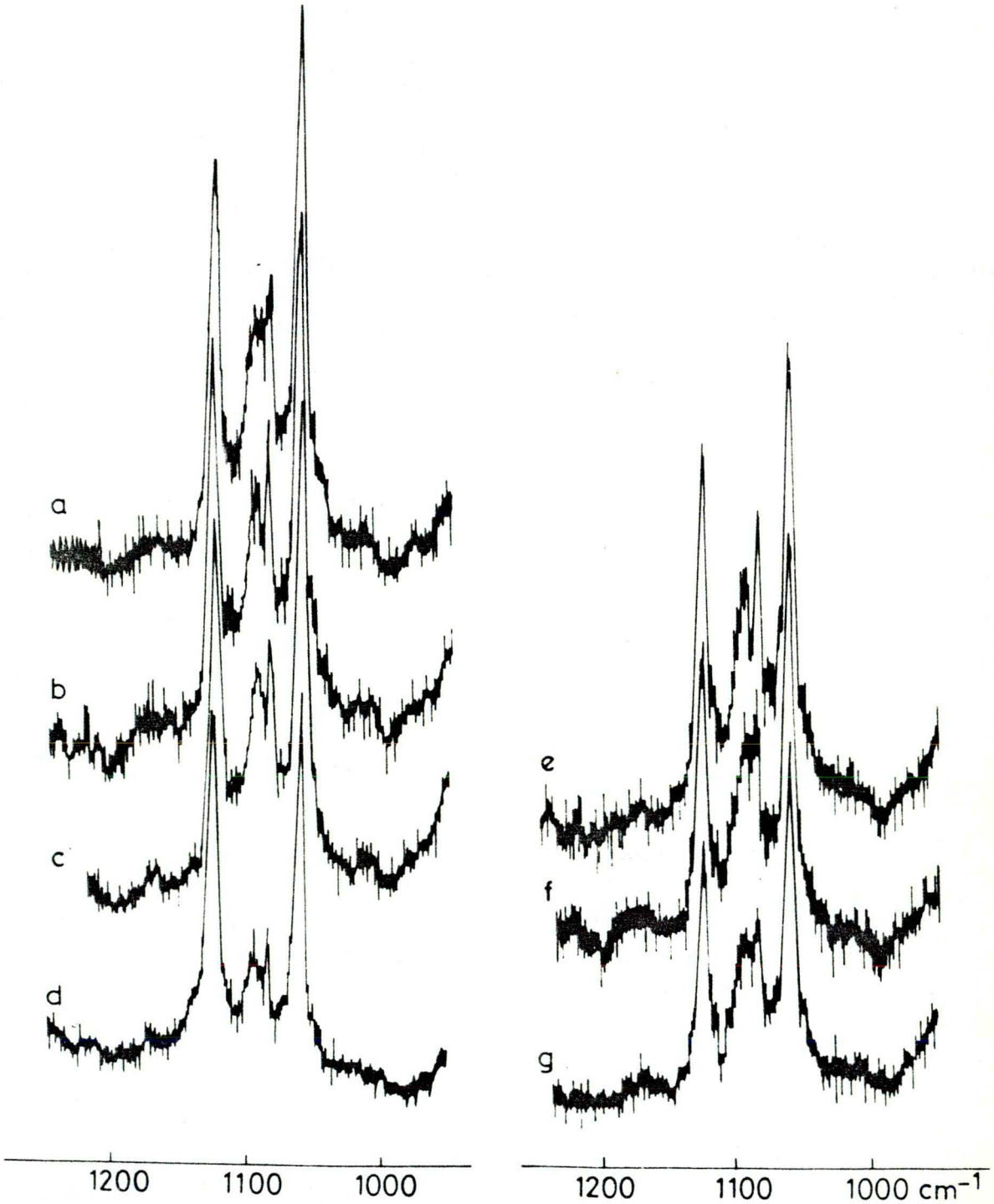
a
b
c
d
e
f
g
1200
1100
1000
1200
1100
1000 cm⁻¹

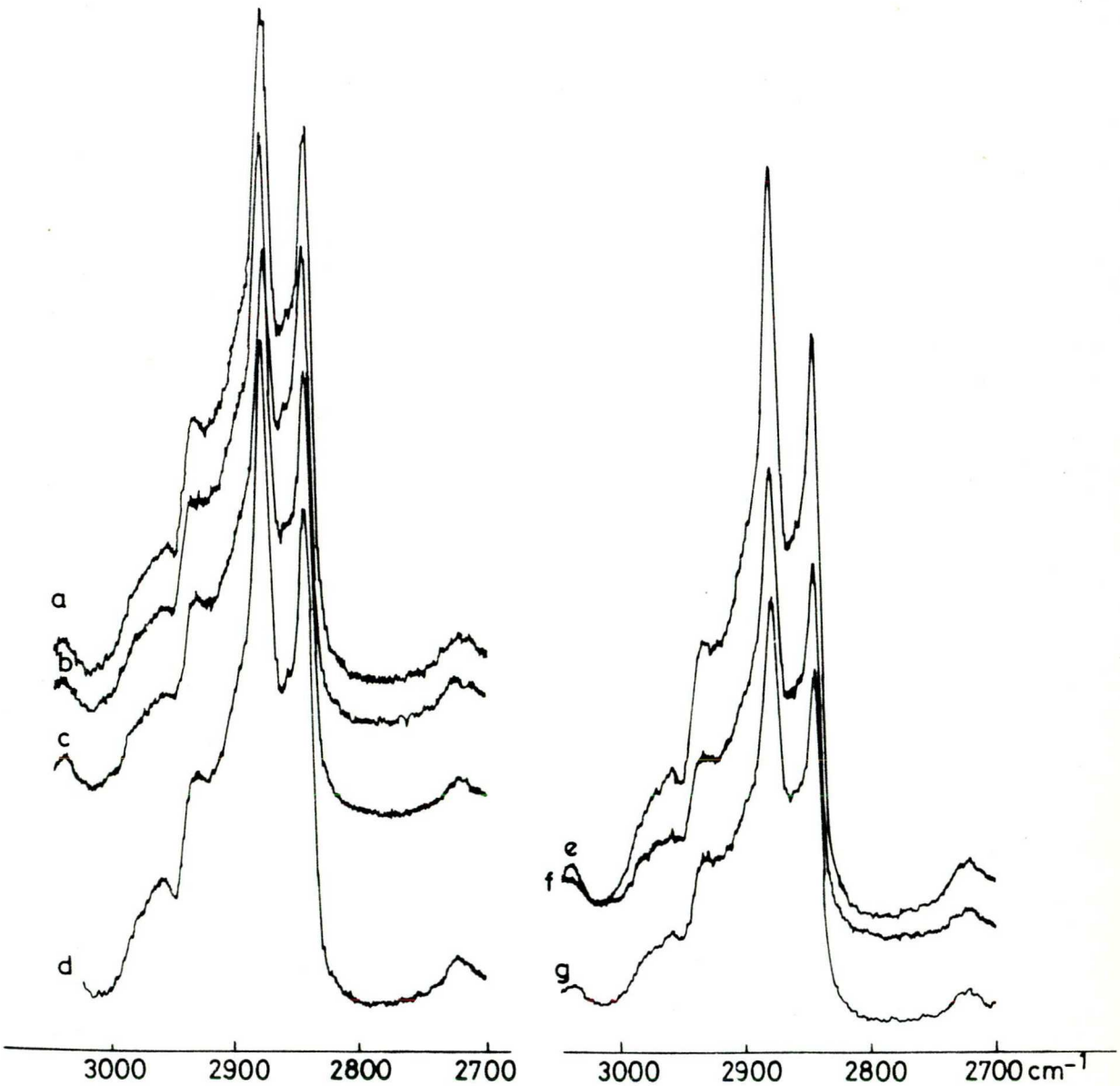

Fig. 18.

Laser Raman spectra of dipalmitoyl phosphatidylcholine in lamellar aqueous disperions containing $CaCl_2$ in different concentrations in the Raman spectral range 2700 - 3050 cm^{-1}.

a - 1M; b - 100 mM; c - 50 mM; d - 10 mM; e - 5 mM; f - 1 mM; g - 0.5 mM;
/from BBA, 514 /1978/ 274-285./

At 1 - 5 mM and/or 1 - 10 mM Ca^{2+}, depending upon the reference line chosen /Fig. 19 and Table 4/, a well-pronounced apparent disordering was observed in the hydrocarbon chains, which is probably related to the partial destruction of the lamellar phase revealed by X-ray diffraction measurements /95/. At higher concentrations the intensity ratios were close to those of ion-free phospholipid-water systems, indicating the "reappearance of the lamellar phase" /95/. It should be emphasized here that the *trans* order parameters calculated from Eqn. 1 with either $I_{ref}=I_{722}$ or $I_{ref}=I_{1100}$ exceed the theoretical maximum value, unity, in the concentration range above 10 mM. On the basis of the corresponding values, strong and concentration-dependent interactions with the head groups can be deduced, the intensity ratios and order parameters used being affected by the changes in head-group polarizability and the PO_2^- vibrations as well /92/, but very probably not in the same way as in the case of monovalent cations. An essential difference between mono- and divalent cations in their overall interactions with polar heads of phosphatidylcholine molecules is exhibited in the opposite behaviour of the 722 cm^{-1} line.

The lower values of the *trans* order parameters α_1 and α_2 in the concentration range of 1-10 mM suggest the existence and the competition of two opposing forces, both Ca^{2+}--dependent; an attractive force favoring close-packing /self--association/ of the membrane constituents, and a repulsive force that is essential to keep the lipid molecules apart and maintains membrane stability. The van der Waals forces, the hydrogen bond network due to the hydration of the polar heads, as well as the blanketing cloud of counter ions provide the main contributions to the resultant attractive force. Primarily, the electrostatic charges on the head

Characteristic intensity ratios and order parameters (S_T^1, S_T^2, α_1 and α_2 for the *all-trans* configuration of hydrocarbon chains; S_L for the lateral packing density) for dry dipalmitoyl phosphatidylcholine and aqueous dipalmitoyl phosphatidylcholine dispersions in the presence of chloride salts of different concentrations. Phospholipid : water = 1 : 4 (w/w).

Composition of lipid sample	$\frac{I_{1100}}{I_{722}}$	$\frac{I_{1128}}{I_{722}}$	$\frac{I_{1128}}{I_{1100}}$	$\frac{I_{2880}}{I_{2850}}$	S_T^1	S_T^2	α_1	α_2	S_L
Dry	1.18	1.76	1.49	1.37	1.00	1.00	—	—	0.45
H_2O	1.20	1.74	1.45	1.28	0.99	0.97	0.00	0.00	0.39
Ca^{2+}									
0.5 mM	1.40	2.01	1.45	1.28	1.15	0.97	+0.17	0.00	0.39
1 mM	1.25	1.65	1.32	1.25	0.94	0.89	—0.05	—0.09	0.37
5 mM	1.24	1.74	1.41	1.22	0.99	0.95	0.00	—0.03	0.35
10 mM	1.23	1.81	1.47	1.25	1.02	0.99	+0.04	+0.01	0.37
50 mM	1.20	1.79	1.49	1.26	1.02	1.00	+0.03	+0.03	0.37
100 mM	1.36	2.12	1.56	1.28	1.20	1.05	+0.22	+0.07	0.39
500 mM	1.30	2.46	1.89	1.30	1.40	1.27	+0.41	+0.30	0.40
1 M	0.98	2.46	2.50	1.32	1.39	1.68	+0.41	+0.72	0.42
2 M	1.07	2.35	2.20	1.46	1.34	1.48	+0.35	+0.52	0.51
Mg^{2+}									
1 mM	1.38	2.00	1.45	1.28	1.14	0.97	+0.15	0.00	0.39
5 mM	1.12	1.58	1.41	1.25	0.90	0.95	—0.08	—0.03	0.37
10 mM	1.17	1.67	1.43	1.25	0.95	0.96	—0.04	—0.01	0.37
50 mM	1.11	1.66	1.49	1.25	0.94	1.00	—0.05	+0.03	0.37
100 mM	1.39	2.16	1.55	1.25	1.22	1.14	+0.24	+0.07	0.37
1 M	1.42	2.30	1.61	1.30	1.30	1.19	+0.31	+0.11	0.40
Ba^{2+}									
1 mM	1.34	2.06	1.54	1.28	1.17	1.03	+0.18	+0.06	0.39
10 mM	1.24	1.88	1.52	1.28	1.07	1.02	+0.08	+0.05	0.39
100 mM	1.47	2.20	1.49	1.28	1.24	1.00	+0.26	+0.03	0.39
1 M	1.38	2.03	1.47	1.26	1.15	0.92	+0.17	+0.01	0.37
Cd^{2+}									
10 mM	1.46	2.09	1.43	1.25	1.18	0.96	+0.20	—0.01	0.37
100 mM	1.11	1.61	1.45	1.26	0.92	0.97	—0.07	0.00	0.37
1 M	0.98	1.79	1.82	1.41	1.01	1.22	+0.02	+0.25	0.47

Fig. 19.

Dependences of the phenomenological order parameters α_1 and α_2 for dipalmitoyl phosphatidylcholine in lamellar aqueous dispersions upon the $CaCl_2$ concentration.

/from BBA, 514 /1978/ 274-285/

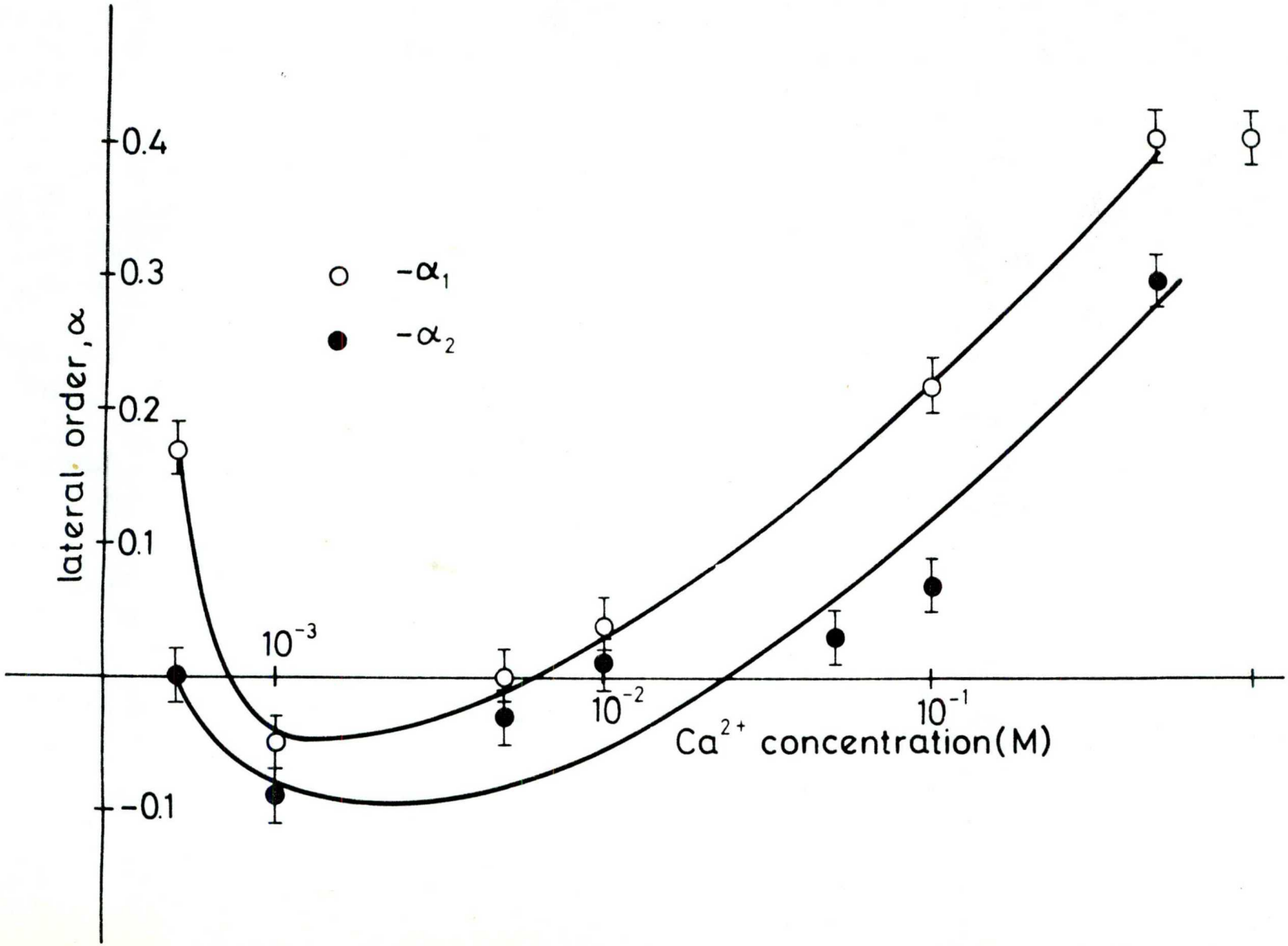
0.4
0.3
0.2
0.1
-0.1
lateral order, α
-α1
-α2
10-3
10-2
10-1
Ca2+ concentration(M)

groups, which may come either from zwitterionic charges, or from adsorption of foreign ions from the surrounding solution furnish the repulsive interactions. /A further aspect of the hydration of the polar head is similar to the role of identical electric charges; it tends to cause the lipid molecules to keep apart/. Obviously, the balance between net attractive and repulsive forces, as well as the hydration shell will determine the existing structure of lipid-water dispersion.

The measurements of Seimiya and Ohko /106/ and those of Belmonte et al. /122/ indicate that : /a/ when the interlipid specing is relatively large the divalent cation interacts only with one lipid molecule; /b/ when the interlipid distance is relatively small the dipositive ion binds two lipid molecules. Keeping these in mind our observations presented in Fig. 19 can be qualitatively explained in the following way. In the absence of electrolyte the structure of the lipid dispersion is essentially determined by van der Waals interactions and the hydrogen bond network /as attractive forces/, and by the electrostatic and hydration effects tending to separate the lipid molecules. As a consequence, a rather loose bilayer structure with relatively large intermolecular spacing will be formed. If a small amount of Ca^{2+} /in chloride form/ is introduced, divalent cations will be adsorbed on single lipid molecules, partially dehydrating the polar head and converting the head group's charge into positive. Although the dehydration of the polar moiety and the presence of the Cl^- /as counter ions/ favor close packing of the lipid molecules, the electrostatic repulsion due to the large positive charge on the head groups surmounting the attractive forces and a larger equilibrium distance between lipid molecules with adsorbed Ca^{2+} will be

established, resulting in the disordering of hydrocarbon chains / O, Fig. 19/. If the electrolyte concentration is increased, the chloride counter-ions present in sufficient amounts can effectively mask the charge of the adsorbed ion and will not allow the Ca^{2+}-induced disordering to proceed. A further rise in the electrolyte concentration leads to the interpenetration of the blanketing counter-ion clouds of neighbouring lipid molecules with adsorbed Ca^{2+} and hence, to the approach of the bilayer constituents. This process must be manifested in a moderate chain ordering as it was in fact observed /Table 4/. At a certain interlipid distance a fairly sudden drop can be expected in the binding of Ca^{2+} /106/, which must be reflected in increases in the order parameters and S_L; It is believed that this transition occurs already at the concentration of 100 mM and the bridging interaction promotes ordering of hydrocarbon chains /Fig. 19 and Table 4/. The effects of Cd^{2+} and Mg^{2+} and, their concentration dependences are similar to those of Ca^{2+}, but somewhat weaker /Table 4/. Ba^{2+} practically does not affect the lateral structure of the phospholipid multibilayers, but the tendency of the concentration dependence of α_1 is also qualitatively similar to those for Ca^{2+}, Cd^{2+} and Mg^{2+}, with the difference that the minimum apparent order is at higher salt concentrations. This again provides arguments in favor of the possible two-step binding of divalent cations to bilayered neutral phospholipids.

A great variety of effectiveness sequences can be constructed on the basis of intensity ratios and order parameters given in Table 4. These sequences depend, however, not only upon the reference line as was the case for monovalent cations, but even upon the concentration of salt.

The sequence of divalent cation effectiveness for lecithin found above 5 mM /Table 4/ is in good agreement with the results obtained with various other thechniques /29,110,111/, though some other authors reported the reverse order of Mg^{2+} and Ca^{2+}/123/ or the same magnitude of the effect for these two divalent cations/113/. These latter observations can perhaps be attributed to the concentration-effect mentioned. The differences between the influences of different divalent cations on membrane may be due to differences in coordination numbers, geometrical requirements for binding ligands, etc. as suggested by Williams /124/.

Since practically no frequency shift was found for the 2880 cm^{-1} line, S_L defined as in Eqn.23 could be used to evaluate the influence of dipositive ions on the lateral packing of the lipid molequles. There are mostly insignificant differences in the lateral order of hydrocarbon chains for different divalent cations in comparison with aqueous dispersions, even at high ionic concentrations. This suggests thst either the parameter S_L is rather insiensitive to the packing density or these cations interact with the head groups and directly affect mainly the polar region of the bilayers. In this latter case the ordering effect on the fatty acid residues is indirect and their structure may be quite close to that of the ion-free phospholipid-water dispersions. If so, this means that Ca^{2+} and other dipositive ions control the permeability properties primarily not via the structure of the membrane interior, but rather at the interface.

Mono- and divalent anions

We have investigated the structural influences of 1M sodium salts of the anions Cl^-,Br^-,I^- NO_3^-,SO_3^{2-},SO_4^{2-} and the very effective $S_2O_3^{2-}$, and $S_2O_8^{2-}$ in 10 mM concentrations

/Figs.20, 21 and Table5/. In the following it will be assumed, as a first approximation, that anions and cations affectthe lecithin molecules independently of each other, i.e. the changes observed are to be ascribed to anions, the sodium concentration being the same in all cases, except for $S_2O_3^{2-}$ and $S_2O_8^{2-}$.

The results obtained /Table 5/ show that the intensity ratios for various mono- and divalent anions mirror different anion effects. That the anions NO_3^-, SO_3^{2-}, $S_2O_3^{2-}$ and $S_2O_8^{2-}$ may in fact give rise to higher *trans* order follows from the slightly enhanced packing densities monitored by S_L /Table 5/ and from the appearances of the corresponding spectra/Figs.20,21/

Table 5

Characteristic intensity ratios and order parameters for dry dipalmitoyl phosphatidylcholine and aqueous dipalmitoyl phosphatidylcholine dispersions in the presence of sodium salts of various mono- and divalent anions.

Composition of lipid sample	$\frac{I_{1100}}{I_{722}}$	$\frac{I_{1128}}{I_{722}}$	$\frac{I_{1128}}{I_{1100}}$	$\frac{I_{2880}}{I_{2850}}$	S_T^1	S_T^2	α_1	α_2	S_L
Dry	1.18	1.76	1.49	1.37	1.00	1.00			0.45
H_2O	1.20	1.74	1.45	1.28	0.99	0.97	0.00	0.00	0.39
1M NaCl	1.10	1.49	1.35	1.28	0.85	0.91	-0.15	-0.07	0.39
1M NaBr	1.27	1.93	1.52	1.28	1.10	1.02	+0.11	+0.05	0.39
1M NaI	5.3	4.1	0.77	1.02	2.33	0.52	+1.36	-0.47	0.21
1M $NaNO_3$	1.06	1.58	1.49	1.30	0.90	1.00	-0.09	+0.03	0.40
1M Na_2SO_3	1.46	2.06	1.41	1.30	1.17	0.95	+0.18	-0.03	0.40
1M Na_2SO_4	1.44	2.09	1.45	1.28	1.19	0.97	+0.20	0.00	0.39
10^{-2}M $Na_2S_2O_3$	1.48	2.38	1.61	1.32	1.35	1.08	+0.37	+0.11	0.41
10^{-2}M $Na_2S_2O_8$	1.46	2.08	1.49	1.25	1.18	0.95	+0.02	-0.20	0.37

Fig. 20.

Laser Raman spectra of dipalmitoyl phosphatidylcholine in lamellar disperions containing 1 M sodium salts of different anions in the Raman spectral range 950 - 1200 cm^{-1}.

a - Na_2SO_4; b - NaBr; c - NaCl; d - Na_2SO_3;

e - $NaNO_3$

/from BBA 514 /1978/ 274-285/

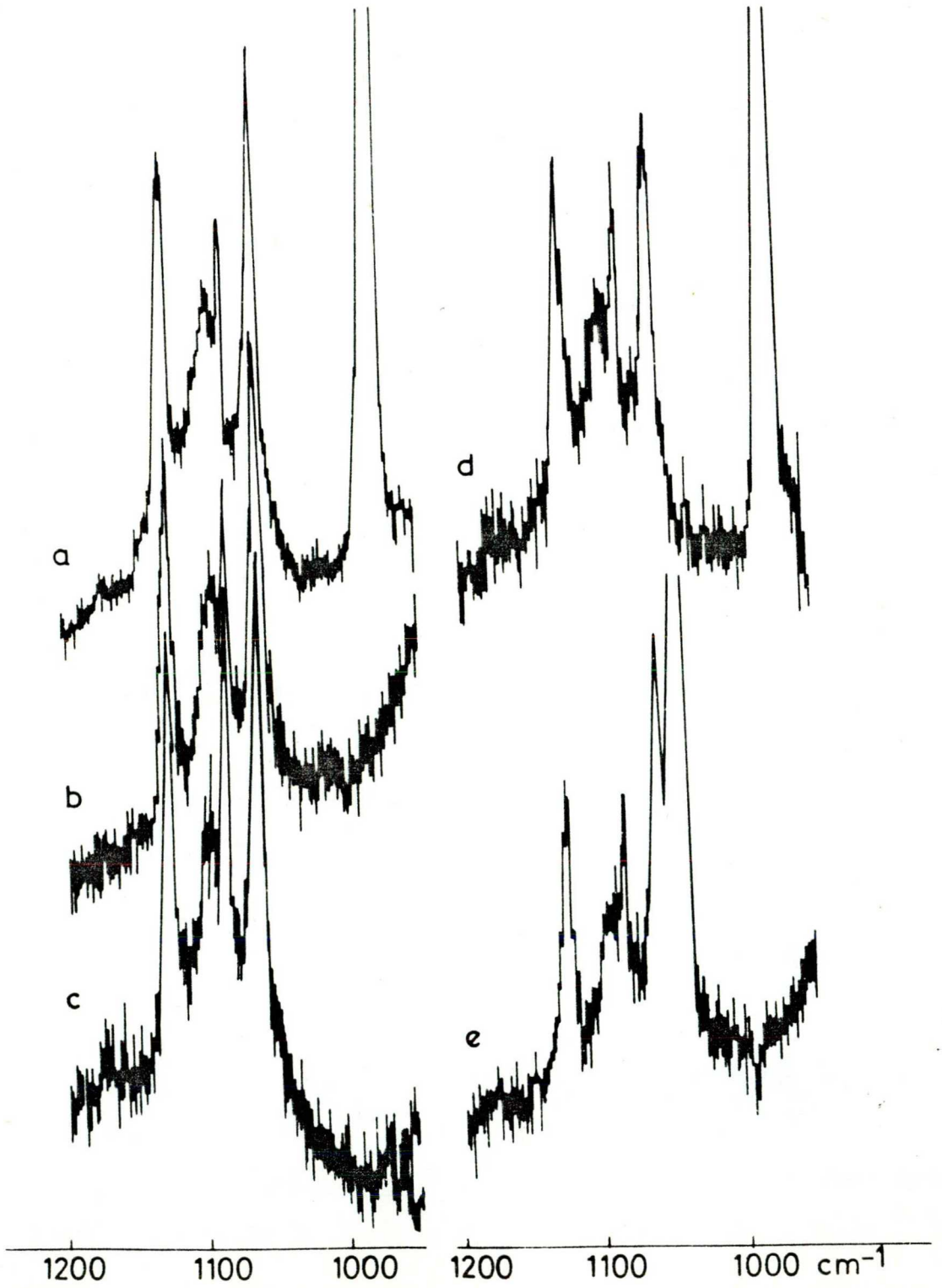
a
b
c
d
e
1200
1100
1000
1200
1100
1000 cm⁻¹

Fig. 21.

Laser Raman spectra of dipalmitoyl phosphatidylcholine in lamellar disperions containing 1 M sodium salts of different anions in the Raman spectral range 2650 - 3100 cm^{-1}.

a - Na_2SO_4; b - NaBr; c - NaCl; d - Na_2SO_3;
e - $NaNO_3$.
/from BBA, 514 /1978/ 274-285/.

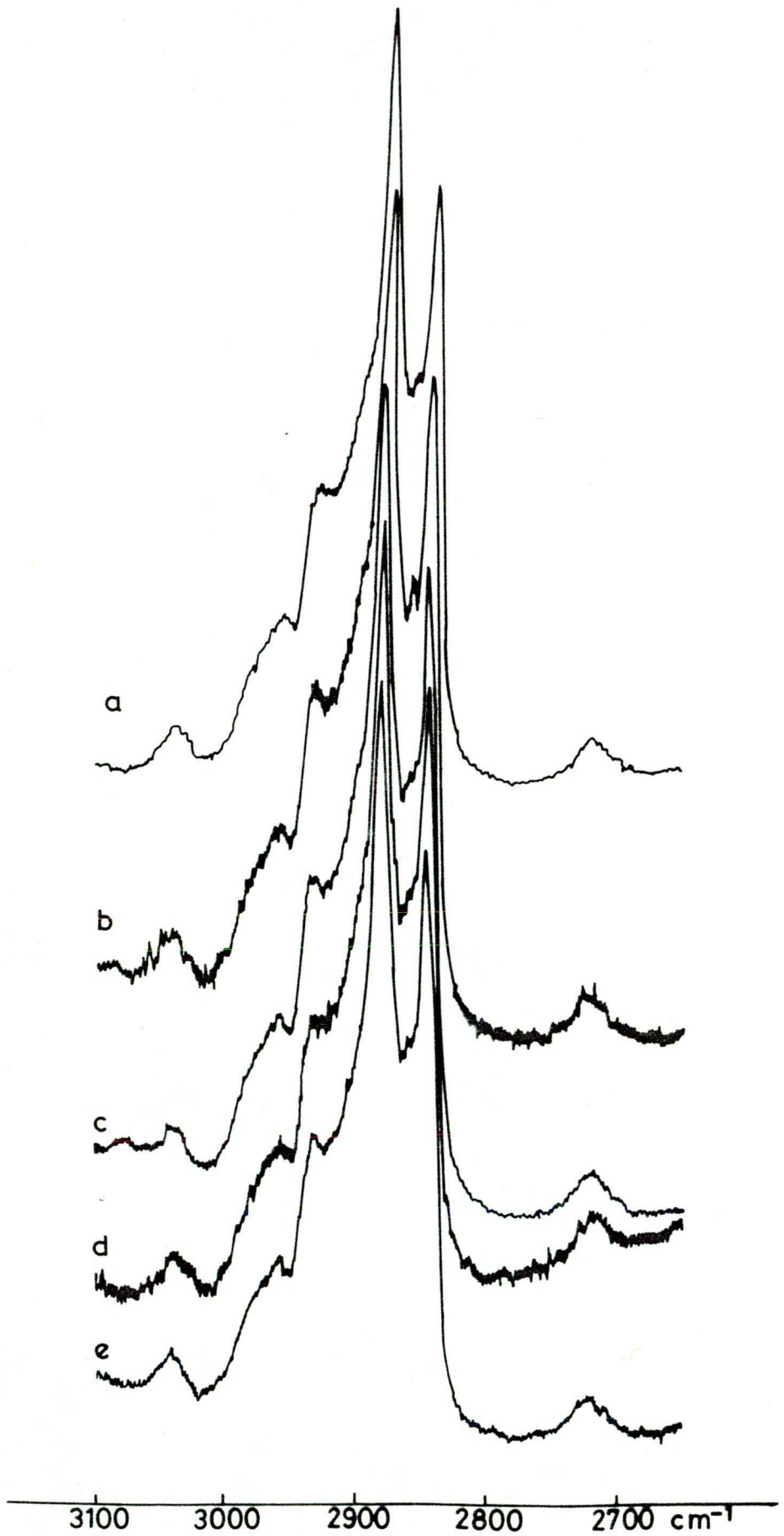
a
b
c
d
e
3100
3000
2900
2800
2700 cm⁻¹

It is very likely that all the anions act as counter-ions for the trimethylammonium groups and they change the conformational states of headgroups, leading to an altered freedom in charge displacement of polarization origin. Besides this, at least NO_3^- and the divalent species have a further particular effect on the polar head motion and polarizability, α being positive. Just for structural reasons, it is plausible that in the presence of divalent anions, the phosphatidylcholine molecules can rearrange themselves so that a divalent anion can be shared by trimethylammonium groups of neighbouring phospholipid molecules and thus, a more closely packed bilayer emerges.

The spectral data suggest that cations, especially the monovalent ones, and anions may have opposite effects on the structure of phospholipid-water systems; anions appear more effective. The structure of the zwitterionic head group of neutral phosphatidylcholine and its orientation indicate that the negative groups, being closer to the hydrocarbon chains and partially neutralized by the quaternary nitrogen of the same molecule/104/, are rather well masked and thus, less accessible for the cations than the trimethylammonium groups for anions. No correlation seems to exist between /either effective or crystal/ ionic radii and strength of interaction of anions with lecithin bilayers, indicating that their effects are rather specific and not entirely of an electrostatic nature. It appears also that the charge distribution on the anion is an important factor in the structural effects. In contrast to the observations of Lis et al./29/on the structure influencing effects of potassium salts of various anions, we found anion-dependent structural changes for the anions investigated. The origin of this discrepancy is not yet well understood. A possible explanation is the different cation used: potassium by Lis et al. /29/ and sodium by us. As mentioned above, sodium was the most effective in altering the structure of DPPC,

and thus, it can be imagined that the anion effects are manifested differently for sodium and potassium. This would mean that the structures and structural transitions of lipid dispersions are determined and governed by cations and anions mutually rather than independently /29/. Whether the effects of anions and cations are interlinked at the level of a certain kind of competition or somehow else, the possible significance of the interactions postulated in the transport and regulatory processes, etc. all remain open, and are interesting tasks of further investigations.

IV. 3. 2. Effect of iodine-iodide system on the lipid bilayer structure

The influence of iodine species /I_2,I^-,I_3^- and other polyiodide ions/ on the electric properties of bimoleculare lipid membranes /BLM/ has been extensively investigated. It was found that in the presense of iodine and iodide the conductivity of a BLM is drastically increased. Different basic mechanisms for their action have been proposed, such as ionic conduction /125,126/, electronic conduction with donor-acceptor complex formation /127,128/, transport of electro-chemically injected holes via triiodide chains /129/, interfacial electron/hole injection /130-133/, charge injection by a catalized redox reaction /134/ and electrostenolysis /135/. It was shown that molecular iodine is necessary to produce the resistance-lowering effect /125,126,136/ and it was suggested that I_2 is a carrier of I^-, forming I_3^-, which diffuses through the membrane /125,126,136,137/. Although the role of iodine and its species is of secondary importance in biology, except for the thyrogenous function, the mechanism of electric conduction of BLMs in the presence of iodide has become a matter of principle and its understan-ing requires clarification of the nature of iodine species interactions with lipids and lipid membranes. In our work Raman spectroscopy has been applied to study the interactions of iodine, iodide and triiodide with phosphati-

dylcholine multilayers in order to find supporting data for conduction mechanisms of iodine-doped bimolecular lipid membranes. The intensity ratios I_{1066}/I_{1100}, I_{1128}/I_{1100} and I_{2880}/I_{2850} were mainly used to characterize and compare interactions between iodine species $/I_2, I^-, I_3^-/$ and lamellar dispersions of DPPC /143/.

In order to investigate the influence of I^- ion, potassium iodide solutions in different concentrations were used. Increasing KI concentration made the lecithin spectra noisy and caused changes in the positions, shapes and intensities of the Raman bands /Fig.22/In the region 1000-1200 cm^{-1} iodide in concentrations 2.10^{-3}M and 2.10^{-2}M has no influence on the lecithin spectra /Fig.23,b and c/, the intensity ratios being very similar to those obtained for the aqueous dispersion /Table 6/.At 2.10^{-1}M KI the intensities of the 1066 and 1128 cm^{-1} bands decrease, while that at 1096 cm^{-1} broadens, its intensity strongly increasing/Fig.23d/.In the presence of 2M KI the bands at 1066 and 1128 cm^{-1} almost disappear, and the spectrum becomes noisy and unsuitable for quantitative analysis. These data imply that the original all-*trans* configuration of the fatty acid chains starts breaking up, leading to gauche conformation. On the other hand, the interaction of iodine and its ionic species with polar head groups, which can be reflected in the modification of the symmetric vibrations of the phosphate groups, may also contribute to the broadening and intensification of the 1096 cm^{-1} line. Changes in the configuration and motion of polar heads attacked by iodine may result in the loosening of the hydrocarbon phase, therby promoting gauche formation in the fatty acid region. Although the presence of gauche structures in thr hydrocarbon region is favorable in principle to ionic charge-transport, little is known for the time being about the posibility of ionic charge-transfer through the polar head group layer.

Fig. 22.

Spectra of dipalmitoyl phsophatidylcholine lamellar dispersions in the Raman spectral range 600 - 1600 cm^{-1}.

a - 1:4 w/w DPPC- H_2O lamellar system.

b - 1:4 w/w DPPC- H_2O lamellar system in the presence of 10^{-2} M KI.

/from Chem. Phys. Lipids 19 /1977/ 159-168/

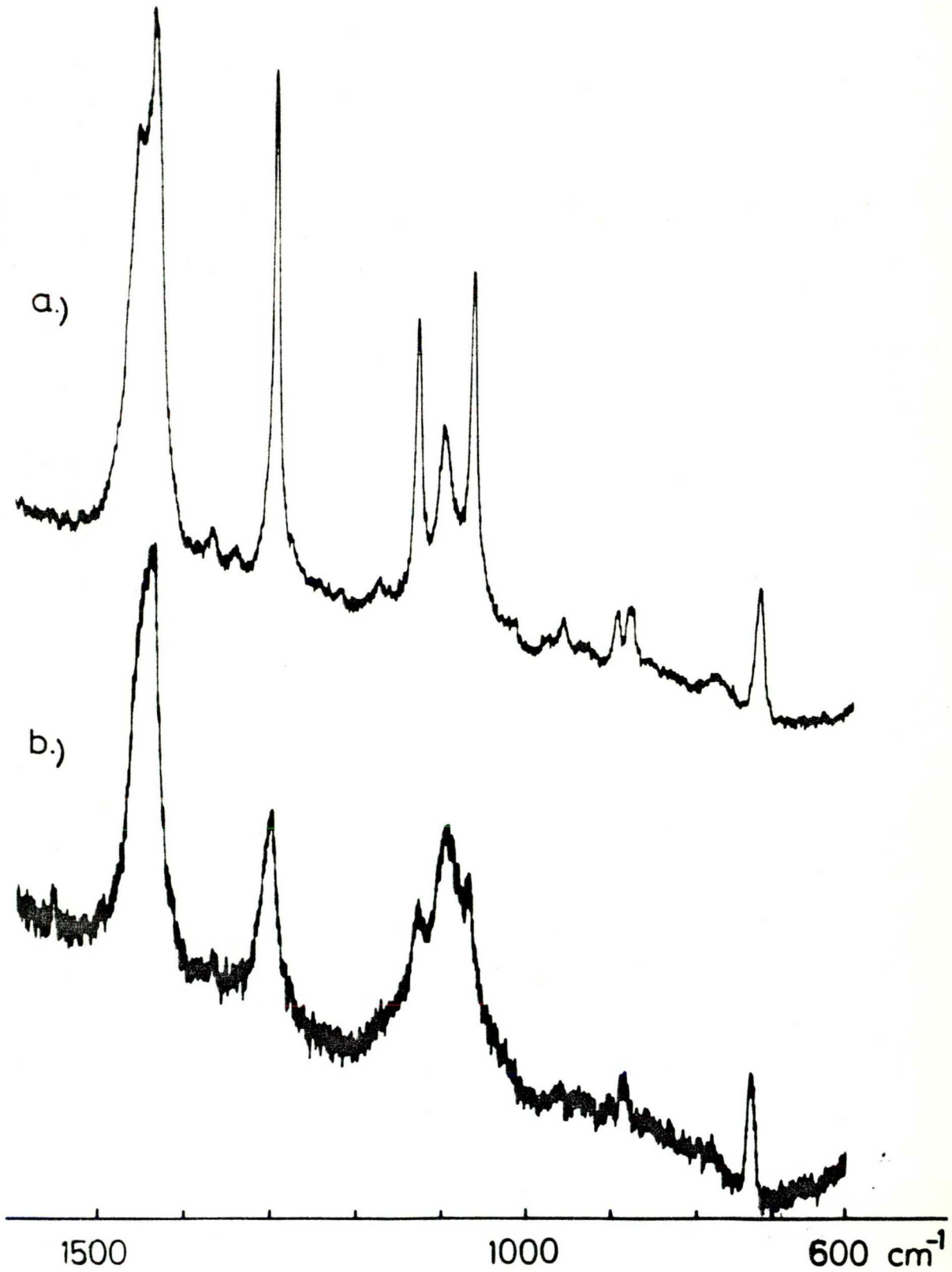
a.)
b.)
1500
1000
600 cm⁻¹

Fig. 23.

Raman spectra of dipalmitoyl phosphatidylcholine lamellar dispersions with different concentrations of KI in the Raman spectral ranges 950 - 1200 cm^{-1}, and 2650 - 3100 cm^{-1}. Iodide concentrations: a - 0; b - 2.10^{-3} M; c - 2.10^{-2} M; d - 10^{-1} M.

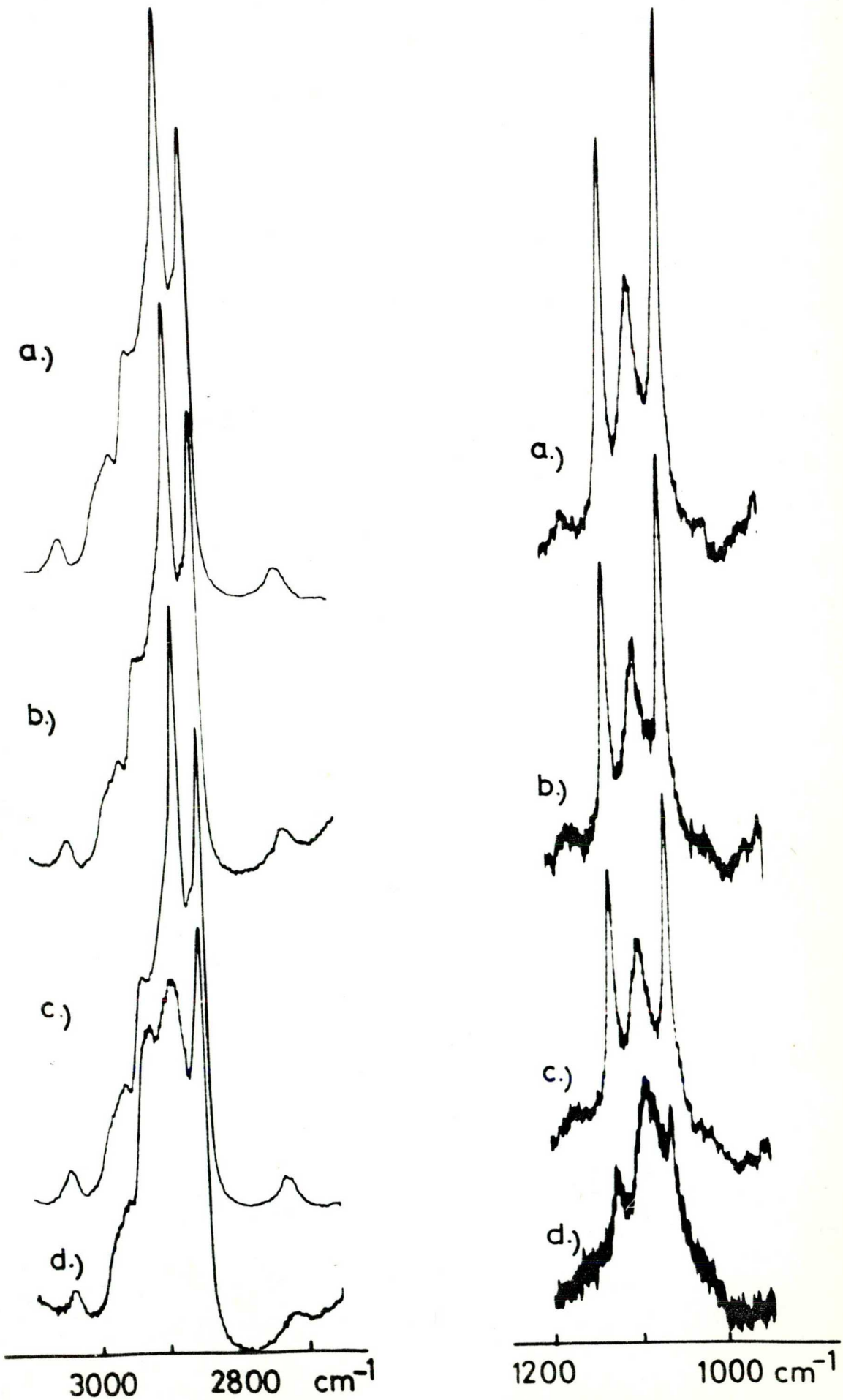
a.)
b.)
c.)
d.)
3000
2800
cm⁻¹
a.)
b.)
c.)
d.)
1200
1000 cm⁻¹

Table 6

Intensity ratios for dipalmitoyl phosphatidylcholine-water dispersions in the presence of different iodine species.

Composition of lipid sample	$\frac{I_{1066}}{I_{1100}}$	$\frac{I_{1128}}{I_{1100}}$	$\frac{I_{2880}}{I_{2850}}$
Dry	1.58	1.49	1.37
H_2O	1.96	1.45	1.28
3.10^{-3}M I_2	1.49	1.17	1.16
2.10^{-3}M KI	1.96	1.49	1.23
2.10^{-2}M KI	1.81	1.38	1.25
2.10^{-1}M KI	0.96	0.51	0.89
$1.5.10^{-3}$M I_2 + 5.10^{-3}M KI	1.49	1.23	1.19
$1.5.10^{-3}$M I_2 + 10^{-2}M KI	1.61	1.20	1.09
$1.5.10^{-3}$M I_2 + 10^{-1}M KI	0.89	0,62	0.90
$1.5.10^{-3}$M I_2 + 1M KI	0.74	0.52	0.89
1M KI + 10^{-2}M $Na_2S_2O_3$	1.75	1.42	1.31
$1.5.10^{-3}$M I_2+10^{-2}M $Na_2S_2O_8$	1.31	1.13	1.17

The enhanced mechanical and dielectric strength of the bilayers doped with iodine indicate that the altered surface properties need special consideration and further investigations from the point of view of ion translocation. Similarly, the possible significance of the gauche density in membrane stability still remains unanswered, and the influence of the interactions with polar heads on the liquid-crystalline-gel transition is also to be explored. Important questions such as the change in the water content of the hydrocarbon region during gauche formation, the physical state of intramembrane water, etc. are still open.

The bands in the region 1200 - 1500 cm^{-1} /Fig.22b/, assigned to bending and rocking vibrations of the methylene groups in the hydrocarbon chains, undergo alterations as the concentration of KI exeeds 10^{-1}M. The band at 1299 cm^{-1}, attributed to a CH_2 twisting vibration, broadens and shifts to 1302 cm^{-1}, and its intensity decreases in comparison to that of the CH_2 deformational vibration at 1450 cm^{-1}. At low KI concentrations there is a sharp band at 1441 cm^{-1} and a shoulder at 1460 cm^{-1}while at concentrations above 10^{-1}M KI there appears a single peak at 1440 cm^{-1}. These changes are characteristic of completely disordered hydrocarbon chains /26/. The same is confermed by the decrease of the intensity ratio I_{2880}/I_{2850} at high KI concentrations /Fig.23/.

Using several intermediate concentrations, it was found that the order-disorder transition occurs in the concentration range 6.10^{-2} - 10^{-1}M KI. Our results differ from those of Lis et al. /29/ who did not find any influence of 1M KI on theDPPC Raman spectra under experimental conditions similar to ours. During exposure to the laser beam tha samples changed in colour to yellowish, probably due to the formation of I_2 and polyiodide ions as a result of oxidation process. In order to establish whether the effect obtained at high KI concentrations is produced by I^- or I_2or even by polyiodide ions, a reducing agent /10^{-2}M $Na_2S_2O_3$/ was used besides 1M KI in the aqueous phase. The intensity ratios had values very close to those of water dispersions, suggesting that I^- itself, even at a concentration of 1M has a negligible effect on DPPC /Fig. 24d/ and the observed effects are due to oxidation products of iodide /I_2, I_3^- /.

The next question to be answered is whether the disordering effect is caused by I_2or by polyiodide ions formed in the simultaneous presence of I_2 and I^-. Accordingly, the

Fig. 24.

Raman spectra of dipalmitoyl phosphatidylcholine lamellar dispersion in the presence of different iodine species in the Raman spectral ranges 950 - 1200 cm^{-1} and 2650 - 3100 cm^{-1}.
a - 10^{-1} M KI; b - 3.10^{-3} M I_2; c - 10^{-1} M KI+$1.5.10^{-3}$M I_2
d - 1 M KI + 10^{-2} M $Na_2S_2O_3$.

/from Chem. Phys. Lipids 19 /1977/ 159-168/.

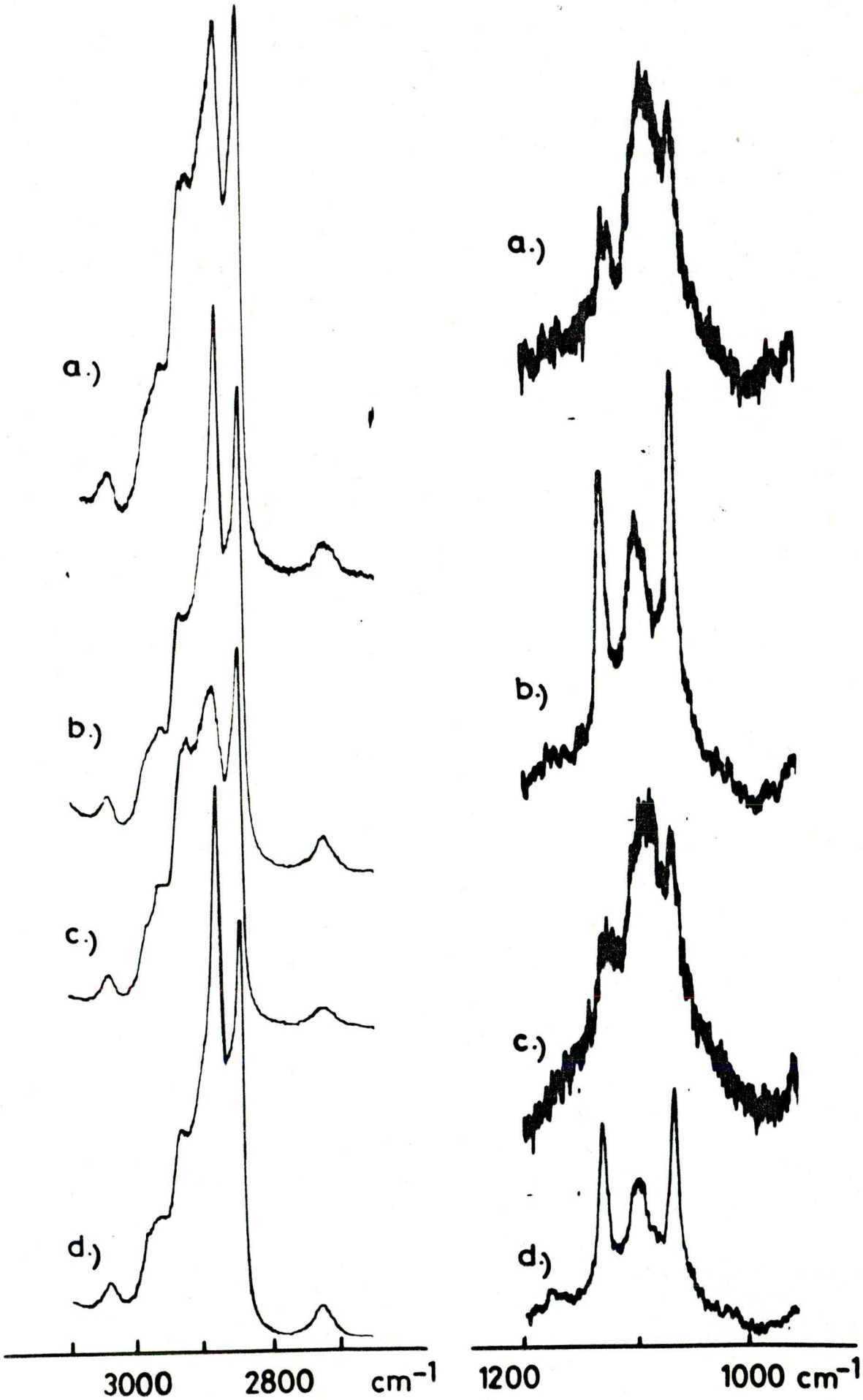
a.)
b.)
c.)
d.)
3000
2800
cm⁻¹
a.)
b.)
c.)
d.)
1200
1000 cm⁻¹

Raman spectra of lecithin dispersions containing $1.5.10^{-3}$M I_2 alone /i.e. the water added was saturated with I_2/, and mixtures of $1.5.10^{-3}$M I_2 and KI in four different concentrations /5.10^{-3}M, 10^{-2}, 10^{-1}M and 1M/ were taken. It was found that I_2 caused a slight disorder /Fig.24b/ and that the mixtures of $1.5.10^{-3}$M I_2 and 5.10^{-3}M KI as well as $1.5.10^{-3}$M I_2 and 10^{-2}M KI had the same effect as I_2 alone /Table 6/. Just the same was established by ESR spectroscopy for egg yolk lecithin vesicles by Jendrasiak and Haves /138/, thuogh they interpreted their results as a rapid conversion of I_2 to I_3^- and interaction of the latter with the membrane. This interpretation is not, however, free from objections, since inour latter two cases the triiodide concentration is much higher than in the presence of I_2 alone. If the differences in the orders of magnitude of triiodide concentrationare not reflected in the Raman spectra, it is hard to believe, that the dominant effect can be attributed to any triiodide interaction. To eliminate triiodide and iodide ions from the aqueous iodine solution, 2.10^{-2}M potassium persulfate was used as an oxidizing agent. Although the spectra obtained in the presence of iodine and persulfate are more noisy, the order-disorder relations estimated on the basis of the intensity ratios do not change noticeably /Table 6/. These observations clearly demonstrate that the primary effect has to be attributed to iodine and not to complex iodide species. An enhanced disordering effect of iodide-iodine mixtures was observed when iodide was present in 10^{-1}M or higher concentrations, whichwere effective even without iodine as seen earlier/Fig 24,a and c/. It can be concluded that I_3^- at 10^{-3}M or higher concentrations has practically no effect different from that of iodine on the structure of lecithin lamellar dispersions. Here again, the disordering effect is probably

due to the I_2 molecules, which may in part penetrate in the hydrocarbon region and also interact with the polar heads. These conclusions are in agreement with the complexing ability and the lipophilic character of I_2 /the partition coefficient of I_2 between water and hexadecane ie 1:50 /139//.

To check the state of iodine in the hydrocarbon phase, iodine transferred from aqueous iodine and triiodide solutions into tetradecane was investigated through its Raman spectrum. In the first case the well-known fundamental vibration of iodine at 211 cm^{-1} with two overtones was found /140/., whereas in the second case Raman lines characteristic of triiodide could not be detected in any of the tetradecane samples. Thus, supporting evedence for the appearance of triiodide ions in the hydrocarbon phase was not obtained.

At concentrations of 10^{-1}M and 1M KI a strong band appeared at 106 cm^{-1} in the spectra of DPPC dispersions, peculiar to the symmetric stretching vibration of I_3^-. During exposure to the laser beam its intensity increased, reaching a constant value, probably because of I_3^- formation from I_2, appearing in the sample during illumination, and I^- present in the aqueous phase. According to refs. 140 and 141, the spectra obtained belong to free, non-complexed form of I_3^-. Thus, I_3^- is probably present in the aqueous phase rather than in the hydrocarbon region of the lipid system /see also the data of the tetradecane experiments/

On the basis of the present studies, therefore, no supporting data could be found for an ionic conduction mechanism based upon triiodide formation and for the existence of triiodide chains as hole pathways in iodine-dopped bilayers. Conversely, the data presented demonstrate that phospholipids interact with iodine rather than with its ionic forms. These results conferm that the primary event in the resistance-lowering effect of iodine could be based upon direct lipid-iodine interaction and iodine penetration into the bilayer membrane /130-134/.

V. CONCLUSIONS

On the basis of the results obtained in the present work the following conclusions were made:

1. Raman spectroscopy is applicable to structural studies of model membrane systems in general and lipid-ion interactions in particular.

2. S_T order parameter introduced by Gaber and Peticolas /43/ as a measure of the all-*trans* probability in lipids, has a restricted applicability in the case of order-disorder transitions in the lipid hydrocarbon chains, induced by interactions of ions with the polar heads and, in general, in transitions affecting the motion and conformation of the polar groups.

3. A phenomenological parameter α, analogous to S_T, was introduced for monitiring the conformational states of fatty acid residues and polar head groups in the presence of ions, accounting for the structural changes in lipids upon hydration.

4. Lateral order parameter S_L, as defined by Gaber and Peticolas /43/, proved to be suitable for the evaluation of the lipid chain packing even in the case of lipid-ion interactions.

5. Monovalent cations /Na^+, K^+, Rb^+, Cs^+/ in high concentrations caused detectable alterations in the Raman spectra of DPPC.

6. Different effectivness sequences in affecting the bilayer structure could be constructed for monovalent cations on the basis of S_T and α, depending on the reference line chosen. The slight disordering effect on the lipid bilayer, observed with Na^+ and Cs^+ is in line with the structure breaking effect of these ions on water.

7. Since no appreciable changes in S_L were observed upon exposure of the lipid bilayer to monovalent cations, it is believed that the effectiveness sequences are determined mainly by cation-head group interactions and that a smaller increase, if any, occurs in the gauche formation than would follow from the corresponding intensity ratios and *trans* order parameters.

8. Divalent cations /Ca^{2+}, Mg^{2+}, Cd^{2+}, Ba^{2+}/ were found more effective in changing the structure of lecithin bilayers than the monovalent ones and with divalent cations detectable changes in the DPPC Raman spectra occured even at lower salt concentrations.

9. On the basis of the α values strong and concentration-dependent interactions of divalent cations with the DPPC polar heads could be deduced. At lower concentrations /5-10 mM/ a slight disordering of the lipid systems was observed, but with increasing the cation concentration /10-100 mM/ the order has been restored and at high ionic concentrations /above 100 mM/ a strong ordering effect of divalent cations was found as judged from the values of the order parameters.

10. Two-step binding mode of divalent cations to DPPC was suggested on the basis of the experimental data.

11. The most pronounced effect was observed with Ca^{2+}. The mode of action and the concentration dependences of Cd^{2+} and Mg^{2+} were similar to those of Ca^{2+} but somewhat weaker. Ba^{2+} proved to be the least effective.

12. On the basis of the small changes in the S_L values it was concluded that the divalent cations interact with the head groups and directly affect mainly the polar region of the bilayers. The ordering effect on the fatty acid re-

sidues is indirect and their arrangement might be close to that found in ion-free phospholipid dispersions.

13. Different effects of mono- and divalent anions on the structure of the lecithin bilayer were deduced from the values of the corresponding order parameters. No correlation seems to exist between the ionic radii and the strengths of interaction of anions with DPPC bilayers, indicating that the effects are not entirely of electrostatic nature. It is believed that, at least in some cases, the effects of anions and cations are rather interlinked, than independent.

14. In studies on the influence of the iodine-iodide system on the structure of DPPC bilayers, no supporting data could be found for the ionic conduction mechanism of iodine-doped BLMs. It was demonstrated that DPPC interacts with iodine rather than with its ionic forms.

ACKNOWLEDGEMENTS

I wish to thank Professor Lajos Keszthelyi, director of the Institute, for making these studies possible, Dr. Béla Karvaly, my supervisor, for his continuous interest, valuable suggestions and criticism throughout the work, and the co-workers of the Institute for their help whenever it was necessary.

REFERENCES

1. G. Herzberg, /1945/ Molecular Spectra and Molecular Structure. II Infrared and Raman Spectra of Polyatomic molecules - D. Van Nostrand Co. Toronto, New York, London.

2. M.M. Sushchinski /1972/ Raman Spectra of Molecules and Crystals. Israel Program for Scientific Translations, New York, Jerusalem, London,

3. T.R. Gilson and P.J. Hendra /197o/ Laser Raman Spectroscopy. Wiley /Interscience/, London, New York, Sydney, Toronto.

4. L.A. Woodward /1972/ Introduction to the theory of molecular vibrations and vibrational spectroscopy. Univ. Press, Oxford.

5. D. Steele /1971/ Theory of vibrational spectroscopy. W.B. Saunders company, Philadelphia, London, Toronto.

6. F.A. Cotton /1971/ Chemical Applications of Group Theory. Wiley /Interscience/ New York, London, Sydney, Toronto.

7. R.M. Hochstrasser /1966/ Molecular Aspects of symmetry. W.A. Benjamin, Inc., New York, Amsterdam.

8. P.J. Hendra, /1972/ In "Laboratory Methods in Infrared Spectroscopy" /R.G.J. Miller and B.C.Stace, eds/ Ch. 15, Heyden and Son Ltd., London, New York, Rheine.

9 F.R. Dollish, W. Fateley, F. Bently /1973/ Characteristic Raman Frequencies of Organic Compounds" John Wiley and Sons, New York, London, Sydney, Toronto.

10. L.J. Bellamy /1975/ The Infrared Spectra of Complex-Molecules. Chapman and Hall, London.

11. W. Hendler /1974/ In "Biomembranes" vol.5. /L.A. Manson, ed./ pp. 251-273, Plenum Press, New York, London.

12. M.K. Jain and H.B. White /1977/ Adv. Lipid Res. 15, 1-60.

13. A.G. Lee /1975/ Progr. Biophys. Molec. Biol. 29, 3-56.

14. Y.K. Levine, /1972/ Progr. Biophys. Molec. Biol. 24, 1-74.

15. F.A. Vandenheuvel /1971/ Adv. Lipid Res. 9, 161-248.

16. L.M. Van Deenen /1965/ Progr. Chem. Fats Other Lipids 8, 1-127.

17. H. Träuble /1972/ in "Biomembranes " vol. 3, /F. Kreutzer, and F.J. G. Slegers, eds./ pp. 197-227, Plenum Press, New York, London.

18. D. Chapman /1975/ Quart. Rev. Biophys. 8, 185-235.

19. B. Fourcans and M.K. Jain /1974/ Adv. Lipid Res. 12, 148-226.

20. D. Chapman, J.C. Gomez-Fernandez and F.M. Goni /1979/ FEBS Lett. 29, 211-228.

21. H. Sandermann, Jr. Biochim. Biophys. Acta. 515, 209-237. /1978/

22. J.L.Lippert, and W.L. Peticolas /1971/ Proc. Natl. Acad. Sci. USA, 68, 1572-1576.

23. J.L Lipprt, and W.L. Peticolas /1972/ Biochim. Biophys. Acta 282, 8-17.

24. R. Mendelsohn /1972/ Biochim. Biophys. Acta 290, 15-21.

25. K. Larsson /1973/ Chem. Phys. Lipids 10, 165-176.

26. K.G. Brown, W.L. Peticolas and E. Brown /1973/ Biochim. Biophys. Res. Comm. 54, 358-364.

27. K. Larsson and R.P. Rand /1973/ Biochim. Biophys. Acta 326, 245-255.

28. R.C. Spiker, Jr. and I.W. Levin /1975/ Biochim. Biophys. Acta 388, 361-373.

29. L.J. Lis, J.W. Kauffman and D.F. Shriver /1975/ Biochim. Biophys. Acta 406, 453-464.

30. R. Mendelsohn, S. Sunder and H.J. Bernstein /1975/ Biochim. Biophys. Acta 413, 329-340.

31. R. Mendelsohn, S. Sunder and H.J. Bernstein /1976/ Biochim. Biophys. Acta 419, 563-569.

32. R. Faiman and D.A. Long /1975/ J. Raman Spectrosc. 3, 371-377.

33. J.B.R. Faiman and D.A. Long /1975/ J. Raman Spectrosc. 3, 379-385.

34. S.P. Verma and D.F.H. Wallach /1976/ Biochim. Biophys. Acta 426, 616-623.

35. R.C. Spiker, Jr. and I.W. Levin /1976/ Biochim. Biophys. Acta 433, 457-468.

36. R. Faiman and K. Larsson /1976/ J. Raman Spectrosc. 4, 387-394.

37. R. Faiman, K. Larsson and D.A. Long /1976/ J. Raman Spectrosc. 5, 3-7.

38. R. Faiman and D.A. Long /1976/ J. Raman Spectrosc. 5, 87-92.

39. S. Sunder, R. Mendelsohn and H.J. Bernstein /1976/ Chem. Phys. Lipids, 17, 456-465.

40. R.C. Spiker, Jr. and I.W. Levin /1976/ Biochim. Biophys. Acta 455, 560-575.

41. R.C. Spiker, Jr., T.J- Pinnavaia and I.W. Levin /1976/. Biochim. Biophys. Acta 455, 588-596.

42. M.R. Bunow and I.W. Levin /1977/ Biochim. Biophys. Acta 464, 202-216.

43. B.P. Gaber and W.L. Peticolas /1977/ Biochim. Biophys. Acta 465, 260-274.

44. N. Yellin and I.W. Levin /1977/ Biochim. Biophys. Acta 468, 490-494.

45. S.A. Simon, L.J. Lis, R.C. MacDonald and J.W. Kauffman /1977/ Biophys. J. 19, 83-90.

46. S.C. Goheen, J.L. Lis and J.W. Kauffman /1977/ Chem. Phys. Lipids 20, 253-262.

47. L.J. Lis, S.C. Goheen and J.W. Kaufmann /1977/ Biochem. Biophys. Res. Comm. 78, 492-497.

48. S.P. Verma, and D.F.H. Wallach /1977/ Biochim. Biophys. Acta 486, 217-227.

49. M.R. Bunow, and I.W. Levin /1977/ Biochim. Biophys. Acta 487, 388-394.

50. N. Yellin and I.W. Levin /1977/ Biochim. Biophys. Acta 489, 177-190.

51. N. Yellin and I. W. Levin /1977/ Biochemistry, 16, 642-647.

52. M.R. Bunow and I.W. Levin /1977/ Biochim. Biophys. Acta 489, 191-206.

53. B.P. Gaber P. Yager and W.L. Peticolas /1978/ Biophys. J. 21, 161-176.

54. B.P. Gaber, P.Yager and W.L. Peticolas /1978/ Biophys. J. 22, 191-207.

55. B.P. Gaber, P. Yager and W.L. Peticolas /1978/ Biophys. J. 24, 677-688.

56. A.S. Sunder, D. Cameron, H.H. Mantsch /1978/ Can J. Chem. 56, 2121-2126.

57. E. Weidekamm, E. Bamberg, K. Janko and R. Weber /1978/ Arch. Biochim. Biophys. 187, 339-345.

58. R. Mendelsohn and J. Maisano /1978/ Biochim. Biophys. Acta 506, 192-201.

59. R. Mendelsohn and T. Taraschi /1978/ Biochemistry 17, 3944-3949.

60. R. Feiman /1979/ Chem. Phys. Lipids 23, 77-84.

61. H. Okabayashi and T. Kitagawa /1978/ J. Phys. Chem. 82, 1830-1836.

62. S. Sunder, H.J. Bernstein and F. Paltauf /1978/ Chem. Phys Lipids 22, 279-283.

63. J. Lis, J.W. Kaufman and D.F. Shriver /1976/ Biochim. Biophys. Acta 436, 513-522.

64. B.J. Bulkin /1976/ Appl. Spectr. 3, 261-269.

65. Y. Koyama, Sh. Toda and Y. Kyogoku /1977/ Chem. Phys. Lipids 19, 74-92.

66. H. Akutsu, Y. Kyogoku, H. Nakahara and K. Fukuda /1975/ Chem. Phys. Lipids 15, 222-242

67. U.P. Fringeli /1977/ Z. Naturforsch. 23c, 20-45.

68. J.E. Fookson and D.F.H. Wallach /1978/ Arch. Biochem. Biophys. 189, 195-204.

69. T.G. Spiro and B.P. Gaber /1977/ Ann. Rev. Biochem. 46, 553-572.

70. N.-T. Yu /1977/ CRC Critical Reviews in Biochemistry 229-280.

71. A. Warshel /1977/ Ann. Rev. Biophys. Bioengn. 6, 273-300.

72. P.R. Carey /1978/ Quart. Rev. Biophys. 11, 309-370.

73. P.R. Carey and H. Schneider /1978/ Accounts of Chemical Research 11, 122-128.

74. J.L. Lippert, L.E. Gorczyca and G. Meiklejohn /1975/ Biochim. Biophys. Acta 382, 51-57.

75. S.P. Verma and R.Schmidt-Ullrich, D.F.H. Wallach /1975/ Biochim. Biophys. Acta 394, 633-645

76. S.P. Verma and D.F.H. Wallach /1975/ Biochim. Biophys. Acta 401, 168-176.

77. F.P. Milanovich, Y.Yeh, R.J. Baskin and R.C. Harney /1976/ Biochim. Biophys. Acta 419, 243-250.

78. R. Schmidt-Ullrich, S.P. Verma and D.F.H. Wallach /1976/ Biochim. Biophys. Acta 426, 477-488.

79. S.P. Verma and D.F.H. Wallach /1976/ Biochim. Biophys. Acta 436, 307-318.

80. L.J.Lis, J.W. Kauffman and D.F. Shriever /1976/ Biochem. Biophys. Acta 436, 513-522.

81. L.J. Lis, S.G. Goheen, J.W. Kauffman and D.F. Shriver, /1976/ Biochim. Biophys. Acta 433, 331-338.

82. G.J. Thomas, Jr., B. Prescott, R.E. McDonald-Ordzie, and K.A. Hartman /1976/ J. Mol. Biol. 102, 103-124.

83. S.C. Goheen, T.H. Gilman, J.W. Kauffman and J.E. Garvin /1977/ Biochem. Biophys. Res. Comm. 79, 805-814.

84. M. Pezolet, M. Pigeon-Gosselin and J.-P. Caille /1978/ Biochim. Biophys. Acta 533, 263-269.

85. W. Curatolo, S.P. Verma, J.D. Sakura, D.M. Small, G.G. Shipley and D.F.H. Wallach, /1978/ Biochemistry 17, 1802-1807.

86. K.A. Hartman, P.E. McDonald-Ordzie, J.M. Kaper, B. Prescott and G.J. Thomas, Jr. /1978/ Biochemistry, 17, 2118-2123.

87. E.J. East, R.C. Chang, N.-T. Yu and F.J.R. Kuck, Jr. /1978/ J. Biol. Chem. 253, 1436-1441.

88. G. Forrest /1978/ Chem. Phys. Lipids 21, 237-252.

89. D.F.H. Wallach, S.P. Verma and J. Fookson /1979/ Biochim. Biophys. Acta 559, 153

90. A.D. Bangham /1968/ Progr. Biophys. Molec. Biol. 18, 31-95.

91. H. Susi, J. Sampugna, J.W. Hampson and J.S. Ard /1979/ Biochemistry 18, 297-301.

92. B. Karvaly and E. Loshchilova /1977/ Biochim. Biophys. Acta 470, 492-496.

93. N.G. Godin and T.W. Ng /1974/ Mol. Pharmacol. 9, 802-819.

94. B. Karvaly, I. Szundi and K. Nagy /1975/ Bioelectrochem. Bioenerg. 2, 339-347.

95. Y. Inoko, T. Yamaguchi, K. Furuya and T. Mitsui /1975/ Biochim. Biophys. Acta 413, 24-32.

96. T. Gulik-Krzywicki, E. Rivas and V. Luzzati /1967/ J. Mol. Biol. 27, 303-322.

97. A. Tardieu, V. Luzzati and F.C. Reman /1973/ J. Mol. Biol. 75, 711-733.

98. Y.K. Levine and M.H. F. Wilkins /1971/ Nature New Biol. 230, 69-72.

99. P.L. Yeagle and R.B. Martin /1976/ Biochem. Biophys. Res. Comm. 69, 775-780.

100. E. Loschchilova and B. Karvaly /1978/ Biochim. Biophys. Acta 514, 274-285.

101. Anderson, P.J. and Pethica, B.A. /1956/ in Biochemical Problems of Lipids /Popjak, G. and le Breton, E. eds/ pp. 24-29, Butterworths Sci. Publ. London

102. H. Kimizuka, and K. Koketsu /1962/ Nature 196, 995-996.

103. D.O. Shah, and J.H. Schulman /1967/ J. Lipid Res. 8, 215-226.

104. D.O. Shah, and J.H. Schulman /1967/ J. Lipid Res. 8, 227-233.

105. D.O. Shah, and J.H. Schulman /1967/ J. Lipid Res. 6, 341-349.

106. T. Seimiya and S. Ohki /1972/ Nat. New Biol. 239, 26-27.

107. S. Ohki and A. Goldup /1968/ Nature 217, 458-459.

108. T. Seimiya and S. Ohki /1973/ Biochim. Biophys. Acta 298, 546-561.

109. Papahadjopoulos, D. and Ohki, S. /1970/ in Liquid Crystals and Ordered Fluids /Johnson, J.F. and Porter, R.S. eds/ pp. 13-32, Plenum Press, New York.

110. S.A. Simon, L.J. Lis, J.W. Kaufman and D.E. MacDonald /1975/ Biochim. Biophys. Acta 375,317-326.

111. D. Chapman, W.E. Peel, B. Kingston and T.H. Lilley /1977/ Biochim. Biophys. Acta 464, 260-275.

112. H. Hauser, M.C. Philips, B.A. Levine and R.J.P. Williams Eur. J. Biochem. 58, 133-144.

113. K.K. Yabusaki and M.A. Wells /1975/ Biochemistry 14, 162-166.

114. D.G. Dervichian /1956/ in Biochemical Problems of Lipids /Popjak G. and le Breton E. eds./ pp. 3-13, Buttersworths Sci. Publ. London.

115. E. Rojas, and J.M. Tobias /1965/ Biochim. Biophys. Acta 94, 394-404

116. G. Colacicco /1973/ Chem. Phys. Lipids 10, 66-72.

117. G. Colaccico, A.R. Bucklew, Jr., and E.M. Scarpelli /1974/ J. Coll. Interface Sci. 46, 147-151.

118. K. Jacobson and D. Paphadjopoulos /1975/ Biochemistry 14, 152-161.

119. H. Hauser, R.M. C. Dawson /1967/ Eur. J. Biochem. 1, 61-69.

120. P.H. von Hippel and T. Schleich /1969/ Structure and Stability of Biological Macromolecules pp. 417-547 , Dekker, New York.

121. B. Karvaly /1976/ Bioelectrochem. Bioenerg. 3, 545-560.

122. A.A. Belmonte, J. Swarbrick, R.G. Jensen and D.T. Gordon /1972/ Lipids 7, 490-492.

123. K.S. Krishnan and D. Balaram /1976/ Arch. Biochem. Biophys. 174, 420-430.

124. R.G.P. Williams /1975/ in Biological Membranes /Parsons, D.S. ed/ pp. 106-140, Clarendon Press, Oxford.

125. A. Finkelstein and A. Cass /1968/ J. Gen. Physiol. 52, 145S

126. G. Szabo, G. Eisenman, R. Laprade, S.M. Ciani and S. Krashne /1975/ in Membranes /G. Eiseman, ed./ vol. 2, Dekker, New York.

127. B. Rosenberg and F.L. Jendrisiak /1968/ Chem.Phys.Lipids, 2, 47.

128. B. Rosenberg, and H.D. Pant. /1970/ Chem. Phys. Lipids 4, 203.

129. V. Vodyanoj, I. Vodyanoj and N. Fedorovich, /1970/ Fiz. Tverd. Tela /Kharkov/ 12, 3321.

130. H.T. Tien and S.P. Verma /1970/ Nature, 227, 1232.

131. L.I. Boguslavskij, F.I. Bagolepova and A.V. Lebedev /1971/ Chem. Phys. Lipids 6, 269.

132. B. Karvaly, B. Rosenberg, H.C. Pant and G. Kemeny /1973/ Biophysik 10 199.

133. B. Karvaly, /1975/ Bioelectrochem. Bioenerg 2, 124.

135. B. Karvaly, P. Shieh and H.T. Tien

134. B. Karvaly, /1974/ Faraday Symp. Chem. Soc. 9, 182.

136. P. Läuger , J. Richter and W. Lesslauer /1968/ Ber. Bunsenges Phys. Chem. 71, 906.

137. E.A. Liberman, V.P. Topaly, M. Tsofina and A.M. Shkrob, /1969/ Biofizika 14, 56.

138. G.L. Jendrasiak and R. Hayes /1970/ Nature 225, 279.

139. J.H. Heldebrands and C. Jenks /1920/ J. Am. Chem. Soc. 42, 2180.

140. W. Kiefer, /1974/ Appl. Spectr. 28, 115.

141. F. Inagaki, I. Harada, I. Simanonchi and M. Tasumi /1972/ Bull. Chem. Soc. Japan 45, 3384.

142. H.J. Bernstein /1973/ in Advances in Raman Spectroscopy /J.P.Mathieu, ed/ Vol. 1. Heyden and Son, London.

143. E. Loshchilova and B. Karvaly /1977/ Chem. Phys. Lipids 19, 159-168.